THE PHYSICOCHEMICAL PROPERTIES AND STARCH DIGESTIBILITY OF THE TERNARY FOOD SYSTEMS COMPOSED OF POTATO STARCH, MILK PROTEINS, AND SOYBEAN OIL

Guan Yufang

A Thesis Submitted in Partial Fulfillment of the Requirements for the

Degree of Doctor of Philosophy Food Technology

Suranaree University of Technology

Academic Year 2020

สมบัติทางเคมีฟิสิกส์และความสามารถในการย่อยแป้งของระบบอาหารแบบตติยภูมิที่ประกอบด้วยแป้งมันฝรั่ง โปรตีนนม และน้ำมันถั่วเหลือง

นางกวาน หยูฟาง

วิทยานิพนธ์นี้เป็นส่วนหนึ่งของการศึกษาตามหลักสูตรปริญญาปรัชญาดุษฎีบัณฑิต
สาขาวิชาเทคโนโลยีอาหาร
มหาวิทยาลัยเทคโนโลยีสุรนารี
ปีการศึกษา 2563

THE PHYSICOCHEMICAL PROPERTIES AND STARCH DIGESTIBILITY OF THE TERNARY FOOD SYSTEMS COMPOSING OF POTATO STARCH, MILK PROTIENS AND SOYBEAN OIL.

Suranaree University of Technology has approved this thesis submitted in partial fulfillment of the requirements for the Degree of Doctor of Philosophy.

Thesis Examining Committee
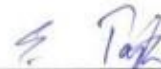
_____
(Assoc. Prof. Dr. Sunanta Tongta)

Chairperson
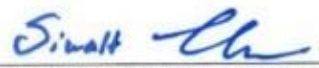
_____
(Asst. Prof. Dr. Siwatt Thaiudom)

Member (Thesis Advisor)

_____
(Prof. Dr. Guohua Zhao)

Member

_____
(Asst. Prof. Dr. Ratchadaporn Oonsivilai)

Member
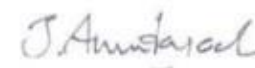
_____
(Assoc. Prof. Dr. Jirarat Anuntagool)

Member

_____
(Prof. Dr. Neung Teaumroong)

_____
(Assoc. Prof. Flt. Lt. Dr. Kontorn Chamniprasart)

Vice Rector for Academic Affairs and

Internationalization

Dean of Institute of Agricultural

Technology

กวาน หยูฟาง : สมบัติทางเคมีฟิสิกส์และความสามารถในการย่อยแป้งของระบบอาหาร
แบบตติยภูมิที่ประกอบด้วยแป้งมันฝรั่ง โปรตีนนม และน้ำมันถั่วเหลือง (THE
PHYSICOCHEMICAL PROPERTIES AND STARCH DIGESTIBILITY OF THE
TERNARY FOOD SYSTEMS COMPOSED OF POTATO STARCH, MILK
PROTEINS, AND SOYBEAN OIL) อาจารย์ที่ปรึกษา : ผู้ช่วยศาสตราจารย์
ดร.ศิวัฒ ไทยอุดม, 181 หน้า.

วัตถุประสงค์ของการศึกษานี้เพื่อเข้าใจถึงผลของการเติมโปรตีนนม (milk protein ; MP)
และน้ำมันถั่วเหลือง (soybean oil ; SBO) ลงในแป้งมันฝรั่ง (potato starch ; PS) ต่อโครงสร้าง
สมบัติทางเคมีฟิสิกส์ และความสามารถในการย่อยของแป้งมันฝรั่งเจลาติไนซ์ (gelatinized potato
starch ; GPS) ระบบจำลองของมันฝรั่งบดแบบทุติยภูมิและแบบติตยภูมิเตรียมได้จาก GPS ผสมกับ
เคซีน (CA) หรือ เวย์โปรตีน (WP) ร้อยละ 10 (คิดเทียบเป็นน้ำหนักแห้งของ PS) โดยอีกสูตรผสม
GPS กับ SBO ร้อยละ 15 (คิดเทียบเป็นน้ำหนักแห้งของ PS) หรือ ผสม GPS กับ CA หรือ WP และ
SBO โดยผสมให้เป็นเนื้อเดียวกันด้วยกระบวนการฮอโมจีไนเซชัน

ภาพจากกล้องจุลทรรศน์คอนโฟคอล แสดงให้เห็นว่า MP และ SBO กระจายอยู่ในโครงสร้าง
สามมิติของ GPS ส่วนผลทางวิทยากระแสแสดงให้เห็นว่าเมื่อเติม SBO เพียงอย่างเดียวลงใน GPS
ทำให้ตัวอย่างมีความหนืดสูงขึ้น ในทางตรงกันข้าม ส่วนผสมของ GPS-CA, GPS-WP, GPS-CA-
SBO และ GPS-WP-SBO แสดงความหนืดที่ต่ำกว่าและแสดงลักษณะเหมือนของเหลวมากกว่า PSP

ผลของการวิเคราะห์ ฟูเรียร์ทรานส์ฟอร์มอินฟราเรด (FTIR) สเปกโทรสโกปี รามันสเปกโทร-
สโกปี และการเลี้ยวเบนรังสีเอกซ์ (XRD) แสดงให้เห็นว่าไม่มีพันธะโควาเลนต์ระหว่าง GSP, MP
และ SBO ในระหว่างกระบวนการทำให้เป็นเนื้อเดียวกัน และ ไม่เกิดลักษณะของโครงสร้างแบบ
ทุติยภูมิและตติยภูมิเกิดขึ้นในตัวอย่างดังกล่าว หลังจากการเกิดเจลาติไนซ์ของ PS และการทำให้เป็น
เนื้อเดียวกันของตัวอย่างผสม พบว่า ส่วนอสัณฐานของ PS เพิ่มขึ้นในขณะที่พันธะโมเลกุลระยะสั้น
และความเป็นผลึกของ PS ลดลง

การเพิ่ม MP และ SBO มีผลเพียงเล็กน้อยต่อความหนืดของ GPS อย่างไรก็ตาม การเติม
เอนไซม์ทำให้ความหนืดของน้ำย่อยอาหารลดลงอย่างมีนัยสำคัญ โดยเฉพาะอย่างยิ่งการเติม MP ลง
ในระบบตัวอย่างมันฝรั่งบดนี้สามารถส่งเสริมการย่อยใน GPS ในขณะที่ SBO กลับชะลอการย่อย
ดังกล่าว อย่างไรก็ตาม การย่อยแป้งมันฝรั่งได้รับการส่งเสริมโดยการเติมโปรตีนและน้ำมัน ตัวอย่าง
ผสมของ SBO และ MP ส่งเสริมการย่อยโปรตีน ในขณะที่การผสม GPS และ MP กลับยับยั้งการ
ย่อยโปรตีน การผสม MP และ/หรือ GPS กับ SBO ส่งเสริมการปลดปล่อย FFA ใน SBO อัตราการ
ปล่อย FFA ที่สูงสุดได้มาจากการผสมระหว่าง MP และ SBO

โดยสรุปแล้ว การเติม MP และ SBO ลงใน GPS สามารถเปลี่ยนโครงสร้าง สมบัติทางเคมี ฟิสิกส์ และความสามารถในการย่อยของ GPS แตกต่างกันไปตามองค์ประกอบของวัตถุดิบที่ใช้ ทดสอบ ทั้งในระบบทุติยภูมิและระบบตติยภูมิ อย่างไรก็ตาม ผลที่ได้จากการศึกษานี้สามารถใช้เป็น แนวทางในการกำหนดองค์ประกอบและได้รับองค์ความรู้เกี่ยวกับปฏิสัมพันธ์ขององค์ประกอบ ดังกล่าวเพื่อนำไปประยุกต์ใช้ในการพัฒนาผลิตภัณฑ์อาหารที่มีแป้งมันฝรั่งเป็นองค์ประกอบหลัก ต่อไปได้
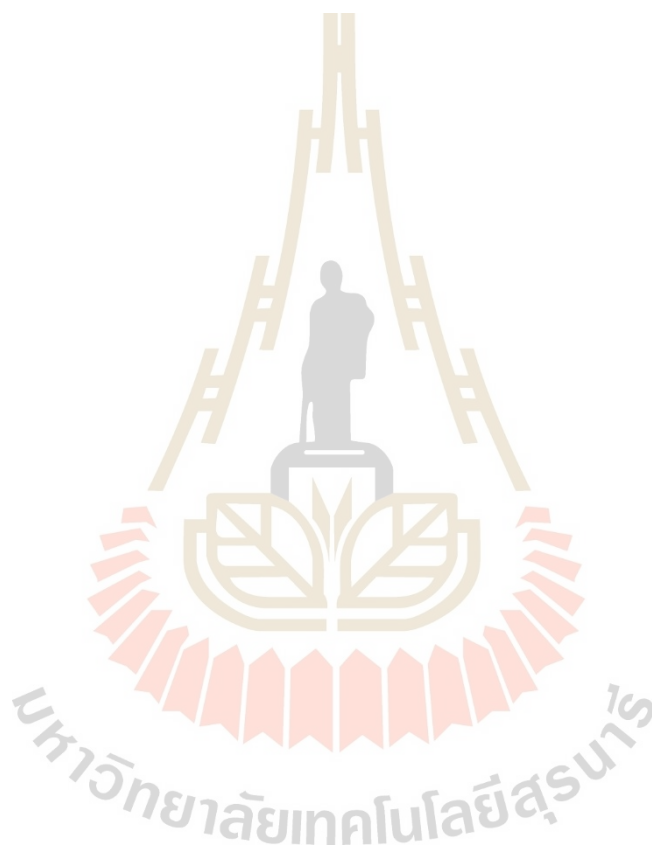
สาขาวิชาเทคโนโลยีอาหาร   ลายมือชื่อนักศึกษา_____

ปีการศึกษา 2563   ลายมือชื่ออาจารย์ที่ปรึกษา_____

                                       ลายมือชื่ออาจารย์ที่ปรึกษาร่วม_____

GUAN YUFANG : THE PHYSICOCHEMICAL PROPERTIES AND
STARCH DIGESTIBILITY OF THE TERNARY FOOD SYSTEMS
COMPOSED OF POTATO STARCH, MILK PROTEINS, AND SOYBEAN
OIL. THESIS ADVISOR : ASST. PROF. SIWATT THAIUDOM, Ph.D., 181 PP.

POTATO STARCH/CASEIN/WHEY PROTEIN/SOYBEAN OIL/DIGESTIBILITY

This study aimed to understand the effects of adding milk protein (MP) and soybean oil (SBO) to potato starch (PS) on the structural, physicochemical and the in vitro digestibility properties of the gelatinized potato starch (GPS). Binary and ternary mixtures were prepared using GPS mixed with 10% w/w dry starch-based MP (casein, CA or whey protein, WP) individually; with 15% w/w dry starch based SBO; or with both the MP and SBO. All samples were then homogenized to initiate binary and tertiary paste samples.

Confocal laser scanning microscopy (CLSM) images showed that MP and SBO were dispersed into the three-dimensional structure of the GPS. The rheological results revealed that with SBO as the only addition into the GPS (GPS-SBO) showed a higher viscosity than with PSP. In contrast, the mixtures of GPS-CA, GPS-WP, GPS-CA-SBO and GPS-WP-SBO, displayed lower viscosity and exhibited a more liquid-like behavior than that of PSP.

The results of Fourier transform infrared (FTIR) spectroscopy, Raman spectroscopy, and X-ray diffraction (XRD) analyses showed that there were no covalent interactions among GSP, MP, and SBO during the homogenization process, and there were no binary and ternary complex formations. After gelatinization of the PS and the homogenization of the mixtures, the amorphous region of the PS increased

while the short-range molecular order and the degree of crystallinity of the PS decreased.

The addition of MP and SBO had little effect on GPS viscosity during digestion. However, with the addition of enzymes, the viscosity of the digestive juice decreased significantly. Specifically, the MP addition promoted GPS digestion, while the SBO slowed down the digestion of potato paste. However, the addition of protein and oil promoted the digestion of potato paste. The mixed sample of SBO and MP promoted protein digestion, while the mixed sample of GPS and MP inhibited protein digestion. The mixture of MP and/or GPS with SBO promoted the release of FFA in SBO. The highest release rate of FFA was attained with a mix of MP and SBO.

In conclusion, the addition of MP and SBO to GPS changed the structure, physicochemical, and digestibility properties of the GPS in different ways depending on the raw material compositions. The results from this study could be used as a guide for assigning food composition while providing knowledge about the interactions of different food compositions or ingredients allowing for further development of potato-based food products.

School of Food Technology

Academic Year 2020

Student's Signature _Yufang Guan_

Advisor's Signature _Sunatt Cu._

Co-Advisor's Signature _Guohua Zhao_

ACKNOWLEDGEMENTS

Thirdly, I would like to thank my workplace, the Institute of biotechnology, Guizhou Academy of Agricultural Sciences, and my colleagues, for their support for my doctoral study.

Fourthly, I would like to thank my family, my parents, husband and sister for their understanding and support over the years, which has made it possible for me to go through this intense and fulfilling study period.

Yufang Guan

CONTENTS

CONTENTS (Continued)

CONTENTS (Continued)

CONTENTS (Continued)

XI

CONTENTS (Continued)

Page

CONTENTS (Continued)

LIST OF TABLES

LIST OF FIGURES

LIST OF FIGURES (Continued)

LIST OF FIGURES (Continued)

LIST OF FIGURES (Continued)

LIST OF FIGURES (Continued)

LIST OF FIGURES (Continued)

LIST OF FIGURES (Continued)

LIST OF ABBREVIATIONS

APTS	=	8-amino-1,3,6-pyrenetrisulfonic acid
AUCexp	=	the areas under the digestograms
C12	=	Lauric acid
C14	=	Myristic acid
C14:0	=	Myristic
C14:1	=	Myristoleic
C16	=	Palmitic acid
C16:0	=	Palmitic
C16:1	=	Palmitoleic
C18	=	Stearic acid
C18:0	=	Stearic
C18:1	=	Oleic acid
C18:1n9c	=	Oleic
C18:2	=	Linoleic acid
C18:2n6c	=	Linoleic
C18:3n3	=	Linolenic
C18:3n6	=	Calendic acid
C20:0	=	Arachidic
C20:2	=	Dihomo-linoleic
C21:0	=	Heneicosylic

LIST OF ABBREVIATIONS (Continued)

C22:0	=	Behenic
C23:0	=	Tricosylic
C24:0	=	Lignoceric
C24:1	=	Nervonic
CA	=	Casein
CA-SBO	=	Casein-soybean oil
CLSM	=	Confocal laser scanning microscopy
D0	=	the digested starch at time t = 0
D∞	=	the digestion at infinite time (D0 + D∞−0)
D∞−0	=	estimated from t = 0–240 min
Dt	=	the digested starch at time t
DSC	=	differential scanning calorimetry
DP		degree of polymerization
eGI	=	estimated glycemic index
FITC	=	Fluorescein isothiocyanate isomer I
FAs		Fatty acids
FFAs		Free fatty acids
FTIR	=	Fourier transform infrared
G'		elastic modulus/storage moduli
G"		viscous modulus/loss modulus
GI	=	glycemic index
GIAVG	=	estimated GI (average)

LIST OF ABBREVIATIONS (Continued)

GL	=	glycemic load
GOPOD	=	glucose oxidase-peroxidase
Gp	=	the amount of glucose produced
GPS		gelatinized potato starch
HI	=	hydrolysis index
HPSEC	=	high performance size exclusion chromatography
K	=	consistency coefficient (charpter III)
K	=	the rate constant (charpter V)
LVR	=	linear viscoelastic region
MALLS	=	multi angle laser scattering
MC	=	Micellar casein concentrates power
MP	=	Milk protein
PS	=	Potato starch
PSP	=	Potato starch paste
PSP-CA	=	Potato starch-casein
PSP-CA-SBO	=	Potato starch-casein-soybean oil
PSP-SBO	=	Potato starch-soybean oil
PSP-WP	=	Potato starch-whey protein
PSP-WP-SBO	=	Potato starch-whey protein-soybean oil
RDS	=	rapidly digested starch
RVA	=	rapid viscosity analyzer
RS	=	resistant starch

LIST OF ABBREVIATIONS (Continued)

SBO	=	Soybean oil
SDS	=	slowly digested starch
Sh	=	the amount of starch hydrolyzed
Si	=	the initial amount of starch
T0	=	onset
Tc	=	conclusion
TCA		trichloroacetic acid
Tp	=	peak
WP	=	Whey protein
WP-SBO	=	Whey-soybean oil
XRD	=	X-ray diffraction
ΔHgel	=	gelatinization enthalpy

CHAPTER I

INTRODUCTION

1.1   Introduction

Potato (*Solanum tuberosum* L.) is the fourth largest crop in the world after wheat, maize and rice (A and Poats, 2009). Potato can be used as a direct edible vegetable and raw material for processing products, such as preformed meals, flour, snacks, potato starch (PS), potato derivatives, starch derivatives, etc. (Singh and Kaur, 2016). Potato tubers contain 13-37% dry matter, 13-30% carbohydrates, 0.7-4.6% proteins, 0.02-0.96% lipids, and about 0.44% ash (Alvani, Qi, Tester, and Snape, 2011; Leivas et al., 2013). Nutrition facts of potatoes are shown in Figure 1.1. Potatoes are not only an important supplier of carbohydrates in the human diet but also a key supplier of nutrients, including minerals, proteins, vitamins, etc. (King and Slavin, 2013). Potatoes are one of the most widely consumed vegetables in the world, with a global per capita consumption of nearly 28 kilograms. In developed countries, the figure is 74 kilograms (Mu, Sun, and Liu, 2017). Various forms of potatoes as cooked, mashed, or fried, have been the main food source in many countries in the world. Potatoes are served as a staple food in some places. The staple foods produced by potatoes are varied and included steamed bread, bread, noodles, sponge cake, mashed potatoes, fried potatoes, cake, and so on (Zhang, Fen, Yu, Hu, and Dai, 2017). Food processing can improve the shelf life of these food products, increase dietary diversity, and provide a range of attractive flavors, colors, aromas, and textures. It can

also change the form of the food for further processing (Fellows, 2009). A better understanding of the structural and physical changes that occur during potato processing is helpful for potato suppliers and manufacturers in order to provide high-quality food products.

Figure 1.1 Potato nutrition facts. (https://www.potatoes.com/item/potato-nutrition).

Mashed potato is a popular side dish served in restaurants and homes. It is consumed with a soft, fine consistency and perceptible moisture or harder, drier consistency. The texture of the cooked tubers is influenced not only by the single chemical composition of the potato, but also by the interactions among them, as well as the interaction during cooking and mashing (Peksa, Apeland, Gronnerod, and Magnus, 2002). Peksa et al. (2002) compared the consistencies of cooked mashed potato made from seven different kinds of potato. They found that the addition potato protein to cooked tubers may not only increase their nutritional value but also their consistency.

The appropriate consistency and uniform texture are the ideal characteristics of frozen/thawed mashed potatoes. The prepared mashed potato is a combination system of native potato-denatured milk protein-water-salt and an added biopolymer, so the complex interaction will affect the properties of these mixtures (Fernandez, Alvarez, and Canet, 2008). Some articles have been published on the effects of milk protein (MP), extra virgin olive oil and hydrocolloids on the consistency of mashed potatoes, which are frozen and directly thawed by microwave equipment (Alvarez, Canet, and Fernandez, 2008; Maria Dolores Alvarez, Fernandez, and Canet, 2010; MarIa Dolores Alvarez, Fernandez, Olivares, Jimenez, and Canet, 2013; Conforti, Lupano, and Yamul, 2013; Fernandez, Canet, and Alvarez, 2009). These articles find that addition of dairy protein, oil, and hydrocolloids will give a good consistency to the mashed potato product. However, these researchers focused on the effect of hydrocolloids on the properties of the mashed potato. More research still needs to be done to understand the molecular and physicochemical basis for the interaction between starches with proteins and oils in mashed potatoes. Starch is the main ingredient of potato. The interaction of PS, MP and plant oils in the mashed potato product can act as a new angle to study the physicochemical properties of potato products.

Potatoes are consumed after cooking. Food processing influences the glycemic index (GI) of potato products (Figure 1.2) (Ek, Brand-Miller, and Copeland, 2012). I*n vitro* and *in vivo* studies of different potato cultivars have shown that cooked potatoes contain a lot of the rapidly digested starch, which will be quickly absorbed by the human body, resulting in high postprandial blood glucose levels (Tian, Chen, Ye, and Chen, 2016). Compared with other processed potatoes, boiled potatoes and mashed potatoes have the highest digestibility (Gracia-Alonso and Goni, 2000). Highly

digestible food is not so popular now because there is evidence that the effect of elevated postprandial blood glucose can lead to physiological complications associated with obesity and diabetes with the consumption of carbohydrates.
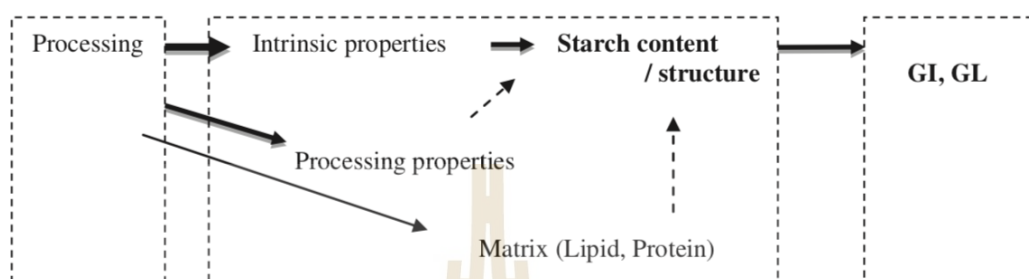
Figure 1.2 Mechanism of processing that effect glycemic Index (GI) and glycemic

load (GL) (Nayak, Berrios, and Tang, 2014).

People are interested in foods that can cause a lower glycemic response after consuming. Starch is the most important glycemic carbohydrate in foods, its digestibility has a close relationship with the increasing incidence rate of obesity and diet-related chronic diseases (Ek et al., 2012; Zaheer and Akhtar, 2016). Some additives, for example, fat or protein, can be added to meal to significantly alleviate the effect of carbohydrates on the glucose response (Ma et al., 2009; Tian et al., 2016). Hatonen et al. (2011) found that chicken breast and rapeseed oil changed the glycemic and insulinemic responses to a mashed potato-based meal. They concluded that oil and protein had an independent lowering effect on the blood glucose responses of healthy subjects to mashed potatoes (Hatonen et al., 2011).

However, the digestibility of starch in processed foods is not very clear, especially the susceptibility of complexes among starch, lipids, and proteins to enzyme decomposition, as well as the potential impact on human nutrition (Parada

and Santos, 2016). Starch digestibility in processed foods is influenced by interactions with other constituents but appear to be independent depending on the degree of starch gelatinization (Wang, Wang, Liu, Wang, and Copeland, 2017). Therefore, it is necessary to further understand the interactions among starch, lipids, and proteins and the properties of resulting complexes. In particular, little information is available on the formation of ternary complexes involving PS, MP, and plant oils.

Protein is an essential component of the human diet. The role of protein in nutrition is to provide adequate essential amino acids. MP is one of the most important proteins in the world because of its excellent nutritional value. MP is a kind of high-quality protein with a good supply of essential amino acids and high bioavailability (Smithers and Augustin, 2012). Protein in dairy products, in particular, is rich in lysine. Therefore, it can be used to supplement poor plant-derived proteins, such as cereal proteins, to greatly increase the nutritional value of the combination (Boland and Singh, 2019). Nutritional studies have shown that the bioactive peptides in MPs have very important biological functions, including antihypertensive, antioxidative, antimicrobial, immunomodulatory, and antidiabetics (Korhonen, 2009; Nongonierma, Mazzocchi, Paolella, and FitzGerald, 2017). Therefore, the food composed of MPs have significant health benefits. MP has many functional properties, which can be used in various foods to improve texture, flavor, color, and protein content. Addition of some milk during potato processing to get better products has been used for a long time (Kluge, Petutschnig, Appoldt, and Seiler, 1979). Also, many researchers showed that they had added some MP or whole milk when they prepared the potato products, especially mashed potato (M Dolores Alvarez, Canet, and Fernandez, 2007; Maria Dolores Alvarez, Fernandez, and Canet, 2009; Maria Dolores Alvarez, Fernandez,

Olivares, and Canet, 2010; MarIa Dolores Alvarez et al., 2013; Chen et al., 2013; McGill, Kurilich, and Davignon, 2013). However, they only used MP as a regular addition without considering the interaction between PS and MP. So far, there has been little discussion about the interaction between the starch in the potato and the protein in the milk.

Plant oils are mainly fluid hydrophobic compounds (at room temperature) obtained from milled grains from different plants such as soybean, peanut, rapeseed/canola, corn, sunflower, palm, cottonseed (O'brien, 2008). These oils are composed of lipids, mainly triacylglycerols, with different fatty acids (FAs) ramifications (Gunstone, 2011). Different types of oil have different proportions of saturated fat, polyunsaturated fat, and monounsaturated fat. Table 1.1 shows the comparison of the composition of dietary plant oils (Vaclavik and Christian, 2008). Edible plant oils are used in food, both in cooking and as supplements. Soybean oil (SBO) is a plant oil extracted from soybean seeds. It is one of the most widely consumed edible oils. The main component of refined SBO is triacylglycerol (TAG), which accounts for 99% (Gunstone, 2011). SBO have a higher content of linoleic acid and linolenic acid. These are all essential FAs and are therefore of dietary importance. TAG is the main neutral lipid in SBO. Commercial SBO consists of 59% polyunsaturated FAs, 25% monounsaturated FAs, and 16% saturated FAs (Dorni, Sharma, Saikia, and Longvah, 2018). The essential FAs linoleic acid (18:2n-6) and alpha-linolenic acid (18:3n-3) accounted for 89% and 11% of the total essential FAs respectively (Gunstone, 2011). SBO contains slightly less n-6 linoleic acid than corn and sunflower, but more than twice as much rapeseed oil. Soybean and rapeseed oil are the only two common vegetable oils that contain abundant n-3 linolenic acid.

Table 1.1 Comparison of the composition of dietary plant oils.

Dietary plant oils	Fatty acid (FAs) content normalized to 100%			
	Saturated fat	Polyunsaturated	Alpha Linoleinc	Monounsaturated fat
Canola oil	7%	21%	11%	61%
Sunflower oil	10%	71%	1%	16%
Corn oil	13%	57%	1%	29%
Olive oil	15%	9%	1%	75%
Soybean oil	15%	54%	8%	23%
Peanut oil	19%	33%	Trace	48%
Cottonseed oil	27%	54%	Trace	19%
Palm oil	51%	10%	Trace	39%
Coconut oil	91%	-	2%	7%

Source: POS Pilot Plant Corporation, Saskatoon, Saskatchewan, Canada June 1994 (Vaclavik and Christian, 2008).

The interactions between food components play an important role in determining the structure, physicochemical properties, and *in vitro* digestion properties of food processing as well as the texture of finished products (Gaonkar and McPherson, 2016). In mashed potato products, PS, protein in milk, and plant oil are three main food components. Their functionalities not only determine the nutritional values of the products but also determines the textural characteristics and shelf life of the product (María Dolores Alvarez, Fernández, Olivares, and Canet, 2012; Álvarez, Fernández, Olivares, Jiménez, and Canet, 2013). It is important to understand the functionality and interactions of food ingredients in a real food system for improving food product quality and designing new food products with desired properties.

However, understanding of the molecular and physicochemical basis of the interactions among starch, proteins and oils in food is still weak, which hinders the development of more healthy food (Chao et al., 2018). In addition, there has been little discussion about the relationship between ternary interactions with the digestibility of the food complexation. In order to determine the key parameters controlling the formation of a complex, it is still necessary to further characterize the complexation mechanism, which will eventually help to expand its production. Previous studies have not investigated the ternary complex using PS. Compared with other commercial starches, PS has some unique properties, which are directly attributable to its granular and molecular structures, including very large and smooth granules, high covalent phosphate content, high-molecular-weight amylose and long amylopectin chains (Bertoft and Blennow, 2016). This study provided an important opportunity to advance understanding of the interaction between PS, MP, and plant oils. Moreover, the relationship between the ternary mixture system's structure, physicochemical properties with its digestibility will be systematically studied.

Therefore, this study intends to use PS, MP, and SBO as the raw materials to build a model system of mashed potato product. Binary and ternary mixtures will be prepared by using gelatinized potato starch (GPS) mixed with MP, SBO, individually and with the combination of MP and SBO, via the homogenization process. The morphological and physicochemical properties of binary or ternary mixture system of GPS, MP and SBO will be investigated. Then the structural bonding of binary or ternary mixture systems of GPS, MP and SBO will be studied by Fourier transform infrared (FTIR) spectroscopy, Raman, and X-ray diffraction (XRD) analyses. Finally, the microstructure, rheological characteristics and digestibility properties of binary or

ternary mixture system of GPS, MP and SBO during the vitro digestion process will be studied. This study will lay a theoretical foundation for the future application and development of mashed potato products. The study of food ingredient interactions can supply meaningful information for the food industry and enhance the understanding of functionalities of food ingredients in real food systems.

1.2 Research objectives

The objectives of this thesis are:

1.2.1 To build a simulated system derived from a mashed potato product.

1.2.2 To better understand the interaction between PS, MP, and SBO and gain a knowledge of the structure and physicochemical properties of ternary-component mixtures and binary-component mixtures.

1.2.3 To investigate the structure and physicochemical properties of ternary-component mixtures and binary-component mixtures during *in vitro* simulated digestion.

1.2.4 To better understand the PS, protein, and oil digestibility properties of ternary-component mixtures and binary-component mixtures during *in vitro* simulated digestion.

1.3 Research hypothesis

The interaction between GPS, MP, and SBO will alter the structure and physicochemical properties of the ternary macronutrient component mixtures. The structure and physicochemical properties of the simulated mashed potato will change during simulated digestion. Furthermore, changes in the molecular structure and

physicochemical properties of ternary macronutrient components will affect the *in vitro* digestibility of starch, protein and oil in the products.

1.4   Scope of this study

PS and SBO were purchased from a market in Nakhon Ratchasima Province, Thailand. Casein (CA) and whey protein (WP) were provided by Vicchi Enterprise Co., Ltd. (Bangkok, Thailand) and Shanghai Yuanye Biological Technology Co., Ltd. (Shanghai, China). PS, MP, and SBO was used as the raw materials to build a model mashed potato product system. Binary and ternary mixtures were prepared by using GPS mixed with MP and SBO, both individually and in combination, via the homogenization process.

The mixtures will be prepared using single, binary and ternary component complex for contrast with 11 samples in total. To better understand the formation and structures of the ternary component complex, the changes in the structure and physicochemical properties of the ternary-component complex will be monitored. The morphological properties of the ternary component complexes were probed using confocal laser scanning microscopy (CLSM). Physicochemical properties will be characterized by rheological tests, including steady shear and oscillatory shear. Meanwhile, the multiscale structures of the ternary complexes will be characterized by a combination of XRD, FTIR, and Raman spectroscopy.

After characterization of the properties of the ternary mixture and the binary mixture, the structure, physicochemical, and digestibility properties of the ternary mixture and the binary mixture will be investigated during the simulated digestion. The starch digestibility of the samples was probed by *in vitro* digestibility and

estimated GI. The protein and oil digestibility of samples also will be probed by *in vitro* digestibility. The morphological and rheological properties of the samples will be investigated during the *in vitro* digestibility study.

1.5   Expected results

Results from this research will lead to develop a fundamental understanding of the interactions of starch with proteins and lipid materials in a simulated mashed potato system. These macronutrients may delay starch digestion and have a lower gastrointestinal reaction, as well as affect protein and lipid digestion. This basic knowledge will contribute to a better understanding of the structures and physicochemical properties of binary and ternary mixtures and their relationship with digestibility. In addition, their rheological properties can affect the digestion rate. The knowledge gained can help guide future food design for food products containing starch, protein, and vegetable oil.

1.6   References

A, W. J., and Poats, S. V. (2009). **The potato in the human diet**: Cambridge University Press.

Alvani, K., Qi, X., Tester, R. F., and Snape, C. E. (2011). Physico-chemical properties of potato starches. **Food Chemistry.** 125(3): 958-965.

Alvarez, M., Canet, W., and Fernandez, C. (2008). Effect of addition of cryoprotectants on the mechanical properties, colour and sensory attributes of fresh and frozen/thawed mashed potatoes. **European Food Research and Technology.** 226(6): 1525-1544.

Alvarez, M. D., Canet, W., and Fernandez, C. (2007). Effect of modified starch concentration and freezing and thawing rates on properties of mashed potatoes (cv. Kennebec). **Journal of the Science of Food and Agriculture.** 87(6): 1108-1122.

Alvarez, M. D., Fernandez, C., and Canet, W. (2009). Enhancement of freezing stability in mashed potatoes by the incorporation of kappa-carrageenan and xanthan gum blends. **Journal of the Science of Food and Agriculture.** 89(12): 2115-2127.

Alvarez, M. D., Fernandez, C., and Canet, W. (2010). Oscillatory rheological properties of fresh and frozen/thawed mashed potatoes as modified by different cryoprotectants. **Food and Bioprocess Technology**. 3(1): 55.

Alvarez, M. D., Fernández, C., Olivares, M. D., and Canet, W. (2012). A rheological characterisation of mashed potatoes enriched with soy protein isolate. **Food Chemistry**. 133(4): 1274-1282.

Alvarez, M. D., Fernandez, C., Olivares, M. D., and Canet, W. (2010). Rheological behaviour and functionality of inulin-extra virgin olive oil-based mashed potatoes. **International Journal of Food Science & Technology.** 45(10): 2108-2118.

Álvarez, M. D., Fernández, C., Olivares, M. D., Jiménez, M. J., and Canet, W. (2013). Sensory and texture properties of mashed potato incorporated with inulin and olive oil blends. **International Journal of Food Properties**. 16(8): 1839-1859.

Bertoft, E., and Blennow, A. (2016). **Structure of potato starch** *Advances in Potato Chemistry and Technology (Second Edition)*: Elsevier. 57-73.

Boland, M., and Singh, H. (2019). **Milk proteins: from expression to food**: Academic Press.

Chao, C., Cai, J., Yu, J., Copeland, L., Wang, S., and Wang, S. (2018). Toward a better understanding of starch-monoglyceride-protein interactions. **Journal of Agricultural and Food Chemistry.** 66(50): 13253-13259.

Chen, J., Pitchai, K., Birla, S., Gonzalez, R., Jones, D., and Subbiah, J. (2013). Temperature-dependent dielectric and thermal properties of whey protein gel and mashed potato. **Transactions of the ASABE.** 56(6): 1457-1467.

Conforti, P. A., Lupano, C. E., and Yamul, D. K. (2013). Rheological, thermal and sensory properties of whey protein concentrate/pectin-fortified mashed potatoes made from dehydrated flakes. **International Journal of Food Science & Technology**. 48(5): 1035-1040.

Dorni, C., Sharma, P., Saikia, G., and Longvah, T. (2018). Fatty acid profile of edible oils and fats consumed in India. **Food Chemistry.** 238: 9-15.

Ek, K. L., Brand-Miller, J., and Copeland, L. (2012). Glycemic effect of potatoes. **Food Chemistry.** 133(4): 1230-1240.

Fellows, P. J. (2009). Food processing technology: principles and practice: Elsevier.

Fernandez, C., Alvarez, M., and Canet, W. (2008). Steady shear and yield stress data of fresh and frozen/thawed mashed potatoes: Effect of biopolymers addition. **Food Hydrocolloids.** 22(7): 1381-1395.

Fernandez, C., Canet, W., and Alvarez, M. (2009). Quality of mashed potatoes: effect of adding blends of kappa-carrageenan and xanthan gum. **European Food Research and Technology.** 229(2): 205.

Gaonkar, A. G., and McPherson, A. (2016). **Ingredient interactions: effects on food quality**: CRC Press.

Gracia-Alonso, A., and Goni, I. (2000). Effect of processing on potato starch: in vitro availability and glycaemic index. **Starch-Stärke.** 52(2-3): 81-84.

Gunstone, F. (2011). Vegetable oils in food technology: composition, properties and uses: John Wiley & Sons.

Hatonen, K. A., Virtamo, J., Eriksson, J. G., Sinkko, H. K., Sundvall, J. E., and Valsta, L. M. (2011). Protein and fat modify the glycaemic and insulinaemic responses to a mashed potato-based meal. **British journal of nutrition**. 106(2): 248-253.

King, J. C., and Slavin, J. L. (2013). White potatoes, human health, and dietary guidance. **Advances in Nutrition.** 4(3): 393S-401S.

Kluge, G., Petutschnig, K., Appoldt, F. S., and Seiler, G. (1979). Process for the preparation of potato puree in flake form and product thereof: Google Patents.

Korhonen, H. J. (2009). Bioactive components in bovine milk. **Bioactive components in milk and dairy products**: 15-42.

Leivas, C. L., da Costa, F. J. O. G., de Almeida, R. R., de Freitas, R. J. S., Stertz, S. C., and Schnitzler, E. (2013). Structural, physico-chemical, thermal and pasting properties of potato (*Solanum tuberosum* L.) flour. **Journal of Thermal Analysis and Calorimetry.** 111(3): 2211-2216.

Ma, J., Stevens, J. E., Cukier, K., Maddox, A. F., Wishart, J. M., Jones, K. L., Rayner, C. K. (2009). Effects of a protein preload on gastric emptying, glycemia, and gut hormones after a carbohydrate meal in diet-controlled type 2 diabetes. **Diabetes Care**. 32(9): 1600-1602.

McGill, C. R., Kurilich, A. C., and Davignon, J. (2013). The role of potatoes and potato components in cardiometabolic health: a review. **Annals of Medicine.** 45(7): 467-473.

Mu, T., Sun, H., and Liu, X. (2017). **Potato staple food processing technology**: Springer.

Nayak, B., Berrios, J. D. J., and Tang, J. (2014). Impact of food processing on the glycemic index (GI) of potato products. **Food Research International**. 56: 35-46.

Nongonierma, A. B., Mazzocchi, C., Paolella, S., and FitzGerald, R. J. (2017). Release of dipeptidyl peptidase IV (DPP-IV) inhibitory peptides from milk protein isolate (MPI) during enzymatic hydrolysis. **Food Research International**. 94: 79-89.

O'brien, R. D. (2008). Fats and oils: formulating and processing for applications: CRC press.

Parada, J., and Santos, J. L. (2016). Interactions between starch, lipids, and proteins in foods: Microstructure control for glycemic response modulation. **Critical Reviews in Food Science and Nutrition.** 56(14): 2362-2369.

Peksa, A., Apeland, J., Gronnerod, S., and Magnus, E.M. (2002). Comparison of the consistencies of cooked mashed potato prepared from seven varieties of potatoes. **Food Chemistry.** 76(3): 311-317.

Singh, J., and Kaur, L. (2016). **Advances in potato chemistry and technology**: Academic press.

Smithers, G. W., and Augustin, M. A. (2012). **Advances in dairy ingredients** (Vol. 79): John Wiley & Sons.

Tian, J., Chen, J., Ye, X., and Chen, S. (2016). Health benefits of the potato affected by domestic cooking: A review. **Food Chemistry.** 202: 165-175.

Vaclavik, V. A., and Christian, E. W. (2008). **Fat and oil products** *Essentials of Food Science* : Springer. 273-309.

Wang, S., Wang, S., Liu, L., Wang, S., and Copeland, L. (2017). Structural orders of wheat starch do not determine the in vitro enzymatic digestibility. **Journal of Agricultural and Food Chemistry.** 65(8): 1697-1706.

Zaheer, K., and Akhtar, M. H. (2016). Potato production, usage, and nutrition-a review. **Critical Reviews in Food Science and Nutrition.** 56(5): 711-721.

Zhang, H., Fen, X., Yu, W., Hu, H.h., and Dai, X.f. (2017). Progress of potato staple food research and industry development in China. **Journal of integrative agriculture.** 16(12): 2924-2932.
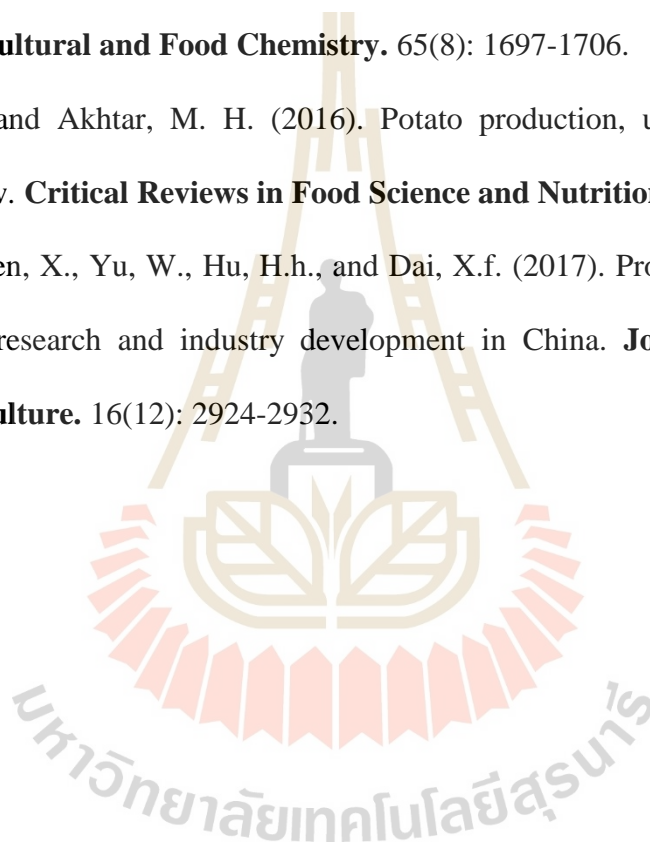
CHAPTER II

LITERATURE REVIEWS

2.1   Mashed potato

As a food crop for human consumption, potato tubers are fourth in the world, only behind rice, maize and wheat (A and Poats, 2009). Cultivated potatoes spread from the Andes in South America to 160 countries around the world. As a food, potatoes can be prepared in many ways: whole or cut, skin or peeled, with or without seasoning. The only requirement is to make the starch granules swell by cooking them. Common potato dishes include mashed potatoes, whole baked potatoes, boiled or steamed potatoes, French fries or chips, home fries, hash browns, potato dishes, and potato snacks (Guenthner, 2001). Potato cubes are also commonly used as a stew ingredient.

Mashed potato is a dish made by mashing boiled potatoes, usually with added milk, oil, salt, and pepper (Álvarez, Fernández, Olivares, Jiménez, and Canet, 2013; Joyner and Meldrum, 2016). It is generally served as a side dish to meat or vegetables. There are many ways to prepare mashed potatoes. It can be made directly from fresh potatoes and then quickly frozen into frozen mashed potatoes. The frozen mashed potatoes can be conveniently sold in shopping malls. It also can be formed by mixing the whole dehydrated potato powder with hot water. The preparation of fresh mashed potato is usually to clean, peel and cut potato tubers, and then cook and mash them (Mu, Sun, and Liu, 2017). The product can be homogenized through stainless steel

screen, or the potato mash can be prepared directly with the mud machine. Mashed potato is characterized by a simple production process, low production cost, rich nutrition, and good texture and flavor. The fresh mashed potato almost retains all the nutrition of potato, but it has the faint smell of potato and soft with glutinous taste. Another way to make mashed potatoes is to use whole potato powder mix with water. According to the different dehydration and drying processes, the whole powder can be divided into snowflake whole powder and granule whole powder (Hadziyev and Steele, 1979; Lamberti, Geiselmann, Conde-Petit, and Escher, 2004). Snowflakes whole powder is made of potato flakes with different thicknesses and irregular sizes by a drum drying process. The whole potato powder is produced by a hot air-drying process and is in the form of monomer particles or several aggregates. The shelf life of mashed potatoes made in this way can reach 2 years. It basically maintains the integrity of cells during processing and can be restored after rehydration. It has the flavor of potato mash and the taste of sand. However, the process of drying and rehydration also lead to the deterioration of texture and flavor, as well as the destruction and loss of some nutrients.

In recent years, the research on the drying technology of potato powder has been very mature, and there are many studies on the frozen storage of potato (Alvarez, Fernández, Olivares, and Canet, 2012; Neilson, Pahulu, Ogden, and Pike, 2006). However, there are few studies on the interaction between the food components in the preparation of mashed potato. The ingredients of mashed potatoes include potato, milk, fat and conditioning, while the main content of potatoes is PS. This section reviewed the main components of mashed potatoes.

2.1.1 PS and its properties

Potatoes are rich in carbohydrates, providing energy but little fat. Starch is the main component of potato tubers, amounting to 15-20% of its weight (Raigond, Singh, Dutt, and Chakrabarti, 2020). Therefore, starch is considered as the major factor affecting the functionality of potatoes for food applications (Bertoft and Blennow, 2009). Consumption of fresh potatoes has declined, while the popularity of processed potato products has increased. In industrial applications, compared with most other starch types, processed PS is considered as a very pure starch due to its low protein and lipid content (Bertoft and Blennow, 2016). PS is a widely used raw material in the manufacture for both food and non-food products. It has its own unique physicochemical, thermal, and rheological characteristics, and is very mild, easy to integrate into food recipes. The functional characteristics of PS depend on its physical and chemical properties including granule size distribution, average granule size, amylose/amylopectin ratio, and mineral content (Kaur, Singh, and Singh, 2005).

2.1.1.1 PS chemistry and structure

In the potato tuber, starch was found to be a unique granule with a diameter of approximately 10-100 μm (Hoover, 2001). PS granules are oval, cuboidal, or irregular in shape (Fig. 2.1). A typical birefringence cross was observed under polarized light in a microscope (Cui, 2005). Corn starch granules are angular-shaped, while rice starch granules are pentagonal and angular. When observed under a scanning electron microscope (SEM), the surfaces of the starch granules of wheat, rice, and corn were less smooth than PS granules (Singh, Singh, Kaur, Sodhi, and Gill, 2003).

(a)   (b)
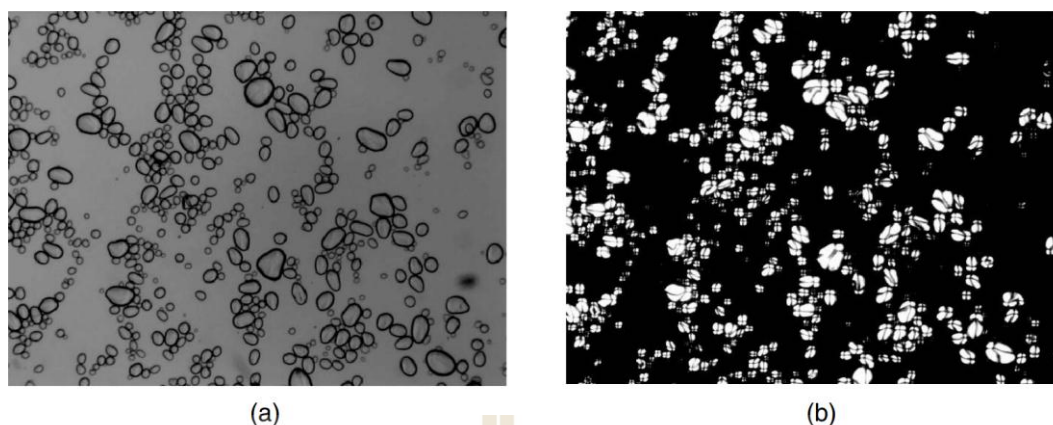
Figure 2.1   Potato starch granules observed under microscope without (a) polarized
light and with (b) polarized light (Singh et al., 2003).

PS granules are composed of two main molecules, amylose and amylopectin, which are polymers of α-D-glucose units in the $^4C_1$ conformation (Kaur, Singh, McCarthy, and Singh, 2007). In starch granules, amylose and amylopectin molecules are arranged into granules in the form of alternate semi-crystalline and amorphous layers, forming a growth ring (Fig. 2.2). Amylopectin is the main component of starch while amylose is a minor component of starch. Amylose is essentially a linear polymer consisting of degree of polymerization (DP) chains on the order of 2000-5000 residues (Hoover, 2001). However, some branches are found in the structure and there are mainly two types of this component, namely linear and branched amylose. The crystallinity of the starch is mainly attributed to the regular arrangement of short amylopectin chains, the formation of double helices, and they packed into one of the well-known A, B, or C polymorphs (Pérez and Bertoft, 2010). The amorphous regions of the semi-crystalline and amorphous layers consist of amylose and unordered amylopectin branches (Jenkins and Donald, 1995; Kaur et al., 2007). PS is a B-type crystalline (Singh et al., 2003).
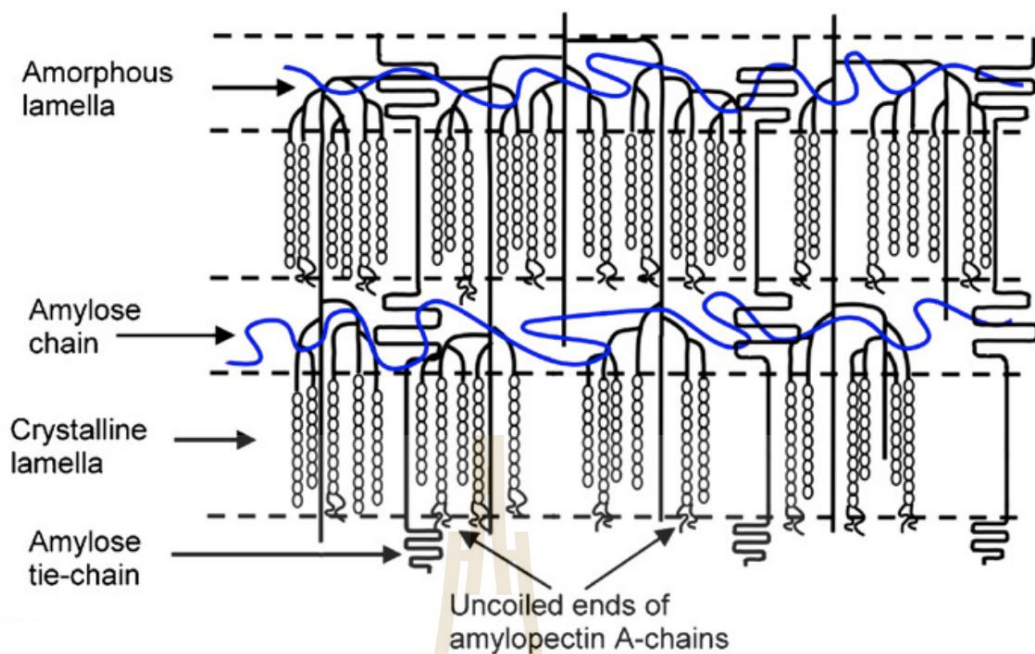
Figure 2.2 Schematic presentation of amylose and amylopectin localization in amylopectin clusters for potato starches (Kozlov, Blennow, Krivandin, and Yuryev, 2007).

In addition to polysaccharide components, PS also contains a very small amount of non-carbohydrate nature. Starch contains some minor components, such as ash, protein, lipid, phosphorus, and other minerals in their granular state. Less than 0.5% of the granules are proteins, which apparently participate in starch synthesis (Yusuph, Tester, Ansell, and Snape, 2003). There is almost no lipid in PS, which is in the same with some other tuber and root starches, but lipid can be found in many other starches, especially from cereals (Hizukuri, Tabata, and Nikuni, 1970; Hoover, 2001). PS also contains phosphorus in the form of phosphate covalently linked to the amylopectin component (Hizukuri et al., 1970). In some cases, these minor components significantly could affect the physicochemical properties of starch (Absar et al., 2009). Trace amounts of different cations, mainly potassium, were also

described as minor components in PS granules. This was obviously coordinated with phosphate groups (Blennow, Sjöland, Andersson, and Kristiansson, 2005).

2.1.1.2 PS swelling power and solubility

When starch molecules are heated in excess water, their crystal structure is destroyed and the water molecules are connected by hydrogen bonds to the exposed hydroxyl groups of amylose and amylopectin, causing the granule particles to swell and increases solubility (Hoover, 2001). The degree of swelling for starch mainly depends on the content and crystallinity of amylose, while the solubility of starch mainly depends on the content of amylose (Srichuwong, Sunarti, Mishima, Isono, and Hisamatsu, 2005). In general, the higher the amylopectin content, the better the expansive ability of starch, and the longer the average chain length of amylopectin, the better the expansive power of starch. The higher the lipid content in starch, the lower the swelling power and amylopectin solubility, while the effect of phosphorus content on the swelling power and solubility has the opposite relationship (Karim et al., 2007; Tester and Morrison, 1990). The average expansibility of PS is much higher than that of cereal starch. Corn and wheat granules can swell up to 30 times while PS granules can swell up to 100 times their original size (Singh et al., 2003). The reason why PS has a higher swelling power and solubility might be related to the existence of large number of phosphate groups in the amylopectin molecules (Kaur et al., 2007). The repulsion between phosphate groups on adjacent chains increased hydration by weakening the degree of bonding within the crystal domain. PS granules with a small particle size had a stronger hydration and expansion ability than those with a large particle size, which was mainly due to the higher specific surface area of the PS granules with their small particle size (Singh, Colussi, McCarthy, and Kaur, 2016).

Amylose could play an important role in suppressing initial swelling because swelling progressed more quickly after the first amylose leached out (Singh, Colussi, McCarthy, and Kaur, 2016). The increase in starch solubility, accompanied by an increase in suspension clarification, was thought to be the result of particle expansion, allowing amylose to leach out. The particles became more and more susceptible to shear collapse as they expanded and release soluble material as they collapsed. Hot starch paste was a mixture of enlarged granules and granule fragments, as well as colloidal and molecularly dispersed starch granules (Uarrota et al., 2013).

The mixture of expanded and crushed particles depended on the plant source of the starch, water content, temperature, and shearing during heating (Varatharajan et al., 2011). The degree of leaching of soluble substances depended primarily on the lipid content of the starch and the ability of the starch to form amylose -lipid complexes since the formation of amylose-lipid complexes could prevent the leaching of amylose (Morrison, Tester, Snape, Law, and Gidley, 1993). Cereal starch contained enough lipids to form a saturated lipid complex with 7-8% amylose in starch (Singh, Colussi, McCarthy, and Kaur, 2016). As a result, the maximum leached amylose was about 20% of the total starch (Tester and Morrison, 1990). The high solubility of PS might be due to the absence of lipids and the lack of starch-lipid inclusion complexes.

2.1.1.3 Starch pasting/rheological Properties

When starch is cooked, the flow behavior of the starch slurry changes significantly with each stage as the suspension becomes swollen granules, then partially disintegrated granules, and finally a dispersion of molecularly dispersed granules. The cooked product is called starch paste (Liu, 2005). Pasting is defined as the state of starch after gelatinization. During the gelatinization process, the starch

granules swelled to several times of their original size and then ruptured, while the amylose leached out and forms a three-dimensional (3D) network (Jenkins and Donald, 1998). With changes in temperature, concentration, and shear rate, starch could exhibits a unique viscous behavior (Nurul, Azemi, and Manan, 1999).

The paste curve of this process can be measured by the Brabender viscometer or a rapid viscosity analyzer (RVA) (Batey and Curtin, 2000; Lee and Purdon, 1969; Liu, 2005). These instruments are configured to simulate the heating and cooling profile of actual processes. The height of the peak for a given concentration reflects the particle's ability to expand freely before physical breakdown. PS had a higher swelling property than cereal starch, and it was not easily broken-down during cooking (Srichuwong et al., 2005). However, the shape of the peak was affected by the initial concentration of the starch suspension. The increase in viscosity during the cooling process showed that the various components of the hot paste (granule fragments, swollen starch granules, colloidally dispersed and molecularly dispersed starch molecules, rate of amylose exudation) were related to the decrease in temperature (Gebre-Mariam, Abeba, and Schmidt, 1996).

The dynamic rheometer allows continuous evaluation of the dynamic modulus during the temperature and frequency sweep test of the starch

suspension (Kaur, Singh, and Sodhi, 2002; Rosalina and Bhattacharya, 2002). The elastic modulus (G') (storage moduli) is a measure of energy stored in the material and recovered from each cycle, while the viscous modulus (G'') (loss modulus) is a measure of energy dissipated or lost per cycle of sinusoidal deformation (Ferry, 1980). The ratio of the energy loss per cycle to the stored energy can be defined by the loss factor (*tan δ*) which is a parameter that indicates the degree of

elasticity of a system. On the dynamic rheometer, the G' of starch gradually increased at a certain temperature, reaching a maximum value (G' peak) and then decreased as the temperature continues to increase (Singh and Singh, 2001). The initial increase in G' was due to the swelling of the starch granules to fill the available volume of the entire system, forming a 3D network of swollen granules. As the temperature further increased, the decrease in G' indicated that the gel structure had been destroyed during the extended heating time. This destruction was due to the melting of the remaining crystalline regions in the expanded starch granules, which deformed and loosened the granules (Eliasson, 1986).

The rheological properties of starch were affected by many factors, such as the ratio of amylose/amylose, the phosphate monoester content, the proportion of long amylopectin branch chains, starch concentration, shear force and strain, and temperature (Eerlingen, Jacobs, Block, and Delcour, 1997; Hermansson and Svegmark, 1996; Vamadevan and Bertoft, 2015). Singh et al. (2007) reported that PS with higher amylose content had a higher G' value in the temperature scanning test. The G' and G'' peaks of corn starch were lower than those of PS. The higher phosphate monoester content and the lack of lipids and phospholipids in PS might also be the reasons for the high G' and G'' (Singh, Kaur, and McCarthy, 2007). The formation of amylose-lipid complexes during corn starch gelatinization reduced G' and G'' (Singh, Singh, and Saxena, 2002).

2.1.1.4 Starch gelatinization and retrogradation

Gelatinization refers to the destruction of the molecular order of starch granules when they are heated by excess water. This is an expansion driven process, which leads to the ordered transition of starch molecules, irreversible granule

expansion, birefringence loss, and crystallinity loss (Donovan, 1979). The gelatinization

phenomenon begins at the hilum of the granule and swells rapidly to the surrounding

area. Gelatinization initially occurs in the amorphous regions, rather than in the

crystalline region of the granules, where the hydrogen bond weakens. The collapse of

the crystalline order within the starch granules is characterized by irreversible changes

in properties, such as granule swelling, gelatinization, loss of crystalline order, loss of

optical birefringence, uncoiling, and dissociation of double helices, and starch

solubility (Hoover, 2001).

The gelatinization transition temperatures (onset, T_0; peak, T_p;

conclusion, T_c) and gelatinization enthalpy (ΔH_{gel}) measured by differential scanning

calorimetry (DSC) were related to the degree of crystallinity. The T_0 reflected the

initiation of the gelatinization process, followed by a peak and conclusion

temperature. After T_c, all amylopectin double helices have been dissociated, but the

swollen granule structures still retained until more widely used in temperature and

shear (Tester and Debon, 2000). A high degree of crystallinity provided structural

stability, making the granule more resistant to gelatinization, leading to higher

transition temperatures, and was influenced by the chemical composition of the starch

(Kong, Zhu, Sui, and Bao, 2015).

Starches from different botanical sources showed different transition

temperatures and gelatinization enthalpy under different compositions. The gelatinization

enthalpy value of various starches was affected by the granule shape, the percentage

of large, small granules, and the presence of phosphate esters effect (Singh, McCarthy,

and Singh, 2006). The small and oval granules in PS exhibited lower storage and loss

modulus and higher tanδ than large and irregular or cuboidal shaped granules (Singh

and Singh, 2001). The gelatinization and swelling properties were partly controlled by the molecular structure of amylopectin (molecular weight, unit chain length, polydispersity, and extent of branching), granule architecture (crystalline-to-amorphous ratio), and starch composition (amylose-to-amylopectin ratio and phosphorus content) (Singh and Singh, 2001, 2003; Tsai, Li, and Lii, 1997). Shewmaker et al. (1994) reported the low viscosity of starch paste made from potato genotypes with low amylose contents.

The cooling of the starch pastes resulted in the aggregation of amylose molecules, leading to a gel formation (Miles, Morris, Orford, and Ring, 1985). These collective processes occured in starch pastes or solutions. As a result, they became less soluble, which was called retrogradation. During retrogradation, amylose forms double-helical associations of 40-70 glucose units (Jane and Robyt, 1984), while amylopectin recrystallized through the outermost short branch associations (Batres and White, 1986; Ring et al., 1987). The crystalline form of retrograded starch is different from that of natural starch granules and may be weaker than the latter because of the recrystallization sequence of amylopectin in the process of retrogradation is weaker than that of native raw starches.

The rate of retrogradation was affected by the starch source, amylose and amylopectin concentration, molecular size/shape, starch/water ratio, temperature, pH, and non-starch components (Singh et al., 2003; Sodhi and Singh, 2003; Yu, Ma, and Sun, 2009). Traditionally, the higher the amylose content, the greater the retrogradation tendency in starches (BeMiller, 2007), but amylopectin and intermediates also played an important role in the starch retrogradation process during refrigerated storage (Yamin, Lee, Pollak, and White, 1999). Amylopectin with longer

chain length also accelerated retrogradation (Yuan, Thompson, and Boyer, 1993). Freezing and thawing accelerated retrogradation (Yuan and Thompson, 1998). In the food industry, starch retrogradation is mostly seen to be associated with the texture and digestibility of foods.

2.1.2 MP

Milk is the fluid secreted by the female of all mammals, and it fully meets the nutritional needs of newborns (O'Mahony and Fox, 2014). Milk is a complex mixture of lipids, proteins, and carbohydrates, as well as minerals (Swaisgood, 2007). In addition, milk contains small amounts of components derived from cell synthesis. Milk also has many physiological functions, including immunoglobulins, enzymes, enzyme inhibitors, growth factors, hormones, and antimicrobials (Mohanty, Mohapatra, Misra, and Sahu, 2016).

Milk contains several proteins, usually grouped into two groups, CA and WP. CA is a protein that is insoluble at pH 4.6 and WP is a protein that remains in solution at pH 4.6 (Smithers and Augustin, 2012). The protein content of normal milk is expressed as N×6.38. Milk contains 30-35 g protein per liter. CA is the main component of MP, accounting for about 78% w/w of the total protein in milk. It has a molecular mass of 20 to 25 kDa. CA is composed of four major components: α_{S1}-casein and α_{S2}- caseins, β-casein, and κ-casein, in an approximate ratio of 40: 10: 40: 10 (O'Kennedy, 2011). In milk, CA mainly exists in macromolecular complexes in the form of micelles. Micelles are spherical complexes with diameters ranging from 50 to 600 nm, with an average of 120 nm (Phillips and Williams, 2011). CA is 92% protein and 8% inorganic salt. The main composition of WP including β-lactoglobulin, α-lactalbumin, bovine serum albumin (BSA), immunoglobulin, etc. In

addition, there are many low abundances of WP active protein such as lactoferrin, lysozyme, lactoperoxidase, a variety of growth factors, etc. (Brumini, Criscione, Bordonaro, Vegarud, and Marletta, 2016; Gupta, Jadhav, Gunaware, and Shinde, 2016).

As proteins, CA and WP have some of the basic functional properties of proteins, such as emulsification, foaming, and hydration (Damodaran and Parkin, 2017). Many studies have reported the functional properties of bioactive ingredients in dairy products. These functional properties include antimicrobial, anti-hypertension, anti-oxidation, anti-cytotoxic, immunomodulatory, and so on (Park and Nam, 2015).

2.1.3 SBO

Soybeans are the world's leading source of vegetable protein and vegetable oil. Soybean has been accounted for 70% of protein powders used globally (Soystat 2020, http://www.soystats.com). Currently, high protein and high oil content soy has been processed into soy food and cooking oil (Hassan, 2013). Soybean seeds contain about 40 percent protein and 20 percent oil. SBO has been accounted for 80% of the fat in most margarine and 65% of the fat in most shortening (Dupont, White, and Feldman, 1991; Hammond, Johnson, Su, Wang, and White, 2005).

SBO is extracted by solvent extraction or mechanical pressing to recover various types of lipids. It consists mainly of neutral lipids, including triacyl, diacyl, monoglycerides, free fatty acids (FFAs), and polar lipids (e.g., phospholipids) (Gunstone, 2011). It also contains small amounts of unsaponifiable substances, including phytosterols, tocopherols, and hydrocarbons such as squalene (Dupont et al., 1991). SBO contains trace amounts of metals in parts per million. As oil is refined, the

concentration of the minor components is reduced. The typical composition of crude and refined SBO is shown in Table 2.1.

Table 2.1 Average composition for crude and refined soybean oil.

Components	Crude oil	Refined oil
Triacylglycerols(%)	95-97	>99
Phospholipids(%)	1.5-2.5	0.003-0.045
Unsaponifiable matter (%)	1.6	0.3
Phytosterols	0.33	0.13
Tocopherols	0.15-0.21	0.11-0.18
Hydrocarbons	0.014	0.01
Free fatty acids (%)	0.3-0.7	<0.05
Trace metals (ppm)		
Iron	1-3	0.1-0.3
Copper	0.03-0.05	0.02-0.06

Source: Adapted from Pryde (Pryde, 1980).

Lipid is one of three nutrients that play an important role in food. It can provide the body with essential FAs and it is the carrier of fat-soluble vitamins (Ozturk, Argin, Ozilgen, and McClements, 2015). It is also an important flavor component in food (Forss, 1973). In addition, lipids have a variety of food technology properties. Fats and oils adhere to food during cooking, making it greasy. The addition of shortening oil to baked food can give the product crispiness, and some polar oils have good emulsification (Bouchemal, Briançon, Perrier, and Fessi, 2004;

McClements, 2015). The characteristics of oils and fats make food rich and varied in taste, for example, baked goods, margarine, ice cream, and chocolate (Akoh, 2017). SBO is a kind of oil, and it also has the unique structural and functional characteristics of oil.

2.2 Interactions among starch, protein, and lipids

2.2.1 Interactions between starch and lipids

The interaction of food components to form structures with specific properties has been well studied in binary systems, such as starch-lipids complex (Tang and Copeland, 2007). Starch is mainly composed of amylose and amylopectin. Amylose could form helical inclusion complexes with various types of lipids, both naturally and during food processing (Zabar, Lesmes, Katz, Shimoni, and Bianco-Peled, 2009). Some experimental evidence suggested that amylopectin migh

also interact with FAs (Batres and White, 1986). As indicated by many studies, the formation of amylose-lipid complexes reduced the solubility and swelling force of starch in water, changed the rheological properties of starch pastes, reduced the hardness of the gel, increased the gelatinization temperature, delayed retrogradation, and reduced susceptibility to enzymic hydrolysis (Crowe, Seligman, and Copeland, 2000; Eliasson, 1994; Goni, Garcia Alonso, and Saura Calixto, 1997; Guraya, Kadan, and Champagne, 1997).

V-type amylose crystals obtained from XRD provided a description of the structure of a starch-lipid complex. V-type amylose was fold through the extended antiparallel helix region (Zobel, French, and Hinkle, 1967). It was known that complex amylose-lipids form two structures: type I and type II (Biliaderis and Galloway, 1989). The melting temperature of type I structures was range from 10°C to

30°C which was lower than that of the melting temperatures for type II structures (Fig. 2.3). Similarly, type II structures could be detected by X-ray crystallography; while type I structures cannot be detected by using this technique, indicating that type I structures might be in an amorphous state. Amylose might form both type I and II structures, while amylopectin might only combine with a lipid through a single chain. The trend for the formation of type II structures by head charged lipids was relatively low (Ann Charlotte Eliasson and Wahlgren, 2004). If the complex was formed rapidly at low temperatures (between 70°C and 80°C), the type I complex was dominant. If the complex was formed at high temperatures, the type II ordered complexes became dominant (Ann Charlotte Eliasson and Wahlgren, 2004).

The formation of starch-lipid complexes and their chemical and physical properties were influenced by many factors, such as the type of starch (Eliasson, Finstad, and Ljunger, 1988) type of lipid (chain length, unsaturation degree) (Kaur and Singh, 2000; Zabar et al., 2009), and the media conditions (temperature, pH, and ionic strength). The complexes between amylose and lipids (FAs, monoacylglycerides, and lysophospholipids) might significantly change the properties and functionality of starch. Changes in starch properties and functions occurred including: the solubility and swelling capacity of starch in water decreased, the rheological properties of paste changed, the gelatinization temperature is increased, the retrogradation was retarded, and the susceptibility to enzymatic hydrolysis decreased (Copeland, Blazek, Salman, and Tang, 2009).
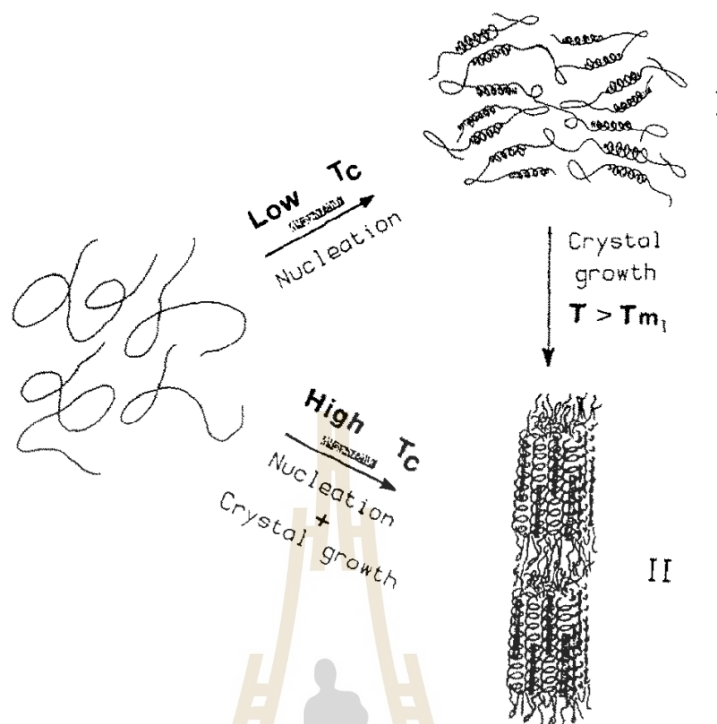
Figure 2. 3 Generalized mechanism for amylose-lipid complex-formation from dilute solutions which can account for the properties and postulated morphological features of Forms I and II (Biliaderis and Galloway, 1989).

Tang et al. (2007) systematically investigated the degree of complex formation between FAs and amylose in gelatinized wheat starch and its rheological properties. Their results indicated that the process was dependent on the type and quantity of FAs. Compared with unsaturated FAs, saturated FAs form a more ordered structure within the lamella (Zabar et al., 2009). With an increase in the unsaturation of FAs, the particle sizes of the complex became higher and broader (Lesmes, Cohen, Shener, and Shimoni, 2009). The chain length and degree of unsaturation of FAs affected the structure and functional properties of starch-fatty acid complexes (Wang, Wang, Yu, and Wang, 2016).

2.2.2   Interaction between starch and protein

Starch and protein are two important components of food and the study of the interactions between them is helpful to improve or modify the functional properties of starch and protein. The interaction between starch and protein is mainly driven by electrostatic and Van der Waals forces, as well as by hydrogen bonds and hydrophobic interactions (Jamilah, Mohamed, Abbas, Rahman, et al., 2009). Three different situations could result from mixing starch and protein in water: (1) a homogeneous and stable system in which the macromolecules do not interact or alternatively they form of soluble complexes, (2) a complex two-phase system in which starch and protein are in the same concentrated phase due to electrostatic interactions and they form insoluble complexes, and (3) a two-phase separation system in which starch and protein are incompatible so they remain at different phases (Sjoo and Nilsson, 2017).

The starch-protein interaction system was mainly dependent on the macromolecular concentration, macromolecules' nature, molecular weight, ionic strength, pH, and temperature (Sjoo and Nilsson, 2017). In general, amylose and amylopectin are considered neutral macromolecules because ionizable groups are not present in their molecular structure except for amylopectin from potato, root, and tubers, which contains phosphate groups, or amylopectin from those which have been chemically modified. PS provided electrostatic interactions between PS and protein due to its anionic properties (Bertolini, Creamer, Eppink, and Boland, 2005). Grega et al. (2003) provided biodegradable complex polymers from PS and CA. PS-whey protein isolate complexes were prepared by the electrochemical method (Zaleska, Ring, and Tomasik, 2001).

Lu et al. (2016) studied the effects of starch-protein interactions on the physicochemical properties of potato starch-protein blends during processing (cooking, cooling, and reheating). This study showed that the interaction between potato starch and potato protein existing in the blended processing system affected the gelatinization and retrogradation of starch. Electrostatic complexing and hydrogen bonding might be the forces driving the interaction as evidenced by the shifted OH stretching bands ($3300 \ cm^{-1}$) with reduced peak intensity in FTIR spectrum. The DSC and dynamic viscoelasticity method showed that the protein blend ratio increased, the swelling of starch granules during the cooking process was proportionally restricted to some extent, and the retrogradation of amylopectin during the cooling process was enhanced (Lu, Donner, Yada, and Liu, 2016). In another study by Zaleska et al. (2001), they confirmed an interaction in the functional group of PS and CA by infrared spectroscopy and electrosynthesis. The results showed that there were possible interactions between the phosphate groups of the PS and the amino groups of the MP.

2.2.3 Interaction between protein and lipids

Protein is an important biopolymer in the food industry. The functionality of protein, exhibiting through such properties as gelling, emulsifying, and foaming is very important for food quality (Zayas, 2012). The types of amino acids and their sequence determined the complexity of the protein structure and their function in food systems (Damodaran, 2008). Interaction with other food components also affected the functionality of protein, such as with lipids, especially polar lipids and FFAs (Kleinschmidt, 2013). Protein-lipid interactions are common for maintaining the structure and stability of a food system.

Proteins have been known to form complexes with a variety of substances, including lipids (El-Motaal, Helmy, Taha, and Shoeb, 1998; McCann, Small, Batey, Wrigley, and Day, 2009; Pokorny et al., 1977; Pokorny, Janicek, and Davidek, 1975). Narayan et al. (1958) reported strongly bound complexes formed between oxidized linoleic acid and protein in egg albumin. Through a simple mixing process, strongly bound adsorption complexes were formed between oxidized lipids and alumina. Real food formulations which were made up of complex emulsifiers had lipids and proteins interacting at the interfaces to maintain structure and stability (Patino, Garcia, and Nino, 2001). Protein-lipid interactions were also important in wheat flour dough systems as they played a vital role in governing the bread-making quality of the flour (McCormack, Panozzo, Bekes, and MacRitchie, 1991; McCormack, Panozzo, and MacRitchie, 1991).

The major driving force of protein-lipid interactions was through electrostatic force and hydrophobic bonding mechanisms (Cornell and Patterson, 1989). The native structure of the components, ionic strength, temperature, and environmental conditions were found to play vital roles in defining these two-way interactions (Perez and Calvo, 1995). Lipid-protein complexes contributed to cause changes in digestibility, color, and flavor binding capacity of foods (Taha and Mohamed, 2004). Taha et al. (2004) also recommended protein denaturation in the presence of oxidized oil to obtain a high lipid-protein complex formation.

2.2.4 Interaction among starch, protein, and lipids

Most of the experimental studies of food ingredient interaction involve mixtures of a single food ingredient with another single food ingredient. However, the situation in a real food system is much complicated than this, as a typical food system

consists of a mixture of starch, protein, other polysaccharides, and lipophilic molecules; each of which could be involved in competitive interaction with the others (Gaonkar and McPherson, 2016). Studying the interaction between food ingredients can provide meaningful information for the food industry and improve people's understanding of the function of food ingredients in the real food systems. Starch, protein, and lipids are the three main food components in cereal-based food. Their interactions among them are of great significance to the functionality and quality of a food system. Only a few studies have reported on the functional and physicochemical property effects on the interaction between two or more components in a food system (Chen et al., 2017; Zhang, Maladen, Campanella, and Hamaker, 2010; Zhang, Maladen, and Hamaker, 2003).

In a study on the pasting properties of sorghum flour, the formation of ternary complexes among starch, protein, and FAs were described (Zhang and Hamaker, 2003). Subsequently, the interaction among starch, protein, and lipids had been studied by DSC, XRD, multi-angle laser scattering (MALLS), and high-performance size exclusion chromatography (HPSEC) (Zhang and Hamaker, 2004, 2005; Zhang et al., 2003). A ternary complex composed of amylose, WP, and FAs had been identified and its iodine binding properties were studied (Liu, Fei, Maladen, Hamaker, and Zhang, 2009). Self-assembly of a ternary complex of amylose, FAs, and WPI mixture formed by heating and cooling was investigated (Zhang, Bhopatkar, Hamaker, and Campanella, 2015). The ternary complex was able to carry a small number of molecules in the spiral lumen of the amylose helix, which had certain application prospects for delivery, nutritional health products, and for the release of hydrophobic drugs.

Recently, the effects of adding soy protein and corn oil to corn starch on the physicochemical properties of the corn starch were investigated (Chen et al., 2017). Results showed that there were more agglomerates of the granules in the ternary blends. The degree of unsaturation of FAs and chain length affected the structure of starch-protein-fatty acid complexes in the model systems (Mengge Zheng et al., 2018). The effect of protein (i.e., WPI and gelatin) on the structure of the starch-linoleic acid-protein complex was investigated (Lin, Yang, Chi, and Ma, 2020). The complexation of linoleic acid with protein significantly increased the ordered structure of starch. Linoleic acid and protein had a synergistic effect on the recombination of starch during cooling, which in turn increased the more ordered structure (short-range ordered structure, helix structure, and crystallinity) of starch. The starch type also affected the formation and the structure of starch-lipid-protein complexes, but the effect was small (Cai et al., 2021). In the presence of β-lactoglobulin, the complex of PS with lauric acid was easier than that of wheat starch and corn starch, which resulted in a small difference in the structural order of the three starch-lipid-protein complexes.

2.3   Digestibility of starch, protein, and lipids in food matrices

2.3.1   Starch digestibility in food matrices

Starch can be classified according to its digestibility, which is generally characterized by the rate and duration of the blood glucose response (Singh, Dartois, and Kaur, 2010; Singh, Kaur, and Singh, 2013). Starch could be classified according to the rate and total degree of hydrolysis as rapidly digested starch (RDS), slowly digested starch (SDS), and resistant starch (RS) (Englyst, Kingman, and Cummings, 1992). A diet containing high doses of RDS could rapidly increase blood glucose

levels in the body compared with a diet containing SDS and RS (Lehmann and Robin, 2007).

Starch is mainly hydrolyzed into glucose by the mammalian amylolytic enzymes in several steps (see Fig. 2.4). Salivary α-amylase is very effective for starch in the mouth, but it is rapidly inactivated and degraded in the gastric acid environment, so it plays a very minor role in the process of starch digestion. Starch-degrading enzymes are present in digestive fluids and the brush border of the small intestine (Kaur and Singh, 2016; Singh, Colussi, McCarthy, and Kaur, 2016a). Most of the starch hydrolysis is carried out by the pancreatic amylase, which is released in the small intestine through the pancreatic duct. α-Amylase catalyzes the hydrolysis of α-1,4 glycosidic bonds in amylose and amylopectin of starch (endo attack) (Lehmann and Robin, 2007). The linear and branched polymers of starch (amylose and amylopectin) are hydrolyzed by virtue of binding their five glucose residues adjacent to terminal reducing glucose units to specific catalytic subsites of α-amylase, and then cleaved between the second and third α-1,4-linked glucosyl residue (Gray, 1992). The final hydrolysates of amylose digestion are maltose, maltotriose, and maltotetraose. α-Amylase has no specificity for α-1,6 branch linkage in amylopectin, so their ability to break α-1,4 links near the branching point is decreased mainly by steric hindrance. The results obtained from an analysis of the intestinal contents of humans showed that the hydrolysate from amylopectin was mainly composed of dextrins or branched oligosaccharides (Kaur and Singh, 2016). The resulting oligosaccharides (maltose, maltotriose, and α-dextrins) are further hydrolyzed efficiently by the intestine brush border enzymes. The enzymes present in the human body are difficult to extract and expensive to buy. Therefore, enzymes from other mammals or microorganisms are

usually used in *in vitro* systems to simulate the digestive process in the human gastrointestinal tract. Mammalian enzymes are very similar to human enzymes, while microbial enzymes have a similar classification, but their functions may work differently.
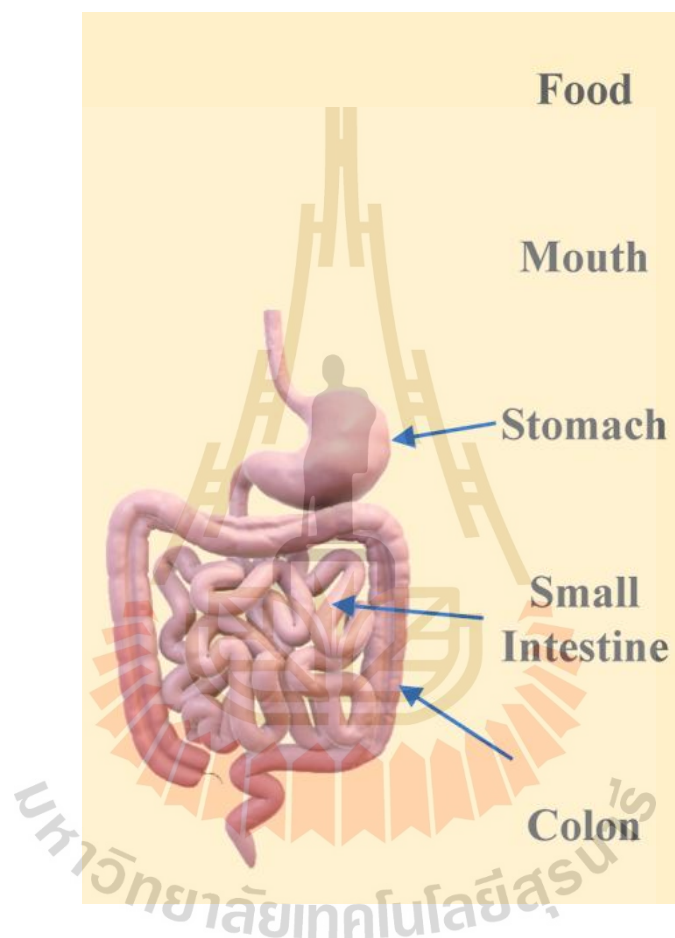
Figure 2.4 The picture of the gastrointestinal tract.

Source: Bornhorst and Singh (2014).

Starch digestion *in vitro* was a technique used to study the glucose release rate of starch and starchy foods which are hydrolyzed into different fractions of sugars under simulated gastro-small intestinal conditions (Dartois, Singh, Kaur, and Singh, 2010; Garcia-Alonso and Goni, 2000; Ramirez et al., 2015). The concept of

glycemic index (GI) was introduced to help classify foods according to the degree to which they released glucose into the bloodstream when they were consumed. GI is defined as the amount of postprandial blood glucose increase after a test meal (a meal of definite composition and quantity given to excite gastric secretion and so furnish material to withdraw for examination), expressed as a percentage of the corresponding area after an equip-carbohydrate portion of a reference food such as glucose or white bread (Goni et al., 1997). Several researchers point out that there was a good relationship between the *in vitro* digestion rate and the glycemic response to food. These studies might be used to identify foods for individuals with diabetes.

Differences in starch digestibility and GI values of PS or potato products were attributed to different factors including: maturity and cultivar (Fernandes, Velangi, and Wolever, 2005); method of cooking (food processing and preparation) (Colussi et al., 2017; Tahvonen, Hietanen, Sihvonen, and Salminen, 2006); cooling after cooking (Tian et al., 2016); properties of the starch, especially the content of amylopectin (Parada and Aguilera, 2009); modification of the starch; and composition of the food matrix (Dartois et al., 2010; Kawai, Takato, Sasaki, and Kajiwara, 2012).

2.3.2 Protein digestibility in food

Protein is abundant in all living cells and is, therefore, a vital part of our diet. The digestion and absorption of food protein is the main source of amino acids in the body (Elango, Ball, and Pencharz, 2009). In order to be useful to the body after digestion, dietary proteins must be hydrolyzed to their basic components, amino acids or small peptides. The digestion of food protein starts from the stomach, but mainly in the small intestine (Joye, 2019). The protein is chewed and mixed in the

mouth, and then enters the stomach through the pharynx and esophagus. Food proteins are hydrolyzed into polypeptides and amino acids by pepsin in the stomach. After a period of non-specific digestion by pepsin, the protein enters the small intestine and is further digested by trypsin, chymotrypsin, and other mixed enzymes (Erickson and Kim, 1990). The small peptides and free amino acids are absorbed in the small intestinal mucosa, and then enter the blood circulation through the capillaries in the small intestinal villi, and finally, they are absorbed and utilized by the body. Proteins, peptides, and even free amino acids that are not digested and absorbed in the small intestine will eventually be fermented in the large intestine by the intestinal flora.

Protein digestibility refers to the ratio of nitrogen absorbed from protein to nitrogen ingested by the human body, reflecting the degree to which food protein is decomposed and absorbed by digestive enzymes. The determination of food protein digestibility mainly includes *in vitro* protein digestibility and in vivo protein digestibility (Hsu, Vavak, Satterlee, and Miller, 1977). Digestibility *in vitro* is a method to simulate the digestion process of protein in the human body. *In vitro* protein digestibility assay mainly includes two steps. The first step is to hydrolyze protein by protease, and the second step is to calculate the digestibility of protein by measuring the degree of hydrolysis of protein or evaluate the degree of digestibility of protein by other methods. There are several methods for the first step including using protease hydrolysis protein to simulate the food in the body's digestive process. This process mainly includes multi-enzyme one-step digestion, human active gastric juice digestion, and pepsin and pancreatin step-by-step digestion (Almaas, Holm, Langsrud, Flengsrud, and Vegarud, 2006; Desai, Brennan, Guo, Zeng, and Brennan, 2019; Fasuan, Gbadamosi, and Omobuwajo, 2018). Methods for analysis of protein

hydrolysates and the calculation of digestibility include the pH-stat method, the trichloroacetic acid (TCA) precipitation method, the SDS-PAGE method, and so on (Malomo and Aluko, 2015; Nunes, Correia, Barros, and Delgadillo, 2004; Xia et al., 2012). The *in vivo* protein digestibility assay is a method to evaluate protein quality by studying and analyzing protein digestibility in animals. A nitrogen balance experiment with rat dung is most used (Silva et al., 2020).

The digestibility of protein depended on internal and external factors of the protein. Internal factors mainly resulted from the protein structure and include the protein amino acid profile, protein folding, and cross-linking (Joye, 2019). External factors included external conditions such as temperature, pH, and the ionic strength during digestion (Mackie, 2020). Also food processing had a large influence on these factors, and therefore on protein digestibility (Wang et al., 2015; Xue et al., 2020).

2.3.3 Lipid digestion and bioavailability

The human body intakes lipids through digestion and absorption, mainly through three sites: the mouth, stomach, and small intestine (McClements, 2020). Different changes occur in these three parts respectively, leading to the final transformation into small molecules that can easily be absorbed by the human body.

After ingestion, food, including lipids, interacts with the tongue, mouth, throat surfaces, and the salivary amylase. Food is initially digested in the mouth and then gradually turns into small pieces of chyme through physical chewing by the teeth (Sarkar, Xu, and Lee, 2019). At the same time, due to the influence of pH, ionic strength, and temperature of the oral environment, its structure becomes looser, which is easier to digest later.

44

The chyme leaving the mouth passes through the esophagus and then into the highly acidic stomach (pH 1~3). The stomach contains a lot of surface-active substances (such as phospholipids, mucin and proteins), which can be fully mixed with chyme (Hur, Decker, and McClements, 2009). The digestion of oil begins in the stomach, where part of the oil is catalyzed by enzymes (gastric lipase) and the oil is partially hydrolyzed, which is conducive to its further digestion in the small intestine. The initial amount of lipid hydrolysis in the stomach is thought to facilitate subsequent lipid digestion in the small intestine (Armand, 2007).

The small intestine is the main site of triglyceride digestion and absorption. In the small intestine, partially hydrolyzed and emulsified oil droplets of chyme are mixed with digestive juices (bile salts, phospholipids, pancreatic lipases, colipases, proteases, salts, etc.) (Gurr, 1999). The pH in the small intestine is close to neutral due to the mixture of chyme and alkaline digestive juices. Most of the digestion of fats is done by pancreatic lipase in the upper small intestine. The lipids enter the small intestine as lipid droplets, and the chemical and physical morphology of the lipids ingested changes significantly under the combined action of bile and pancreatic juice (Macierzanka, Torcello-Gómez, Jungnickel, and Maldonado-Valderrama, 2019). Because the small intestine is the main place for fat digestion and absorption, most of the current studies on human fat digestion also take the small intestine as the reaction environment for digestion and hydrolysis (Akoh, 2017).

There are many factors that affected the digestibility of oil (Golding and Wooster, 2010; Tan, Zhang, Mundo, and McClements, 2020). Dietary lipid content, lipid composition and other components in the food could affect the digestibility of fats and oils (Dias, Zhu, Thompson, Singh, and Garg, 2019; A. Ye,

Wang, Lin, Han, and Singh, 2020). Temperature and salinity in the digestive environment also affected the digestibility of fats (Olsen and Ringø, 1997). In addition, the results of digestibility differed by the methods used to determine digestibility (Guo, Bellissimo, and Rousseau, 2017; Wan et al., 2020).

2.3.4 Food protein and starch digestibility

The existence of protein in the food matrix might influence the rate of starch digestion. The digestibility of starch and protein in various cereal products was greatly affected by their interactions with each other. It has been reported that functional properties and starch digestibility were influenced by the presence of even small amounts of protein in cereals and other food products (Ezeogu, Duodu, Emmambux, and Taylor, 2008; Guerrieri, Eynard, Lavelli, and Cerletti, 1997). Protein existed on the surface of starch granules, which might be a physical barrier to digestion (Svihus, Uhlen, and Harstad, 2005). The effect of starch-protein interaction in wheat and its effect on starch digestibility were studied by Jenkins et al. (1987). Their reports suggested that the occurrence of a starch-protein interaction in white flour was the reason for the reduced rate of starch digestion and decreased glycemic response (Jenkins et al., 1987). Lu et al. (2016) investigated the effects of starch-protein interactions on physicochemical properties and *in vitro* starch digestibility of composite PS and protein blends during different processing. The results showed that the interactions between starch and protein reduced the starch digestibility of the processed blends (Lu et al., 2016).

2.3.5 Food lipids and starch digestibility

Amylose-lipid complexes are resistant to the degradation of enzymatic (α-amylase, amyloglucosidase, and isoamylase) (Kitahara, Suganuma, and Nagahama,

1996; Szezodrak and Pomeranz, 1992). It escapes from the digestion of the small intestine and then it is fermented into short-chain fatty acids in the large intestine by the gut microflora (Gelders, Duyck, Goesaert, and Delcour, 2005).

Ai et al. (2013) studied the effects of different food lipids on the enzymatic hydrolysis, pasting properties, and gel formation of starch of different structures. Different food lipids compose of triglycerides, FAs of different chain-lengths and phospholipids (Ai, Hasjim, and Jane, 2013). The mechanisms of interactions between the starch and lipids were elucidated. Results showed that after cooking with the starch, all the lipids used in the study significantly decreased the starch-hydrolysis rates except waxy corn starch because of the lack of amylose. This was attributed to complex formation between amylose and the lipids.

The effects of long-chain fatty acids (including lauric acid (C12), myristic acid (C14), palmitic acid (C16), stearic acid (C18), oleic acid (C18:1), and linoleic acid (C18:2)) on the *in vitro* digestibility of GPS were investigated (Kawai et al., 2012). The result showed that lauric acid and oleic acid had the largest reduction in hydrolyzed starch content among the long-chain fatty acids. This result might be related to the extent and thermal stability of the complexes.

The effects of the amount and type of FAs presenting in millets on *in vitro* starch digestibility and estimated glycemic index (eGI) were investigated (Annor, Marcone, Corredig, Bertoft, and Seetharaman, 2015). FAs presenting in millet starch played an important role in their hypoglycemic property. The amount and the type of FAs present in the millet flour were very important in maintaining the low digestibility of millet starch. Oleic acid was very effective in reducing the hydrolysis rates of the millet starches.

2.3.6 Food lipids, protein and starch digestibility

The effect of endogenous protein and lipids on the starch digestibility of Kodu millet flour and rice flour were investigated. The results showed that endogenous lipids and proteins could inhibit starch digestion (Annor, Marcone, Bertoft, and Seetharaman, 2013; Ye et al., 2018). Proteins and lipids might slow down the hydrolysis of starch by forming a coating around starch granules, which could inhibit their swelling and restrict the entry of digestive enzymes into the underlying starch molecules. Chen et al. (2017) carried out research by adding soy protein and corn oil to corn starch. The complex reduced the content of RDS and increased the sum of SDS and RS content. The effect of soy protein on the digestibility of the ternary blends was greater than that of corn oil. The physical barrier of corn oil, protein-starch matrix, and amylose-lipid complex could provide resistance to starch digestion (Chen et al., 2017). The degree of unsaturation of FAs and chain length affected the *in vitro* digestibility of starch-protein-fatty acid complexes (Mengge Zheng et al., 2018).

Some treatments might affect the digestibility of starch-protein-lipid mixtures. Alkali treatment could significantly change the functionality and *in vitro* digestibility of wheat starch granules by removing lipids and the surface proteins, rather than significantly changing the internal structure of starch granules (Wang et al., 2014). Heating treatment at 40 °C resulted in the lowest RDS fraction for both cooked and uncooked three-component mixtures (maize starch, zein protein, and maize oil) (Chen et al., 2018).

2.4 Methods used to study binary complex and ternary complex

Many analytical methods have been used to characterize the formation and structure of binary and ternary complexes. These methods include thermal, spectral, diffraction, imaging techniques, and so on (Wang et al., 2020).

DSC has been the most widely used thermal analysis technique in food research. It is used to measure the changes in energy for samples that have been heated or cooled (Wang et al., 2020). It was widely used to study the melting properties of starchy-lipid complexes, where endothermic transition temperatures provide information on structural stability and enthalpy changes related to ordered structure quantities (A. Eliasson and Krog, 1985). Some studies had detected the formation of starch-lipid complexes (such as maize starch-fatty acid, amylose-lipid, maize starch- palmitic acid complex) by DSC (Cervantes-Ramírez et al., 2020; Eliasson, 1994; Q. Li, Shi, Du, Dong, and Yu, 2021). It was also an effective analytical tool to describe the thermal characteristics of protein-lipid interactions (Cañadas and Casals, 2013). The thermal transition parameters of the starch-lipid-protein complex (maize starch, β-lactoglobulin and FAs) had also been measured by DSC (Cai et al., 2021; Wang, Zheng, Yu, Wang, and Copeland, 2017).

FTIR has also been used to detect the formation of starch-lipid complexes and starch-lipid-protein complexes because the interaction between starch and lipids could change the position of the lipid band (Wang et al., 2018; Wang et al., 2017). FTIR was widely used for the structural characterization of proteins or peptides (Li, Li, Fox, Gidley, and Dhital, 2020; Tatulian, 2013). Although this method did not provide precise atomic resolution of the molecular structure, it was very sensitive to the conformational changes that occurred in protein-functional transitions or

intermolecular interactions. The interaction of the functional group of PS and CA also could be detected by infrared spectroscopy (Grega et al., 2003).

Raman spectroscopy could be used for quality control, component identification, or detection of adulteration, as well as for basic research to illuminate structural or conformational changes occurring during food processing (Chan, 1996). As a non-destructive technique, it has been widely used to characterize the short-range molecular sequence of the double helix in starch samples (Mingjing Zheng et al., 2020). Natural starches usually showed very strong bands at 480, 865, 943, 1264, and 2900 cm^{-1}, which become weaker after starch gelatinization. The half-peak full width (FWHM) at 480 cm^{-1} could be used to predict the formation of starch-lipid complexes and characterized the degree of their ordered structure. In recent years, Raman spectroscopy was used to detect short-range molecular order changes of starch-lipid complex and starch-lipid-protein complex (Chao et al., 2018; L. Wang et al., 2018; Wang et al., 2017).

XRD techniques are widely used to characterize crystalline materials and provide information about crystal structure and cell size (Blazek and Gilbert, 2011). The distant structural sequence of natural starches is usually characterized using XRD, resulting in three diffraction patterns, namely A-, B-, and C- (Fig. 2.5) (Sarko and Wu, 1978). The C-structure is a mixture of A- and B-unit cells. In contrast, starch-lipid complexes exhibited a different XRD pattern, known as V-type (Zobel, French, & Hinkle, 1967). The long-range ordered structure of starch-lipid-protein complex by XRD showed the same V-shaped diffraction peak as starch-lipid complex (Hai and Yinxia, 2016). Chen et al. (2018) found that the relative crystallinity of swollen maize starch, maize oil, and Zain protein blends decreased when treatment temperature using

XRD increased. It was mainly attributed to the residue of amylopectin double helices and newly formed starch-lipid complexes.
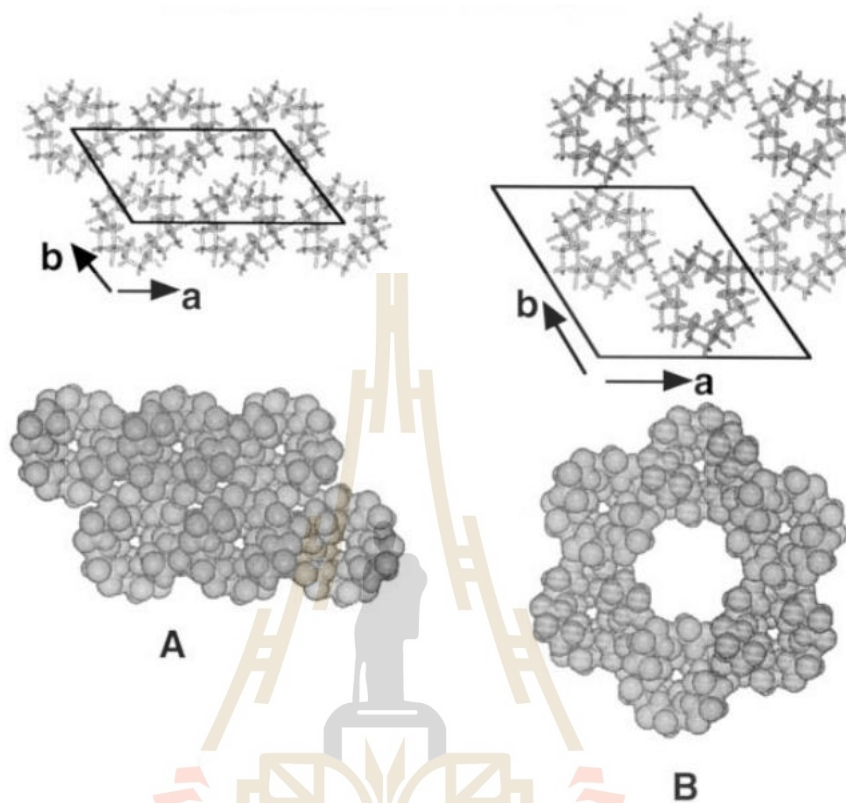
Figure 2.5 Crystalline packing of double helices in A-type (A) and B-type (B) amylose. Projection of the structure onto the (a, b) plane.

Source: (Buleon, Colonna, Planchot, and Ball, 1998).

Rheological tests can also be used to detect the interactions of complex or mixture. The rheological methods provide the rheological changes during heating and cooling in the mode of oscillatory test only (Autio, 1990). The composition and structure of food determined the rheological properties of food. Basic rheological testing provided key information on the time-dependent viscoelastic behavior and molecular mechanisms surrounding structural changes in proteins when they

underwent gelation in food (Jamilah, Mohamed, Abbas, Abdul Rahman, et al., 2009). The rheological properties and functional properties of starch paste in mixed foods also varied with types and varieties of starch (Joshi, Aldred, Panozzo, Kasapis, and Adhikari, 2014; Wu, Wang, Ge, Yu, and Xiong, 2018). Rheological methods were also used to analyze the viscoelasticity of starch-lipid complexes to detect the effect of lipid addition on the rheology of the starch (Handarini, Sauman Hamdani, Cahyana, and Siti Setiasih, 2020).

Morphological characteristics of starch-lipid/starch-protein-lipid complexes could be observed by scanning electron microscopy, transmission electron microscopy, and atomic force microscopy (Chen et al., 2018; Wang et al., 2020). CLSM was a relatively new method that was reported to be able to detect starch-lipid complexes and starch-protein mixtures (Li et al., 2020; Oyeyinka, Singh, Venter, and Amonsou, 2017; Thaiudom and Pracham, 2018).

2.5 References

A, W. J., and Poats, S. V. (2009). **The potato in the human diet**: Cambridge University Press.

Abd El-Motaal, E., Helmy, H., Taha, F., and Shoeb, Z. (1998). **Effect of dry and moist heating on the formation of lipid–protein complex in soybean products**. Paper presented at the Proceedings of the 47th oil seed conference, New Orleans, Louisiana, March.

Absar, N., Zaidul, I., Takigawa, S., Hashimoto, N., Matsuura-Endo, C., Yamauchi, H., and Noda, T. (2009). Enzymatic hydrolysis of potato starches containing different amounts of phosphorus. **Food Chemistry.** 112(1): 57-62.

Ai, Y., Hasjim, J., and Jane, J. (2013). Effects of lipids on enzymatic hydrolysis and physical properties of starch. **Carbohydrate Polymers.** 92(1): 120-127.

Akoh, C. C. (2017). Food lipids: chemistry, nutrition, and biotechnology: CRC press.

Almaas, H., Holm, H., Langsrud, T., Flengsrud, R., and Vegarud, G. E. (2006). In vitro studies of the digestion of caprine whey proteins by human gastric and duodenal juice and the effects on selected microorganisms. **British Journal of Nutrition**. 96(3): 562-569.

Alvarez, M. D., Fernández, C., Olivares, M. D., and Canet, W. (2012). Comparative Characterization of Dietary Fibre-Enriched Frozen/Thawed Mashed Potatoes. **International Journal of Food Properties.** 15(5): 1022-1041.

Álvarez, M. D., Fernández, C., Olivares, M. D., Jiménez, M. J., and Canet, W. (2013). Sensory and texture properties of mashed potato incorporated with inulin and olive oil blends. **International Journal of Food Properties.** 16(8): 1839-1859.

Annor, G. A., Marcone, M., Bertoft, E., and Seetharaman, K. (2013). In vitro starch digestibility and expected glycemic index of kodo millet (Paspalum scrobiculatum) as affected by starch–protein–lipid interactions. **Cereal Chemistry**. 90(3): 211-217.

Annor, G. A., Marcone, M., Corredig, M., Bertoft, E., and Seetharaman, K. (2015). Effects of the amount and type of fatty acids present in millets on their in vitro starch digestibility and expected glycemic index (eGI). **Journal of Cereal Science.** 64: 76-81.

Armand, M. (2007). Lipases and lipolysis in the human digestive tract: where do we stand?. **Current Opinion in Clinical Nutrition & Metabolic Care.** 10(2): 156-164.

Autio, K. (1990). Rheological and microstructural changes of oat and barley starches during heating and cooling. **Food Structure.** 9(4): 5.

Batey, I. L., and Curtin, B. M. (2000). Effects on pasting viscosity of starch and flour from different operating conditions for the Rapid Visco Analyser. **Cereal Chemistry.** 77(6): 754-760.

Batres, L. V., and White, P. J. (1986). Interaction of amylopectin with monoglycerides in model systems. **Journal of the American Oil Chemists' Society.** 63(12): 1537-1540.

BeMiller, J. N. (2007). **Carbohydrate chemistry for food scientists**: American Association of Cereal Chemists, Inc (AACC).

Bertoft, E., and Blennow, A. (2009). **Structure of potato starch** Advances in potato chemistry and technology: Elsevier. 83-98

Bertoft, E., and Blennow, A. (2016). **Structure of potato starch** Advances in potato chemistry and technology: Elsevier. 57-73

Bertolini, A. C., Creamer, L. K., Eppink, M., and Boland, M. (2005). Some rheological properties of sodium caseinate-starch gels. **Journal of Agricultural and Food Chemistry.** 53(6): 2248-2254.

Biliaderis, C. G., and Galloway, G. (1989). Crystallization behavior of amylose-V complexes: structure-property relationships. **Carbohydrate Research.** 189: 31-48.

Blazek, J., and Gilbert, E. P. (2011). Application of small-angle X-ray and neutron scattering techniques to the characterisation of starch structure: A review. **Carbohydrate Polymers.** 85(2): 281-293.

Blennow, A., Sjöland, A. K., Andersson, R., and Kristiansson, P. (2005). The distribution of elements in the native starch granule as studied by particle-

induced X-ray emission and complementary methods. **Analytical Biochemistry.** 347(2): 327-329.

Bouchemal, K., Briançon, S., Perrier, E., and Fessi, H. (2004). Nano-emulsion formulation using spontaneous emulsification: solvent, oil and surfactant optimisation. **International Journal of Pharmaceutics.** 280(1-2): 241-251.

Brumini, D., Criscione, A., Bordonaro, S., Vegarud, G. E., and Marletta, D. (2016). Whey proteins and their antimicrobial properties in donkey milk: a brief review. **Dairy Science & Technology.** 96(1): 1-14.

Buleon, A., Colonna, P., Planchot, V., and Ball, S. (1998). Starch granules: structure and biosynthesis. **International Journal of Biological Macromolecules.** 23(2): 85-112.

Cai, J., Chao, C., Niu, B., Copeland, L., Yu, J., Wang, S., and Wang, S. (2021). New insight into the interactions among starch, lipid and protein in model systems with different starches. **Food Hydrocolloids**. 112: 106323.

Cañadas, O., and Casals, C. (2013). **Differential scanning calorimetry of protein-lipid interactions.** Lipid-protein interactions: Springer. 55-71.

Cervantes-Ramírez, J. E., Cabrera-Ramirez, A. H., Morales-Sánchez, E., Rodriguez-García, M. E., de la Luz Reyes-Vega, M., Ramírez-Jiménez, A. K., . . . Gaytán-Martínez, M. (2020). Amylose-lipid complex formation from extruded maize starch mixed with fatty acids. **Carbohydrate Polymers.** 246: 116555.

Chao, C., Cai, J., Yu, J., Copeland, L., Wang, S., and Wang, S. (2018). Toward a better understanding of starch–monoglyceride–protein interactions. **Journal of Agricultural and Food Chemistry.** 66(50): 13253-13259.

Chen, He, X., Zhang, B., Fu, X., Li, L., and Huang, Q. (2018). Structure, physicochemical and in vitro digestion properties of ternary blends containing swollen maize starch, maize oil and zein protein. **Food Hydrocolloids.** 76: 88-95.

Chen, X., He, X., Zhang, B., Fu, X., Jane, J., and Huang, Q. (2017). Effects of adding corn oil and soy protein to corn starch on the physicochemical and digestive properties of the starch. **International Journal of Biological Macromolecules.** 104: 481-486.

Colussi, R., Singh, J., Kaur, L., da Rosa Zavareze, E., Dias, A. R. G., Stewart, R. B., and Singh, H. (2017). Microstructural characteristics and gastro-small intestinal digestion in vitro of potato starch: Effects of refrigerated storage and reheating in microwave. **Food Chemistry.** 226: 171-178.

Copeland, L., Blazek, J., Salman, H., and Tang, M. C. (2009). Form and functionality of starch. **Food hydrocolloids.** 23(6): 1527-1534.

Cornell, D. G., and Patterson, D. L. (1989). Interaction of phospholipids in monolayers with. beta.-lactoglobulin adsorbed from solution. **Journal of Agricultural and Food Chemistry**. 37(6): 1455-1459.

Crowe, T. C., Seligman, S. A., and Copeland, L. (2000). Inhibition of enzymic digestion of amylose by free fatty acids in vitro contributes to resistant starch formation. **The Journal of nutrition.** 130(8): 2006-2008.

Cui, S. W. (2005). Food carbohydrates: chemistry, physical properties, and applications: CRC press.

Silva, M. E. T., de Paula Correa, K., Martins, M. A., da Matta, S. L. P., Martino, H. S. D., and dos Reis Coimbra, J. S. (2020). Food safety, hypolipidemic and hypoglycemic activities, and in vivo protein quality of microalga Scenedesmus

obliquus in Wistar rats. **Journal of Functional Foods.** 65: 103711.

Damodaran, S. (2008). **Amino acids, peptides and proteins** (Vol. 4): CRC Press: Boca Raton, FL.

Damodaran, S., and Parkin, K. L. (2017). **Amino acids, peptides, and proteins** Fennema's food chemistry.: CRC Press. 235-356

Dartois, A., Singh, J., Kaur, L., and Singh, H. (2010). Influence of guar gum on the in vitro starch digestibility-rheological and microstructural characteristics. **Food Biophysics**. 5(3): 149-160.

Desai, A. S., Brennan, M. A., Guo, X., Zeng, X. A., and Brennan, C. S. (2019). Fish protein and lipid interactions on the digestibility and bioavailability of starch and protein from durum wheat pasta. **Molecules.** 24(5): 839.

Dias, C. B., Zhu, X., Thompson, A. K., Singh, H., and Garg, M. L. (2019). Effect of the food form and structure on lipid digestion and postprandial lipaemic response. **Food & function**. 10(1): 112-124.

Donovan, J. W. (1979). Phase transitions of the starch–water system. **Biopolymers.** 18(2): 263-275.

Dupont, J., White, P. J., and Feldman, E. B. (1991). Saturated and hydrogenated fats in food in relation to health. **Journal of the American College of Nutrition.** 10(6): 577-592.

Eerlingen, R. C., Jacobs, H., Block, K., and Delcour, J. A. (1997). Effects of hydrothermal treatments on the rheological properties of potato starch. **Carbohydrate Research**. 297(4): 347-356.

Elango, R., Ball, R. O., and Pencharz, P. B. (2009). Amino acid requirements in humans: with a special emphasis on the metabolic availability of amino acids.

Amino Acids. 37(1): 19-27.

Eliasson, A., Finstad, H., and Ljunger, G. (1988). A Study of Starch-Lipid Interactions for Some Native and Modified Maize Starches. **Starch-Stärke**. 40(3): 95-100.

Eliasson, A., and Krog, N. (1985). Physical properties of amylose-monoglyceride complexes. **Journal of Cereal Science.** 3(3): 239-248.

Eliasson, A.-C. (1994). Interactions between starch and lipids studied by DSC. **Thermochimica Acta**. 246(2): 343-356.

Eliasson, A. C. (1986). Viscoelastic behaviour during the gelatinization of starch I. Comparison of wheat, maize, potato and waxy-barley starches. **Journal of texture studies**. 17(3): 253-265.

Eliasson, A. C. (1994). Interactions between starch and lipids studied by DSC. **Thermochimica Acta.** 246(2): 343-356.

Eliasson, A. C., and Wahlgren, M. (2004). Starch-lipid interactions and their relevance in food products. **Starch in food: Structure, function and applications.** 441-460.

Englyst, H. N., Kingman, S., and Cummings, J. (1992). Classification and measurement of nutritionally important starch fractions. **European journal of clinical nutrition.** 46: S33-50.

Erickson, R. H., and Kim, Y. S. (1990). Digestion and absorption of dietary protein. **Annual Review of Medicine.** 41(1): 133-139.

Ezeogu, L. I., Duodu, K. G., Emmambux, M. N., and Taylor, J. R. (2008). Influence of cooking conditions on the protein matrix of sorghum and maize endosperm flours. **Cereal Chemistry.** 85(3): 397-402.

Fasuan, T. O., Gbadamosi, S. O., and Omobuwajo, T. O. (2018). Characterization of protein isolate from Sesamum indicum seed: In vitro protein digestibility,

amino acid profile, and some functional properties. **Food science & nutrition.** 6(6): 1715-1723.

Fernandes, G., Velangi, A., and Wolever, T. M. (2005). Glycemic index of potatoes commonly consumed in North America. **Journal of the Academy of Nutrition and Dietetics.** 105(4): 557-562.

Ferry, J. D. (1980). **Viscoelastic properties of polymers**: John Wiley & Sons.

Forss, D. A. (1973). Odor and flavor compounds from lipids. **Progress in the Chemistry of Fats and other Lipids.** 13: 177-258.

Gaonkar, A. G., and McPherson, A. (2016). **Ingredient interactions: effects on food quality**: CRC press.

Garcia-Alonso, A., and Goni, I. (2000). Effect of processing on potato starch: in vitro availability and glycaemic index. **Food/Nahrung.** 44(1): 19-22.

Gebre-Mariam, T., Abeba, A., and Schmidt, P. (1996). Isolation and physico-chemical properties of enset starch. **Starch-Stärke.** 48(6): 208-214.

Gelders, G. G., Duyck, J. P., Goesaert, H., and Delcour, J. A. (2005). Enzyme and acid resistance of amylose-lipid complexes differing in amylose chain length, lipid and complexation temperature. **Carbohydrate Polymers**. 60(3): 379-389.

Golding, M., and Wooster, T. J. (2010). The influence of emulsion structure and stability on lipid digestion. **Current Opinion in Colloid & Interface Science.** 15(1-2): 90-101.

Goni, I., Garcia Alonso, A., and Saura Calixto, F. (1997). A starch hydrolysis procedure to estimate glycemic index. **Nutrition Research.** 17(3): 427-437.

Gray, G. M. (1992). Starch digestion and absorption in nonruminants. **The Journal of nutrition.** 122(1): 172-177.

Grega, T., Najgebauer, D., Sady, M., Baczkowicz, M., Tomasik, P., and Faryna, M. (2003). Biodegradable complex polymers from casein and potato starch. **Journal of Polymers and the Environment.** 11(2): 75-83.

Guenthner, J. (2001). **The international potato industry**: Elsevier.

Guerrieri, N., Eynard, L., Lavelli, V., and Cerletti, P. (1997). Interactions of protein and starch studied through amyloglucosidase action. **Cereal Chemistry.** 74(6): 846-850.

Gunstone, F. (2011). Vegetable oils in food technology: composition, properties and uses: John Wiley & Sons.

Guo, Q., Bellissimo, N., and Rousseau, D. (2017). Role of gel structure in controlling in vitro intestinal lipid digestion in whey protein emulsion gels. **Food Hydrocolloids**. 69: 264-272.

Gupta, A., Jadhav, J., Gunaware, K., and Shinde, B. (2016). Whey proteins and its impact on human health nutrition: review. **Journal of Analytical & Pharmaceutical Research**. 3(8): 00083.

Guraya, H. S., Kadan, R. S., and Champagne, E. T. (1997). Effect of rice starch-lipid complexes on in vitro digestibility, complexing index, and viscosity. **Cereal Chemistry.** 74(5): 561-565.

Gurr, M. I. (1999). Lipids in nutrition and health: A reappraisal: Elsevier.

Hadziyev, D., and Steele, L. (1979). **Dehydrated mashed potatoes—chemical and biochemical aspects.** Advances in Food Research Vol. 25: Elsevier. 55-136

Hai, L., and Yinxia, C. (2016). Review on Theory and Technology Research of Starch-lipid Complex. **Agricultural Science & Technology.** 17(8).

Hammond, E. G., Johnson, L. A., Su, C., Wang, T., and White, P. J. (2005). Soybean oil. **Bailey's industrial oil and fat products**.

Handarini, K., Sauman Hamdani, J., Cahyana, Y., and Siti Setiasih, I. (2020). Functional and pasting properties of a starch-lipid complex formed with gaseous ozone and palm oil. **International Journal of Food Properties.** 23(1): 1361-1372.

Hassan, S. M. (2013). Soybean, nutrition and health. **Soybean–Bio-Active Compounds. London, United Kingdom: InTech**: 453-473.

Hermansson, A.M., and Svegmark, K. (1996). Developments in the understanding of starch functionality. **Trends in Food Science & Technology.** 7(11): 345-353.

Hizukuri, S., Tabata, S., and Nikuni, Z. (1970). Studies on Starch Phosphate Part 1. Estimation of glucose-6-phosphate residues in starch and the presence of other bound phosphate (s). **Starch-Stärke.** 22(10): 338-343.

Hoover, R. (2001). Composition, molecular structure, and physicochemical properties of tuber and root starches: a review. **Carbohydrate Polymers.** 45(3): 253-267.

Hsu, H., Vavak, D., Satterlee, L., and Miller, G. (1977). A multienzyme technique for estimating protein digestibility. **Journal of Food Science.** 42(5): 1269-1273.

Hur, S. J., Decker, E. A., and McClements, D. J. (2009). Influence of initial emulsifier type on microstructural changes occurring in emulsified lipids during in vitro digestion. **Food Chemistry.** 114(1): 253-262.

Jamilah, B., Mohamed, A., Abbas, K., Abdul Rahman, R., Karim, P., and Hashim, D. (2009). Protein-starch interaction and their effect on thermal and rheological characteristics of a food system: A review. **J. Food Agric. Env.** 7: 169-174.

Jamilah, B., Mohamed, A., Abbas, K., Rahman, R. A., Karim, R., and Hashim, D. (2009). Protein-starch interaction and their effect on thermal and rheological characteristics of a food system: A review. **J. Food Agric. Env**. 7: 169-174.

Jane, J.l., and Robyt, J. F. (1984). Structure studies of amylose-V complexes and retro-graded amylose by action of alpha amylases, and a new method for preparing amylodextrins. **Carbohydrate Research**. 132(1): 105-118.

Jenkins, D., Thorne, M. J., Wolever, T., Jenkins, A. L., Rao, A. V., and Thompson, L. U. (1987). The effect of starch-protein interaction in wheat on the glycemic response and rate of in vitro digestion. **The American journal of clinical nutrition.** 45(5): 946-951.

Jenkins, P., and Donald, A. (1995). The influence of amylose on starch granule structure. **International Journal of Biological Macromolecules**. 17(6): 315-321.

Jenkins, P. J., and Donald, A. M. (1998). Gelatinisation of starch: a combined SAXS/WAXS/DSC and SANS study. **Carbohydrate Research.** 308(1-2): 133-147.

Joshi, M., Aldred, P., Panozzo, J., Kasapis, S., and Adhikari, B. (2014). Rheological and microstructural characteristics of lentil starch–lentil protein composite pastes and gels. **Food Hydrocolloids.** 35: 226-237.

Joye, I. (2019). Protein digestibility of cereal products. **Foods.** 8(6): 199.

Joyner, H. S., and Meldrum, A. (2016). Rheological study of different mashed potato preparations using large amplitude oscillatory shear and confocal microscopy. **Journal of Food Engineering.** 169: 326-337.

Karim, A., Toon, L., Lee, V., Ong, W., Fazilah, A., and Noda, T. (2007). Effects of phosphorus contents on the gelatinization and retrogradation of potato starch. **Journal of Food Science.** 72(2): C132-C138.

Kaur, K., and Singh, N. (2000). Amylose-lipid complex formation during cooking of rice flour. **Food Chemistry,** 71(4): 511-517.

Kaur, L., and Singh, J. (2016). **Microstructure, Starch Digestion, and Glycemic Index of Potatoes.** Advances in Potato Chemistry and Technology (Second Edition): Elsevier. 369-402.

Kaur, L., Singh, J., McCarthy, O. J., and Singh, H. (2007). Physico-chemical, rheological and structural properties of fractionated potato starches. **Journal of Food Engineering.** 82(3): 383-394.

Kaur, L., Singh, J., and Singh, N. (2005). Effect of glycerol monostearate on the physico-chemical, thermal, rheological and noodle making properties of corn and potato starches. **Food Hydrocolloids.** 19(5): 839-849.

Kaur, L., Singh, N., and Sodhi, N. S. (2002). Some properties of potatoes and their starches II. Morphological, thermal and rheological properties of starches. **Food Chemistry.** 79(2): 183-192.

Kawai, K., Takato, S., Sasaki, T., and Kajiwara, K. (2012). Complex formation, thermal properties, and in-vitro digestibility of gelatinized potato starch-fatty acid mixtures. **Food Hydrocolloids**. 27(1): 228-234.

Kitahara, K., Suganuma, T., and Nagahama, T. (1996). Susceptibility of amylose-lipid complexes to hydrolysis by glucoamylase. **Cereal Chemistry.** 73(4): 428-432.

Kleinschmidt, J. H. (2013). **Lipid-Protein Interactions**: Springer.

Kong, X., Zhu, P., Sui, Z., and Bao, J. (2015). Physicochemical properties of starches from diverse rice cultivars varying in apparent amylose content and gelatinisation temperature combinations. **Food Chemistry.** 172: 433-440.

Kozlov, S. S., Blennow, A., Krivandin, A. V., and Yuryev, V. P. (2007). Structural and thermodynamic properties of starches extracted from GBSS and GWD suppressed potato lines. **International Journal of Biological Macromolecules.**

40(5): 449-460.

Lamberti, M., Geiselmann, A., Conde-Petit, B., and Escher, F. (2004). Starch transformation and structure development in production and reconstitution of potato flakes. **LWT-Food Science and Technology**. 37(4): 417-427.

Lee, G., and Purdon, J. (1969). Brabender viscometry: I. Conversion of brabender curves to instron flow curves. **Polymer Engineering & Science.** 9(5): 360-364.

Lehmann, U., and Robin, F. (2007). Slowly digestible starch–its structure and health implications: a review. **Trends in Food Science & Technology**. 18(7): 346-355.

Lesmes, U., Cohen, S. H., Shener, Y., and Shimoni, E. (2009). Effects of long chain fatty acid unsaturation on the structure and controlled release properties of amylose complexes. **Food Hydrocolloids.** 23(3): 667-675.

Li, H.T., Li, Z., Fox, G. P., Gidley, M. J., and Dhital, S. (2020). Protein-starch matrix plays a key role in enzymic digestion of high-amylose wheat noodle. **Food Chemistry.** 336: 127719.

Li, Q., Shi, S., Du, S.k., Dong, Y., and Yu, X. (2021). Starch–palmitic acid complex formation and characterization at different frying temperature and treatment time. **LWT.** 136: 110328.

Li, C., E. C. (1996). The applications of Raman spectroscopy in food science. **Trends in Food Science & Technology.** 11(7): 361-370.

Lin, L., Yang, H., Chi, C., and Ma, X. (2020). Effect of protein types on structure and digestibility of starch-protein-lipids complexes. **LWT.** 134: 110175.

Liu, J., Fei, L., Maladen, M., Hamaker, B. R., and Zhang, G. (2009). Iodine binding property of a ternary complex consisting of starch, protein, and free fatty acids. **Carbohydrate Polymers.** 75(2): 351-355.

Liu, Q. (2005). Understanding starches and their role in foods. **Food carbohydrates: Chemistry, physical properties and applications**. 340.

Lu, Z., Donner, E., Yada, R. Y., and Liu, Q. (2016). Physicochemical properties and in vitro starch digestibility of potato starch/protein blends. **Carbohydrate Polymers.** 154: 214-222.

Macierzanka, A., Torcello-Gómez, A., Jungnickel, C., and Maldonado-Valderrama, J. (2019). Bile salts in digestion and transport of lipids. **Advances in Colloid and Interface Science.** 274: 102045.

Mackie, A. (2020). Insights and gaps on protein digestion. **Current Opinion in Food Science**.

Malomo, S. A., and Aluko, R. E. (2015). Conversion of a low protein hemp seed meal into a functional protein concentrate through enzymatic digestion of fibre coupled with membrane ultrafiltration. **Innovative Food Science & Emerging Technologies.** 31: 151-159.

McCann, T. H., Small, D. M., Batey, I. L., Wrigley, C. W., and Day, L. (2009). Protein–lipid interactions in gluten elucidated using acetic acid fractionation. **Food Chemistry.** 115(1): 105-112.

McClements, D. J. (2015). Food emulsions: principles, practices, and techniques: CRC press.

McClements, D. J. (2020). Food hydrocolloids: Application as functional ingredients to control lipid digestion and bioavailability. **Food Hydrocolloids**: 106404.

McCormack, G., Panozzo, J., Bekes, F., and MacRitchie, F. (1991). Contributions to breadmaking of inherent variations in lipid content and composition of wheat cultivars. I. Results of survey. **Journal of Cereal Science.** 13(3): 255-261.

McCormack, G., Panozzo, J., and MacRitchie, F. (1991). Contributions to breadmaking of inherent variations in lipid content and composition of wheat cultivars. II. Fractionation and reconstitution studies. **Journal of Cereal Science.** 13(3): 263-274.

Miles, M. J., Morris, V. J., Orford, P. D., and Ring, S. G. (1985). The roles of amylose and amylopectin in the gelation and retrogradation of starch. **Carbohydrate Research.** 135(2): 271-281.

Mohanty, D., Mohapatra, S., Misra, S., and Sahu, P. (2016). Milk derived bioactive peptides and their impact on human health–A review. **Saudi journal of biological sciences.** 23(5): 577-583.

Morrison, W., Tester, R., Snape, C., Law, R., and Gidley, M. (1993). Swelling and gelatinization of cereal starches. IV: some effects of lipid-complexed amylose and free amylose in waxy and normal barley starches. **Cereal Chemistry.** 70(4): 385-391.

Mu, T., Sun, H., and Liu, X. (2017). **Potato staple food processing technology**: Springer.

Neilson, A. P., Pahulu, H. F., Ogden, L. V., and Pike, O. A. (2006). Sensory and nutritional quality of dehydrated potato flakes in long-term storage. **Journal of Food Science.** 71(6): S461-S466.

Nunes, A., Correia, I., Barros, A., and Delgadillo, I. (2004). Sequential in vitro pepsin digestion of uncooked and cooked sorghum and maize samples. **Journal of Agricultural and Food Chemistry.** 52(7): 2052-2058.

Nurul, M., Azemi, B. M., and Manan, D. (1999). Rheological behaviour of sago (Metroxylon sagu) starch paste. **Food Chemistry**. 64(4): 501-505.

O'Kennedy, B. (2011). **Caseins.** Handbook of food proteins: Elsevier. 13-29.

O'Mahony, J., and Fox, P. (2014). **Milk: an overview.** Milk proteins: Elsevier. 19-73.

Olsen, R. E., and Ringø, E. (1997). Lipid digestibility in fish: a review. **Recent Res. Dev. Lipid Res.** 1: 199-265.

Oyeyinka, S. A., Singh, S., Venter, S. L., and Amonsou, E. O. (2017). Effect of lipid types on complexation and some physicochemical properties of bambara groundnut starch. **Starch-Stärke.** 69(3-4): 1600158.

Ozturk, B., Argin, S., Ozilgen, M., and McClements, D. J. (2015). Nanoemulsion delivery systems for oil-soluble vitamins: Influence of carrier oil type on lipid digestion and vitamin D3 bioaccessibility. **Food Chemistry.** 187: 499-506.

Parada, J., and Aguilera, J. M. (2009). In vitro digestibility and glycemic response of potato starch is related to granule size and degree of gelatinization. **Journal of Food Science.** 74(1).

Park, Y. W., and Nam, M. S. (2015). Bioactive peptides in milk and dairy products: a review. **Korean journal for food science of animal resources.** 35(6): 831.

Patino, J. M. R., Garcia, J. M. N., and Nino, M. R. R. (2001). Protein-lipid interactions at the oil-water interface. **Colloids and Surfaces B: Biointerfaces.** 21(1-3): 207-216.

Perez, M. D., and Calvo, M. (1995). Interaction of β-lactoglobulin with retinol and fatty acids and its role as a possible biological function for this protein: a review. **Journal of Dairy Science.** 78(5): 978-988.

Pérez, S., and Bertoft, E. (2010). The molecular structures of starch components and their contribution to the architecture of starch granules: A comprehensive review. **Starch-Stärke.** 62(8): 389-420.

Phillips, G. O., and Williams, P. A. (2011). **Handbook of food proteins**: Elsevier.

Pokorny, J., Davidek, J., Chocholata, V., Panek, J., Bulantova, H., Janitz, W., Vierecklova, M. (1977). Interactions of oxidized lipids with protein. **Riv. Ital. Sostanze Grasse.** 54: 389-393.

Pokorny, J., Janicek, G., and Davidek, J. (1975). Determination of the interaction products of proteins with lipids. **Zesz Probl Postepow Nauk Roln**.

Pryde, E. (1980). Composition of soybean oil. **Handbook of soy oil processing and utilization**: 13-31.

Raigond, P., Singh, B., Dutt, S., and Chakrabarti, S. K. (2020). **Potato: Nutrition and Food Security**: Springer Nature.

Ramirez, C., Millon, C., Nunez, H., Pinto, M., Valencia, P., Acevedo, C., and Simpson, R. (2015). Study of effect of sodium alginate on potato starch digestibility during in vitro digestion. **Food Hydrocolloids.** 44: 328-332.

Ring, S. G., Colonna, P., IAnson, K. J., Kalichevsky, M. T., Miles, M. J., Morris, V. J., and Orford, P. D. (1987). The gelation and crystallisation of amylopectin. **Carbohydrate Research**. 162(2): 277-293.

Rosalina, I., and Bhattacharya, M. (2002). Dynamic rheological measurements and analysis of starch gels. **Carbohydrate Polymers.** 48(2): 191-202.

Sarkar, A., Xu, F., and Lee, S. (2019). Human saliva and model saliva at bulk to adsorbed phases-similarities and differences. **Advances in Colloid and Interface Science.** 273: 102034.

Sarko, A., and Wu, H. C. (1978). The crystal structures of A-, B-and C-polymorphs of amylose and starch. **Starch-Stärke.** 30(3): 73-78.

Singh, J., Colussi, R., McCarthy, O. J., and Kaur, L. (2016). **Potato starch and its modification.** Advances in Potato Chemistry and Technology (Second Edition): Elsevier. 195-247.

Singh, J., Dartois, A., and Kaur, L. (2010). Starch digestibility in food matrix: a review. **Trends in Food Science & Technology.** 21(4): 168-180.

Singh, J., Kaur, L., and McCarthy, O. (2007). Factors influencing the physico-chemical, morphological, thermal and rheological properties of some chemically modified starches for food applications-A review. **Food hydrocolloids.** 21(1): 1-22.

Singh, J., Kaur, L., and Singh, H. (2013). **Food microstructure and starch digestion.** Advances in food and nutrition research (Vol. 70): Elsevier. 137-179

Singh, J., McCarthy, O. J., and Singh, H. (2006). Physico-chemical and morphological characteristics of New Zealand Taewa (Maori potato) starches. **Carbohydrate Polymers.** 64(4): 569-581.

Singh, J., and Singh, N. (2001). Studies on the morphological, thermal and rheological properties of starch separated from some Indian potato cultivars. **Food Chemistry.** 75(1): 67-77.

Singh, J., and Singh, N. (2003). Studies on the morphological and rheological properties of granular cold water soluble corn and potato starches. **Food hydrocolloids.** 17(1): 63-72.

Singh, J., Singh, N., and Saxena, S. (2002). Effect of fatty acids on the rheological properties of corn and potato starch. **Journal of Food Engineering.** 52(1): 9-16.

Singh, N., Singh, J., Kaur, L., Sodhi, N. S., and Gill, B. S. (2003). Morphological, thermal and rheological properties of starches from different botanical sources.

Food Chemistry. 81(2): 219-231.

Sjoo, M., and Nilsson, L. (2017). Starch in food: Structure, function and applications: CRC Press.

Smithers, G. W., and Augustin, M. A. (2012). **Advances in dairy ingredients** (Vol. 79): John Wiley & Sons.

Sodhi, N. S., and Singh, N. (2003). Morphological, thermal and rheological properties of starches separated from rice cultivars grown in India. **Food Chemistry.** 80(1): 99-108.

Srichuwong, S., Sunarti, T. C., Mishima, T., Isono, N., and Hisamatsu, M. (2005). Starches from different botanical sources II: Contribution of starch structure to swelling and pasting properties. **Carbohydrate Polymers.** 62(1): 25-34.

Svihus, B., Uhlen, A. K., and Harstad, O. M. (2005). Effect of starch granule structure, associated components and processing on nutritive value of cereal starch: A review. **Animal Feed Science and Technology.** 122(3-4): 303-320.

Swaisgood, H. E. (2007). **Characteristics of milk.** Fennema's food chemistry: CRC Press. 897-934.

Szezodrak, J., and Pomeranz, Y. (1992). Starch-lipid interactions and formation of resistant starch in high-amylose barley. **Cereal Chemistry.** 69: 626-626.

Taha, F., and Mohamed, S. (2004). Effect of different denaturating methods on lipid-protein complex formation. **LWT-Food Science and Technology.** 37(1): 99-104.

Tahvonen, R., Hietanen, R., Sihvonen, J., and Salminen, E. (2006). Influence of different processing methods on the glycemic index of potato (Nicola). **Journal of Food Composition and Analysis.** 19(4): 372-378.

Tan, Y., Zhang, Z., Mundo, J. M., and McClements, D. J. (2020). Factors impacting lipid digestion and nutraceutical bioaccessibility assessed by standardized gastrointestinal model (INFOGEST): Emulsifier type. **Food Research International.** 137: 109739.

Tang, M. C., and Copeland, L. (2007). Analysis of complexes between lipids and wheat starch. **Carbohydrate Polymers.** 67(1): 80-85.

Tatulian, S. A. (2013). Structural characterization of membrane proteins and peptides by FTIR and ATR-FTIR spectroscopy. Lipid-protein interactions: Springer. 177-218.

Tester, R. F., and Debon, S. J. (2000). Annealing of starch-a review. **International Journal of Biological Macromolecules**. 27(1): 1-12.

Tester, R. F., and Morrison, W. R. (1990). Swelling and gelatinization of cereal starches. I. Effects of amylopectin, amylose, and lipids. **Cereal Chemistry.** 67(6): 551-557.

Thaiudom, S., and Pracham, S. (2018). The influence of rice protein content and mixed stabilizers on textural and rheological properties of jasmine rice pudding. **Food Hydrocolloids,** 76: 204-215.

Tian, J., Chen, S., Wu, C., Chen, J., Du, X., Chen, J., Ye, X. (2016). Effects of preparation methods on potato microstructure and digestibility: An in vitro study. **Food Chemistry.** 211: 564-569.

Tsai, M.L., Li, C.F., and Lii, C.Y. (1997). Effects of granular structures on the pasting behaviors of starches. **Cereal Chemistry.** 74(6): 750-757.

Vamadevan, V., and Bertoft, E. (2015). Structure-function relationships of starch components. **Starch-Stärke.** 67(1-2): 55-68.

Varatharajan, V., Hoover, R., Li, J., Vasanthan, T., Nantanga, K., Seetharaman, K., . Chibbar, R. (2011). Impact of structural changes due to heat-moisture treatment at different temperatures on the susceptibility of normal and waxy potato starches towards hydrolysis by porcine pancreatic alpha amylase. **Food Research International.** 44(9): 2594-2606.

Wan, L., Li, L., Harro, J. M., Hoag, S. W., Li, B., Zhang, X., and Shirtliff, M. E. (2020). In Vitro Gastrointestinal Digestion of Palm Olein and Palm Stearin-in-Water Emulsions with Different Physical States and Fat Contents. **Journal of Agricultural and Food Chemistry**. 68(26): 7062-7071.

Wang, L., Wang, W., Wang, Y., Xiong, G., Mei, X., Wu, W., Liao, L. (2018). Effects of fatty acid chain length on properties of potato starch-fatty acid

complexes under partially gelatinization. **International Journal of Food Properties.** 21(1): 2121-2134.

Wang, S., Luo, H., Zhang, J., Zhang, Y., He, Z., and Wang, S. (2014). Alkali-induced changes in functional properties and in vitro digestibility of wheat starch: the role of surface proteins and lipids. **Journal of Agricultural and Food Chemistry.** 62(16): 3636-3643.

Wang, S., Wang, J., Yu, J., and Wang, S. (2016). Effect of fatty acids on functional properties of normal wheat and waxy wheat starches: a structural basis. **Food Chemistry.** 190: 285-292.

Wang, S., Chao, C., Cai, J., Niu, B., Copeland, L., and Wang, S. (2020). Starch–lipid and starch-lipid-protein complexes: A comprehensive review. **Comprehensive Reviews in Food Science and Food Safety.** 19(3): 1056-1079.

Wang, S., Zheng, M., Yu, J., Wang, S., and Copeland, L. (2017). Insights into the Formation and Structures of Starch-Protein-Lipid Complexes. **Journal of Agricultural and Food Chemistry.** 65(9): 1960-1966.

Wang, Y., Wang, R., Chang, Y., Gao, Y., Li, Z., and Xue, C. (2015). Preparation and thermo-reversible gelling properties of protein isolate from defatted Antarctic krill (Euphausia superba) byproducts. **Food Chemistry.** 188: 170-176.

Wu, M., Wang, J., Ge, Q., Yu, H., and Xiong, Y. L. (2018). Rheology and microstructure of myofibrillar protein-starch composite gels: comparison of native and modified starches. **International Journal of Biological Macromolecules.** 118: 988-996.

Xia, N., Wang, J.M., Gong, Q., Yang, X.Q., Yin, S.W., and Qi, J.R. (2012). Characterization and In Vitro digestibility of rice protein prepared by enzyme-assisted microfluidization: Comparison to alkaline extraction. **Journal of Cereal Science.** 56(2): 482-489.

Xue, S., Wang, C., Kim, Y. H. B., Bian, G., Han, M., Xu, X., and Zhou, G. (2020). Application of high-pressure treatment improves the in vitro protein digestibility of gel-based meat product. **Food Chemistry.** 306: 125602.

Yamin, F., Lee, M., Pollak, L. M., and White, P. J. (1999). Thermal properties of starch in corn variants isolated after chemical mutagenesis of inbred line B73. **Cereal Chemistry.** 76(2): 175-181.

Ye, A., Wang, X., Lin, Q., Han, J., and Singh, H. (2020). Dynamic gastric stability and in vitro lipid digestion of whey-protein-stabilised emulsions: Effect of heat treatment. **Food Chemistry.** 318: 126463.

Ye, J., Hu, X., Luo, S., McClements, D. J., Liang, L., and Liu, C. (2018). Effect of endogenous proteins and lipids on starch digestibility in rice flour. **Food Research International**.

Yu, S., Ma, Y., and Sun, D.W. (2009). Impact of amylose content on starch retrogradation and texture of cooked milled rice during storage. **Journal of Cereal Science.** 50(2): 139-144.

Yuan, R., and Thompson, D. (1998). Freeze-thaw stability of three waxy maize starch pastes measured by centrifugation and calorimetry. **Cereal Chemistry**. 75(4): 571-573.

Yuan, R., Thompson, D., and Boyer, C. (1993). Fine structure of amylopectin in relation to gelatinization and retrogradation behavior of maize starches from three wx-containing genotypes in two inbred lines. **Cereal Chemistry.** 70: 81-81.

Yusuph, M., Tester, R. F., Ansell, R., and Snape, C. E. (2003). Composition and properties of starches extracted from tubers of different potato varieties grown under the same environmental conditions. **Food Chemistry.** 82(2): 283-289.

Zabar, S., Lesmes, U., Katz, I., Shimoni, E., and Bianco-Peled, H. (2009). Studying different dimensions of amylose–long chain fatty acid complexes: Molecular, nano and micro level characteristics. **Food Hydrocolloids.** 23(7): 1918-1925.

Zaleska, H., Ring, S., and Tomasik, P. (2001). Electrosynthesis of potato starch-casein complexes. **International Journal of Food Science & Technology**. 36(5): 509-515.

Zaleska, H., Ring, S., and Tomasik, P. (2001). Electrosynthesis of potato starch–whey protein isolate complexes. **Carbohydrate Polymers.** 45(1): 89-94.

Zayas, J. F. (2012). **Functionality of proteins in food**: Springer science & business media.

Zhang, G., Bhopatkar, D., Hamaker, B. R., and Campanella, O. H. (2015). Self-assembly of amylose, protein, and lipid as a nanoparticle carrier of hydrophobic small molecules. **Nanotechnology and Functional Foods: Effective Delivery of Bioactive Ingredients**: 263-271.

Zhang, G., and Hamaker, B. R. (2003). A three component interaction among starch, protein, and free fatty acids revealed by pasting profiles. **Journal of Agricultural and Food Chemistry.** 51(9): 2797-2800.

Zhang, G., and Hamaker, B. R. (2004). Starch-free fatty acid complexation in the presence of whey protein. **Carbohydrate Polymers.** 55(4): 419-424.

Zhang, G., and Hamaker, B. R. (2005). Sorghum (Sorghum bicolor L. Moench) flour pasting properties influenced by free fatty acids and protein. **Cereal Chemistry.** 82(5): 534-540.

Zhang, G., Maladen, M., Campanella, O. H., and Hamaker, B. R. (2010). Free fatty acids electronically bridge the self-assembly of a three-component nanocomplex consisting of amylose, protein, and free fatty acids. **Journal of Agricultural and Food Chemistry.** 58(16): 9164-9170.

Zhang, G., Maladen, M. D., and Hamaker, B. R. (2003). Detection of a novel three component complex consisting of starch, protein, and free fatty acids. **Journal of Agricultural and Food Chemistry.** 51(9): 2801-2805.

Zheng, M., Chao, C., Yu, J., Copeland, L., Wang, S., and Wang, S. (2018). Effects of Chain Length and Degree of Unsaturation of Fatty Acids on Structure and in Vitro Digestibility of Starch-Protein-Fatty Acid Complexes. **Journal of Agricultural**

and Food Chemistry. 66(8): 1872-1880.

Zheng, M., Lin, Y., Wu, H., Zeng, S., Zheng, B., Zhang, Y., and Zeng, H. (2020). Water migration depicts the effect of hydrocolloids on the structural and textural properties of lotus seed starch. **Food Chemistry.** 315: 126240.

Zobel, H., French, A., and Hinkle, M. (1967). X-ray diffraction of oriented amylose fibers. II. Structure of V amyloses. **Biopolymers**. 5(9): 837-845.

Uarrota, V. G., Amante, E. R., Demiate, I. M., Vieira, F., Delgadillo, I., and Maraschin, M. (2013). Physicochemical, thermal, and pasting properties of flours and starches of eight Brazilian maize landraces (*Zea mays* L.). **Food Hydrocolloids.** 30(2): 614-624.
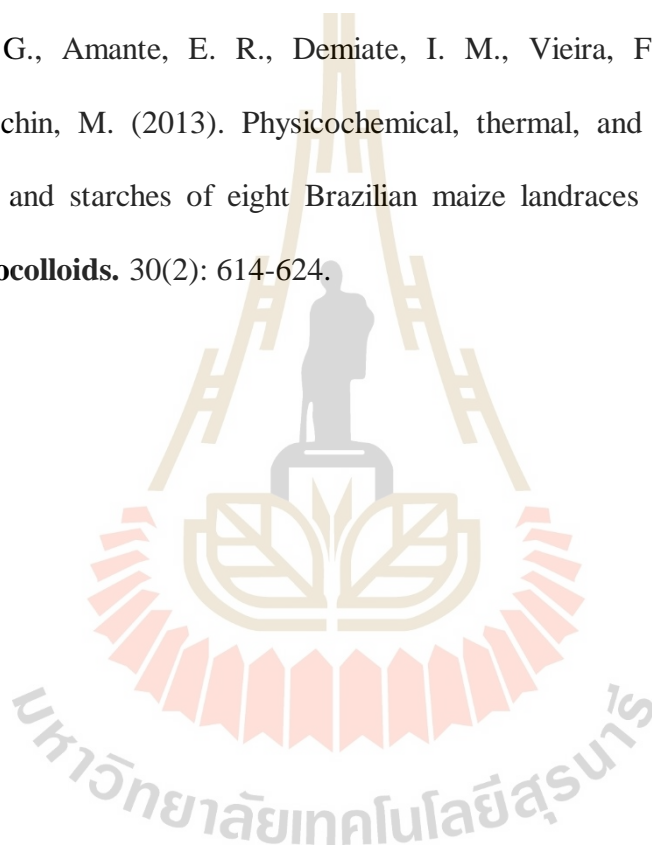
CHAPTER III

CHAPTER I THE MORPHOLOGICAL AND
PHYSICOCHEMICAL PROPERTIES OF BINARY OR
TERNARY MIXTURE SYSTEM OF GELATINIZED
POTATO STARCH, MILK PROTEIN AND SOYBEAN OIL

3.1   Abstract

This study aimed to understand the effects of the addition of MP and SBO to GPS on the structural and physicochemical properties of the GPS. Binary and ternary mixtures were prepared using GPS mixed with 10% dry starch-based MP (CA or WP) individually; with 15% dry starch based SBO; or with both the MP and SBO. The samples (potato starch paste, PSP; gelatinized potato starch-casein, GPS-CA; gelatinized potato starch-whey protein, GSP-WP; gelatinized potato starch-soybean oil, GPS-SBO; gelatinized potato starch-casein-soybean oil, GPS-CA-SBO; and gelatinized potato starch-whey protein-soybean oil, GSP-WP-SBO) were then homogenized. For the microstructural study by CLSM, MP and SBO dispersed into the 3D structure of the GPS. The rheological results revealed that GPS mixed with SBO possessed a higher viscosity and exhibited more solid-like characteristic than typical PSP. In contrast, the mixtures of GPS-CA, GPS-WP, GPS-CA-SBO, and GPS-WP-SBO, displayed a lower viscosity and exhibited more liquid-like rather than PSP. This research provides an understanding of the effect of food ingredient interactions

on structural arrangement and provides the knowledge about physicochemical properties of the interactions mimicking the real food systems.

Keywords: Potato starch, Casein, Whey protein, Soybean oil

3.2   Introduction

Starch, protein, and lipids are the main components of staple foods. During the process of food processing, changes in these components lead to complex interactions which impact the quality, physicochemical properties, and nutritional characteristics of the products. Starch is the main energy storage material for most plants. It is widely used as a source of carbohydrates in food. The complex between starch and lipids may exist in natural starch or be formed in the process of food processing or during storage. The interaction between starch and lipid was widely studied in previous work (Tang and Copeland, 2007; Zabar, Lesmes, Katz, Shimoni, and Bianco-Peled, 2009). The complex formed by amylose and fat could reduce the swelling power and solubility of starch, improve the gelatinization stability of starch, and delay the retrogradation of starch (Crowe, Seligman, and Copeland, 2000; Eliasson, 1994; Goni, Garcia Alonso, and Saura Calixto, 1997; Guraya, Kadan, and Champagne, 1997). As an important part of the human diet, protein, especially MP provided enough essential amino acids for human-beings. However, the binary mixture of protein and starch in aqueous solution could present three different equilibrium states: compatibility, thermodynamic incompatibility, and complex coacervation (or complexation) (Sjoo and Nilsson, 2017). On the other hand, protein-lipid interactions were also found in many foods which help to maintain the structure and stability of the food system (Alzagtat and Alli, 2002; Patino, García, and Niño, 2001). The main driving force of protein-lipid

interaction was electrostatic force and the water dispersing bonding mechanism (Ioffe, Gorbenko, Deligeorgiev, Gadjev, and Vasilev, 2007). Lipoprotein complexes could change the digestibility and flavor binding ability of foods (Taha and Mohamed, 2004).

In recent years, much research focused on the interaction between starches, proteins, and lipids, in both binary and ternary mixtures. Zhang et al. (2003) studied the ternary interaction of maize starch, protein, and FFA in the process of starch gelatinization. Wang et al. (2017) monitored the gelatinization and gelatinization characteristics of the starch system model in the presence of FAs and/or lactoglobulin, to better understand the formation of starch-protein-lipid complexes (Wang, Wang, Liu, Wang, and Copeland, 2017; Wang, Zheng, Yu, Wang, and Copeland, 2017). They also found that the length and unsaturation of FAs had an impact on the structure of the ternary complex (Wang, Wang, Yu, and Wang, 2016). Huang et al. (2018) prepared three-component blends of expanded corn starch, corn oil, and zein using high-speed homogenization and heat treatment. The heat treatment affected the structure and physicochemical properties of the blends.

Mashed potato made from 100% fresh potato tubers was a kind of natural vegetable semi-solid food. It was a popular side dish served in restaurants and homes. It was consumed with a soft and delicate consistency with a clearly perceptible moisture or with a harder and drier consistency. In order to improve the taste and texture of mashed potatoes, milk and oil were typically added during the mashed potato cooking process (Alvarez, Canet, and Fernandez, 2008; Alvarez, Fernandez, and Canet, 2010; Alvarez, Fernandez, Olivares, Jimenez, and Canet, 2013; Conforti, Lupano, and Yamul, 2013; Fernandez, Canet, and Alvarez, 2009). Mashed potato was

a mixture of PS, milk, salt, oil, and water. Complex interactions could influence the properties of the mashed potato mixture (Fernandez, Alvarez, and Canet, 2008). Therefore, the study of the molecular and physicochemical basis of starch-protein interactions with or without oils in mashed potatoes was important for the development of protein and plant oil in starchy food technology. In this study, PS, MP (CA or WP), and SBO as the raw materials were used to create a model system for mashed potato products. Binary and ternary mixtures were prepared by mixing GPS and MP or SBO separately and by mixing both MP and SBO with GPS via homogenization. Confocal microscope and rheometer were used to study the interactions for different combinations of the raw materials in order to better understand the structure of starch, protein and oil mixtures and the interaction among them during food processing.

3.3 Material and Methods

3.3.1 Materials

The potato starch was purchased from Bangkok Inter Food Co., Ltd. (Bangkok, Thailand). Micellar Casein concentrates powder with 82% (w/w) total protein was received from Vicchi Enterprise Co., Ltd. (Bangkok, Thailand). WP was purchased from Shanghai Yuanye Biological Technology Co., Ltd. (Shanghai, China). The SBO (Cook Brand, Bangkok, Thailand) used in the study was purchased from a local supermarket in Nakhon Ratchasima province, Thailand. 8-amino-1,3,6-pyrenetrisulfonic acid (APTS), Fluorescein isothiocyanate isomer I (FITC), Nile Red, ethyl alcohol, acetone, and other chemicals used in this study were of analytical grade.

3.3.2   Proximate analysis

The fat, protein, ash, and moisture content of the raw materials were measured using official AOAC methods (AOAC 2000). FAs of the SBO were determined according to the method of AOAC 969.33 (2000) by Gas chromatography (7890 GC system, Agilent Technologies Inc., Santa Clara, USA).

The total starch content of the samples (initial amount of starch) was analyzed using a method derived from Megazyme (Megazyme International Ireland Ltd., Wicklow, Ireland). About 100 mg of the sample was wetted with 0.2 ml of 80% v/v ethanol before it was stirred in an ice/water bath in the presence of 2 ml of KOH. Eight ml of 1.2 M sodium acetate buffer (pH 3.8) was added to each tube, allowed to rotate on a magnetic stirrer. Thermostable α-amylase and amyloglucosidase (0.1 ml each) were immediately added and mixed well. Then the tubes were placed in a water bath at 50°C. Afterwards, the tubes were incubated for 30 min with intermittent mixing on a vortex mixer. The glucose content (starch = 0.9×glucose) was determined using D-glucose assay and the absorbance was measured at 510 nm against a reagent blank. D-glucose assay procedure see appendix A.

3.3.3   Sample preparation

The binary and ternary component system were prepared according to the methods of Huang et. al (2018) with a slight modification, following a real mashed potato system.

For the ternary-component system, the ratio of PS, MP, and SBO was 10:1:1.5. Deionized water was added to make the proportion of PS to be 10% in total concentration. First, 6 g of PS (dry starch base) was weighted in a 100 ml centrifuge tube. Then, deionized water (nearly 40 g) was added to the tube to prepare a potato

starch suspension. The suspension was heated to 95°C in a water bath for 30 minutes. The suspension was stirred for the first 4 mins to prevent the potato starch from caking, resulting in a gelatinized potato starch (GPS). In a mean time, the CA or WP (0.6 g, dry starch base) was weighed in a beaker, and deionized water (nearly 8 g) was added to prepare a CA or WP solution. MP (CA or WP) solution (pH: CA solution = 7.07; WP solution = 5.86) and SBO (0.9 g) were heated in a 95°C water bath for 30 mins. After the formation of the GPS, the tubes which contained MP or SBO were taken out from the water bath, and the milk solution and/or SBO were added to the GPS. Water (95°C) was also added to make the total weight of mixture as 60 g. These mixtures were mixed at room temperature for 1 min. After the temperature of the sample reduced from 95°C to 60°C, the sample was blended by homogenization (IKA T25 digital, Staufen, German) at 10,000 rpm for 3 min, with break intervals every 60 s. Finally, the binary or ternary-component mixture paste was cooled to 50°C. These mixtures were structural observed by CLSM and were determined for their rheological property. The details of these analyses would be mentioned further in the following.

SBO, PSP, CA or WP solutions were individually used as negative controls. The composition of each sample is shown in Table 3.1. The methods to make a one phase-water mixture (PSP, CA, WP, SBO) and a binary-component mixture (GSP-CA, GSP-WP, GPS-SBO, CA-SBO, WP-SBO) were the same as the method used for the ternary-component mixture but only use corresponding ingredients (see Table 3.1). Supplementary notes, PSP was obtained by homogenizing GPS after adding water. GPS-CA, GPS-WP and GPS-SBO were obtained by homogenizing GPS with MP or SBO and water. GPS-CA-SBO and GPS-WP-SBO were obtained by homogenizing GPS after adding MP, SBO, and water.

Table 3.1 The samples with different ingredient compositions.

Number	Name	Ingredients				
		Gelatinized potato starch (GPS)	Casein	Whey protein	Soybean oil	Water
1	Potato starch paste (PSP)	√				√
2	Casein (CA)		√			√
3	Whey protein (WP)			√		√
4	Soybean oil (SBO)				√	√
5	Gelatinized potato starch-Casein (GPS-CA)	√	√			√
6	Gelatinized potato starch-Whey protein (GPS-WP)	√		√		√
7	Gelatinized potato starch-Soybean oil (GPS-SBO)	√			√	√
8	Casein-Soybean oil (CA-SBO)		√		√	√
9	Whey protein-Soybean oil (WP-SBO)			√	√	√
10	Gelatinized potato starch-Casein-Soybean oil (GPS-CA-SBO)	√	√		√	√
11	Gelatinized potato starch-Whey protein-Soybean oil (GPS-WP-SBO)	√		√	√	√

3.3.4 Microstructure analysis

3.3.4.1 Digital photograph analysis

All freshly prepared samples were packed in a 5 ml transparent glass bottle. All prepared samples were placed in a black 3D camera box with a digital of 60 cm. Eleven samples were placed in a straight line, and each sample was separated by 0.5 cm. The samples were photographed with a digital camera (Canon EOS80D, Canon Crop., Tokyo, Japan). Fresh samples were also poured into the Petri dish, which was placed in the camera box. Each sample was marked and photographed with Canon EOS80D camera.

3.3.4.2 Microstructure analysis

The microstructures of the fresh samples were revealed using CLSM (Nikon A1R, Nikon Crop., Tokyo, Japan), following Thaiudom and Pracham (2018). CLSM was equipped with 405, 488, and 561 nm lasers. GPS was dyed with APTS in distilled water while CA or WP was dyed with FITC in acetone. SBO was dyed with Nile Red (0.1% w/v, dissolving in absolute ethyl alcohol). APTS gave blue color while FITC and Nile red provided green and red colors, respectively. The fluorescence excited at 405 nm for the blue channel (425-475 nm), at 488 nm for the green channel (500-550 nm), and at 561 nm for the red channel (570-620 nm). The fresh sample (around 0.2 ml) was placed in a tube, then a drop of APTS (around 10 μl) was thoroughly mixed with a fresh sample and the stained samples were stored at ambient temperature for 10 min. Then the samples were continuously strained with FITC, for 10 min. After that, the samples were strained for 10 mins with Nile red. Finally, the stained samples were placed on slides and covered with cover slides. The samples were observed by an objective lens magnified 20 or 40 times. There were at least 6 images taken for the microstructure of each sample.

3.3.5 Rheological measurements

3.3.5.1 Steady shear

The rheological properties of the fresh samples were measured using an Anton-Paar MCR302 (Anton Paar, Graz, Austria) with a cone-plate probe (cone angle of 1° and a plate radius of 60 mm). A 2 min balance was performed before each test (Li, Ye, Zhou, Lei, and Zhao, 2019). The shear rate range of steady shear measurements was gradually increased from 0.01 s^{-1} to 100 s^{-1}. The samples were measured at 37 °C simulated the human body temperature. The data of shear stress (τ)

and shear rate ($\dot{\gamma}$) were fitted to the Herschel-Bulkley model (Equation (3.1)) to characterize the rheological behavior of the samples in terms of yield stress (τ_0, Pa), consistency coefficient (K, Pa s^n) and flow behavior index (n, dimensionless), respectively (Wang et al., 2018). Herein, τ is the shear stress (Pa), and ($\dot{\gamma}$) is the shear rate (s^{-1}).

$$\tau = \tau_0 + K\dot{\gamma}^n \tag{3.1}$$

3.3.5.2 Oscillatory shear

In small amplitude oscillatory shear, the frequency varied from 0.01 Hz to 10 Hz, and an amplitude strain of 0.1% were applied, within the linear viscoelastic region (LVR). In order to determine the LVR, strain sweep was performed at a constant frequency of 0.5Hz in a range of 0.01% to 100% strain. For the dynamic oscillatory shear measurements, the G' and G'' with a frequency in the range of 0.01-10 Hz were recorded, and the corresponding loss tangent (tan $\delta = G''/G'$) was also documented. The tracks of both moduli were fitted to the power models of $G'(\omega) = k'\omega^{n'}$ and $G''(\omega) = k''\omega^{n''}$. Here, k' and k'' are consistency coefficients (Pa s^n), n' and n'' are behavior indices (Gao et al., 2019).

3.3.6 Statistical analysis

Measurements of all experiments were carried out in triplicate. The results were expressed as mean±standard deviation. Statistical analyses were conducted using SPSS 23.0. In all statistical analyses, $p<0.05$ was considered significant.

3.4 Results and Discussions

Before this part of the experiment begins, some preliminary experiments have been done. The preliminary experiments aimed to understand the effects of adding CA and SBO on the structural and rheological properties of the PSP. Binary and ternary mixtures were prepared using GPS mixed with CA (10% w/w of dry starch basis) and/or 15% w/w SBO (dry starch basis). GPS, CA, and SBO were mixed by homogenization process at 12500 rpm for 1 min and the final mixture had a starch content of 10% (w/w, dry basis). The rheological property results revealed that with the addition of CA, no matter addition of SBO or not, the mixture displayed a lower viscosity and exhibited a more liquid-like behaviour. Freeze-dried samples were made to detect the structural-bonding study of the mixtures. FTIR spectroscopy and XRD were used to analyze the short-range structure and long-range structure of the freeze-dried samples. It was found that there was no covalent interaction among GPS, CA, and SBO. The experimental methods and results are shown in Appendix B.

3.4.1 Chemical composition

Table 3.2 shows the chemical composition of potato starch, CA, WP, and SBO. The main component of PS is starch, with a starch content of 76.77% w/w, and an amylose content of 31.14% w/w. Protein was the main component of CA and WP and the protein content was 81.25% w/w and 78.67% w/w, respectively. The main component of SBO was fat and the fat content is 99.9% w/w.

The composition and proportion of fatty acids in fat are shown in Table 3.3. The GC chromatogram of FAs in SBO is shown in Appendix Fig C.1. SBO contained a large number of polyunsaturated FAs, accounting for 61% of SBO. Linoleic, Oleic, Palmitic, Linolenic, and Stearic were the main FAs in SBO.

Table 3.2 Chemical composition of the raw materials.

Chemical compositions	Potato starch	Micellar casein	Whey protein concentrate	Soybean oil
Moisture (%)	17.90±0.03	7.92±0.08	5.08±0.09	0.06±0.00
Protein (%)	0.13±0.13	81.25±2.86	78.67±4.65	0.00±0.00
Ash (%)	0.23±0.04	7.38±1.45	3.14±0.06	0.05±0.00
Fat (%)	0.22±0.06	0.492±0.04	0.795±0.06	99.9±0.01
Starch (%)	76.77±2.80			
Amylose/Starch (%)	31.14±0.01			

Table 3.3 Fatty acid profile of soybean oils sold in the maket.

Name	The proportion (%)	Ret Time (min)
C14:0 (Myristic)	0.081	24.127
C14:1 (Myristoleic)	0.017	26.006
C16:0 (Palmitic)	10.839	28.562
C16:1 (Palmitoleic)	0.0913	30.558
C18:0 (Stearic)	3.621	35.778
C18:1n9c (Oleic)	22.983	39.019
C18:2n6c (Linoleic)	53.666	43.575
C20:0 (Arachidic)	0.344	44.960
C18:3n6 (Calendic acid)	0.334	45.927
C18:3n3 (Linolenic)	7.326	47.115
C21:0 (Heneicosylic)	0.028	48.492
C20:2(Dihomo-linoleic)	0.031	50.014
C22:0 (Behenic)	0.453	51.735
C23:0 (Tricosylic)	0.045	55.129
C24:0 (Lignoceric)	0.114	58.726
C24:1(Nervonic)	0.025	60.561
Total Saturated FAs	15.526	
Total Monounsaturated FAs	23.117	
Total Polyunsaturated FAs	61.024	
Totals	100	

3.4.2 Microstructure analysis

3.4.2.1 Digital photograph

Figure 3.1   Photos of the fresh samples. 1. PSP: Potato starch paste; 2. CA: Casein solution; 3. WP: Whey protein solution; 4. SBO: Soybean oil-water mixture; 5. GPS-CA: Gelatinized potato starch-Casein; 6. GSP-WP: Gelatinized potato starch-Whey protein; 7. GPS-SBO: Gelatinized potato starch-Soybean oil; 8. CA-SBO: Casein-Soybean oil; 9. WP-SBO: Whey protein - Soybean oil; 10. GSP-CA-SBO: Gelatinized potato starch-Casein-Soybean oil; 11. GSP-WP-SBO: Gelatinized potato starch-Whey protein-Soybean oil.

All freshly prepared samples are shown in Fig. 3.1. The fresh samples were poured into the petri dishes and were photographed, as shown in the first column of the figure in Appendix D. Although the transparency and color depth of each sample were different, all samples were relatively uniform, without an obvious stratification or particles. Fig. 3.1-1 shows the image of PSP. The PSP has a certain transparency (Zhou et al., 2014). Transparency value depended on granule size, swelling capabilities, amylose content, amylose/amylopectin ratio, and level of swollen and non-swollen granule remnants. CA and WP are milky white particles, so

the solution of CA and WP in this study also exhibited the white and opaque solution. It liked the color of milk. Oil and water were incompatible (Damodaran, Parkin, and Fennema, 2007) but after homogenizing, the oil dispersed into the water, making the solution cloudy and opaque. In other binary or ternary systems, mixtures containing MP (GPS-CA, GPS-WP, GPS-CA-SBO, and GPS-WP-SBO) also showed the milky white only the binary sample of GPS-SBO possessed a color similar to that of PSP.

3.4.2.2 CLSM analysis

Microstructures of all fresh samples were determined by CLSM (Fig. 3.2). Their images from different channels (405 nm, 488 nm, or 561 nm) are shown in Appendix D 1-3. PSP was stained by APTS giving a blue color as shown in Fig. 3.2 (1-PSP). From this figure, there was no granular substance in the PSP sample, indicating that PS was completely gelatinized and the texture of the PSP was uniform (Chen et al., 2011). Moreover, the figure illustrated that the PS granules were nearly completely destroyed after homogenization since the image revealed that there were no discernible particles and the PS granules formed a continuous integrated matrix (Chen et al., 2017). CA and WP were stained with FITC, giving a brighter green color as shown in Fig. 3.2 (2-CA and 3-WP). It was found that CA exhibited larger particles than WP because CA possessed calcium phosphate as a coexisting composition in a unique highly hydrated spherical complex that made CA form micelles which were larger than WP molecules (Horne, 2017). SBO was stained by Nile Red, giving a red color in Fig. 3.2 (4-SBO).
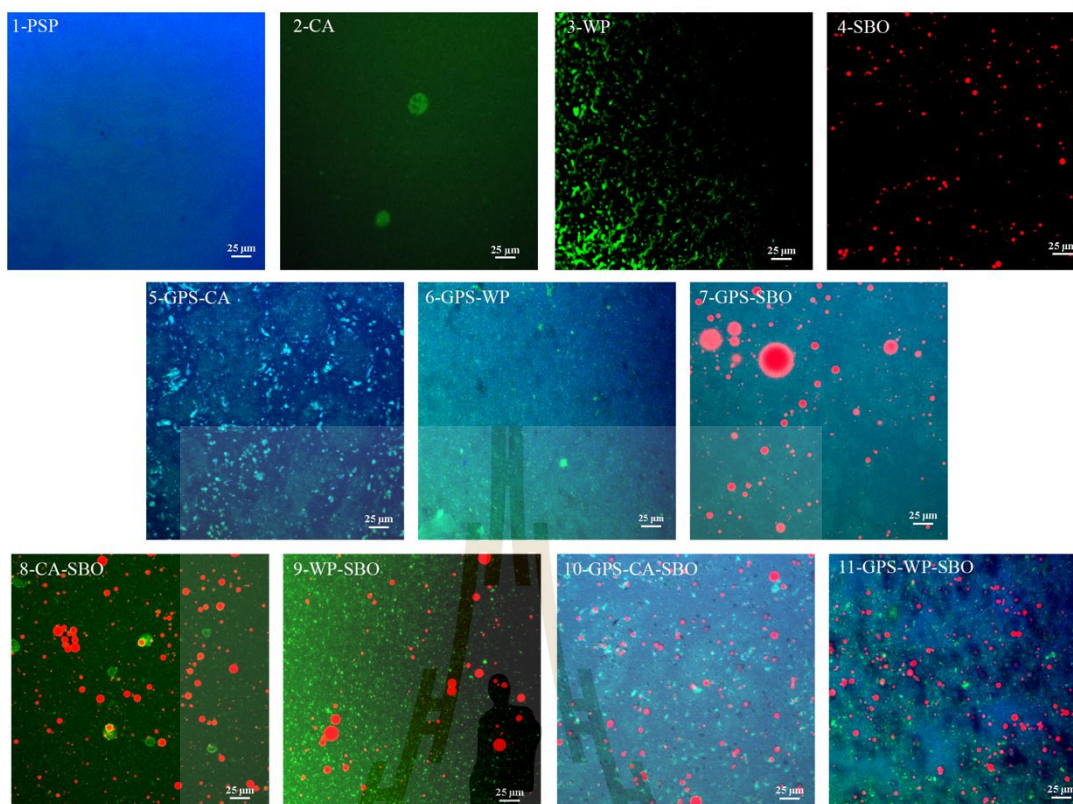
Figure 3.2 Confocal laser scanning microscopy (CLSM) images of fresh samples.
Sample code: 1. PSP; 2. CA; 3. WP; 4.SBO; 5. GPS-CA; 6. GPS-WP;
7.GPS-SBO; 8. CA-SBO; 9. WP-SBO; 10. GPS-CA-SBO; 11.GPS-WP-
SBO.

In a binary system, for the GPS-CA sample, Fig. 3.2 (5-GPS-CA)
shows that CA was scattered in the 3D networks of GSP. This phenomenon was
similar to the phenomenon of separation between polysaccharide and protein
(Doublier, Garnier, Renard, and Sanchez, 2000; Kett et al., 2013). For the GPS-SBO
interaction sample (Fig. 3.2 (7-GPS-SBO)), the distribution of SBO droplets in GSP-
3D networks seemed to be inhomogeneous since there are large and small round sized
SBO particles in this image which identified that SBO and PS overlapped each other

(Chen et al., 2018). This implied that there were interactions between SBO and GPS in this sample and the starch-lipid complex might be formed. For the Casein- Soybean oil (8-CA-SBO) sample, the yellow color in the image represented that the SBO overlapped with the CA. CA could be absorbed on the surface of the SBO because there were many non-polar amino acids in CA and the polarity of amino acid in CA was not uniform so that the CA could form hydrophobic interactions with the hydrophobic parts of the SBO at the boundary of oil-water interface (Kruif, Huppertz, Urban, and Petukhov, 2012; Fernandez et al., 2008). This seemed to make the sample more stable in terms of thermodynamic stability of the oil in emulsion system (Gandova and Balev, 2016). Different from the CA-SBO, the image of the Whey protein-Soybean oil (9-WP-SBO) did not show a yellow color, because the WP dispersed evenly over the whole system. Unlike CA, the distribution sequence of the hydrophobicity, polarity, and charged residues of WP were uniform. As a result, these proteins fold intramolecularly, burying most of their hydrophobic residues so that widespread self-binding or interactions with other proteins did not occur (Damodaran et al., 2007).

For the ternary system samples, GPS-CA-SBO (Fig. 3.2-10) and GPS-WP-SBO (Fig. 3.2-11) showed that the CA or WP and SBO were dispersed into the 3D networks of PSP. SBO was more homogenous in the ternary system than in the GPS-SBO binary system. A possible explanation for this phenomenon might be that MP played the emulsifying role during the homogenization process when MP and SBO were both added into the GPS (Liang et al., 2017).

3.4.3   Rheological properties

3.4.3.1   Steady shear measurement

Steady shear flow curves of the PSP, binary, and ternary mixtures are shown in Fig. 3.3 (A). Shear stress as a function of shear rate for PSP, GPS-CA, GPS-WP, GPS-SBO, GPS-CA-SBO, and GPS-WP-SBO is illustrated in Fig. 3.3 (B), and the corresponding parameters of the rheological behaviors are summarized in Table 3.4. For the paste systems with or without MP and/or SBO, the viscosities decreased with an increase of shear rate, resulting in pseudo plastic fluids with shear-thinning behavior. This could be explained that potato starch could hydrate with water for gelatinization, consequently the amorphous region of potato starch granules swelled, and the amylose could leach out from the potato starch granule. This resulted in a loss of the crystalline structure of the potato starch (Olkku and Rha, 1978). Moreover, the physicochemical properties of potato starch might be affected by processing. For this study, amylopectin in the GSP was shear cut at high speed by a homogenizer during the mixing process (Che et al., 2009). Therefore, their viscosity was much lower than that of GPS, while the amylose found in this starch generally possessed a shorter length, resulting in a lower impact on the sample viscosity (Bertoft and Blennow, 2016).

The addition of MP and/or SBO changed the viscosity of the PSP. In comparison with PSP, however, the effect of the addition of SBO into the GPS was not significantly different. This result might be explained by the fact that SBO droplets still existed in the GSP in the form of droplets, and it entered the 3D networks of GSP (Fig. 3.2-7). Different from GSP-SBO, the GSP mixed with CA or WP had a significantly lower viscosity during all the studied shear rates as compared with PSP.
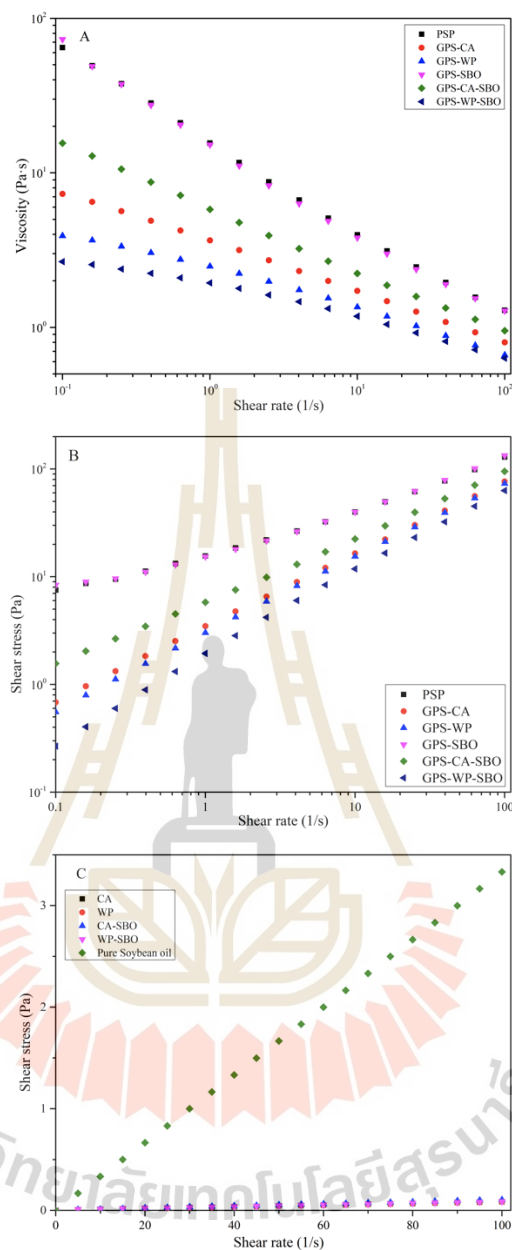
Figure 3.3 (A) Flow curves of the pastes (37°C). (B) Shear stress as a function of shear rate for PSP, GPS-CA, GPS-WP, GPS-SBO, GPS-CA-SBO and GPS-WP-SBO. (C) Shear stress as a function of shear rate for Casein solution (CA), Whey solution (WP), Casein-Soybean oil (CA-SBO), Whey protein - Soybean oil (WP-SBO) and pure Soybean oil.

This might be because CA and WP could disperse into much smaller particles than SBO droplets during homogenization. (See Figure 3.2) The viscosity of GPS-WP was less than that of GPS-CA because WP had a smaller particle size than that of CA, resulting in less resistance to flow in the system when the shear force was applied (Gazi and Huppertz, 2015). On the other hand, the viscosity of SBO, CA solution, WP solution, CA-SBO solution, and WP-SBO solution was less than that of the samples from the binary and/or ternary systems (Fig. 3.3C). The viscosity of these sample solutions without GPS was low viscosity Newtonian fluids.

The Herschel-Bulkley equation is a widely used model for pseudoplastic materials. The flow curves of studied samples were fitted to this model and R^2 values varied between 0.99 to 1 (Table 3.4). The n value for all mixtures was less than 1, which meant that the mixtures exhibited shear-thinning behavior. The smaller the n value, the stronger the pseudoplasticity and the closer to solid-like properties (Li et al., 2019; Wang et al., 2018). The consistency coefficient (K) reflected the viscosity of mixtures. The larger the K value is, the greater the viscosity of the mixture is (Steffe, 1996). Compared with PSP, the addition of SBO into the GPS showed a higher value for yield stress (τ_0) and for flow behavior index (n) but a lower value for K. This result might be due to the increase of solid content and the interaction between starch and SBO (Wang et al., 2018). Different from GPS-SBO, the samples with the addition of MP (GPS-CA and GPS-WPS) presented lower values for τ_0 and K but higher values in n, compared with those for PSP. Potato starch had high polyelectrolyte property due to its high phosphate content (Swinkels, 1985). The GPS appear as a kind of 'super-swelling' polyelectrolyte gel (Donnan effect), and the entanglement density between amylopectin molecules was relatively low (Kelly, Van

Wagenberg, Latham, and Mitchell, 1995). The reduction in viscosity after mixing with

MP was associated with nonspecific ionic strength effects (Considine et al., 2011).

Phosphate has a negative charge, and casein also has a negative charge at this study

condition. They repel each other, so this might lead to phase separation. Interestingly,

to compare GPS-CA-SBO with GPS-CA, GPS-CA-SBO had a higher K value and

lower n value than GPS-CA. Contrarily, GPS-WP-SBO had a lower K value and

higher n value than GPS-WP. It might be related to the differences in the structural

and functional properties between CA and WP. The interaction between CA's

hydrophobic group and SBO occurred as the result of the addition of both CA and

SBO, so the effect of CA on the decrease of PSP viscosity was weakened by SBO

(Liang et al., 2017). On the other hand, WP was an inert filler that prevented amylose

from rearranging and weaken the starch gel (Carvalho, Onwulata, and Tomasula,

2007; Shim and Mulvaney, 2001). The SBO allowed the oil and WP to better disperse

into the GPS in the GPS-WP-SBO sample.

3.4.3.2 Oscillatory shear

Strain sweeps were conducted to study the LVR

characteristics of the paste samples. The LVR and nonlinear viscoelastic regions of the

different samples are shown in Fig. 3.4. The stain in the range of 0.01% to1 % was

within the LVR of these samples. In this test, 0.1% was selected as the strain value for

the dynamic oscillatory shear measurements. Fig. 3.5 (A) shows G', G'', and $tan\ \delta$

versus frequency plots for the paste samples measured at 37°C. The data of Fig. 3.5

(A) were fitted to the power law model and the rheological parameters of the samples

were quantitatively described (Table 3.5).

Table 3.4 Parameters of the Herschel-Bulkley functions describing dependence on shear stress and shear rate of the pastes.

Paste samples	τ_0 (Pa)	K (Pa sn)	n	R^2
PSP	5.66 ± 1.57^a	9.43 ± 1.47^a	0.55 ± 0.03^d	0.99
GPS-CA	0.04 ± 0.065^b	3.46 ± 0.16^{bc}	0.67 ± 0.002^{bc}	0.99
GPS-WP	0	2.72 ± 0.22^c	0.69 ± 0.009^b	0.99
GPS-SBO	6.43 ± 1.29^b	8.60 ± 1.12^a	0.58 ± 0.013^d	0.99
GPS-CA-SBO	0.53 ± 0.36^b	4.75 ± 0.29^b	0.64 ± 0.01^c	0.99
GPS-WP-SBO	0	2.18 ± 0.18^c	0.73 ± 0.001^a	1

The rheological parameters of steady shear including yield stress (τ_0), consistency coefficient (K), and flow behavior index (n), which were obtained by fitting the shear stress (τ) and shear rate ($\gamma\cdot$) data from the steady shear rheological curves across the specific fitting range to Herschel- Bulkley model of $= \tau_0 + K\dot{\gamma}^n$. [a-d] Data bearing different superscript lowercase letters in the same column are significantly different ($p<0.05$).
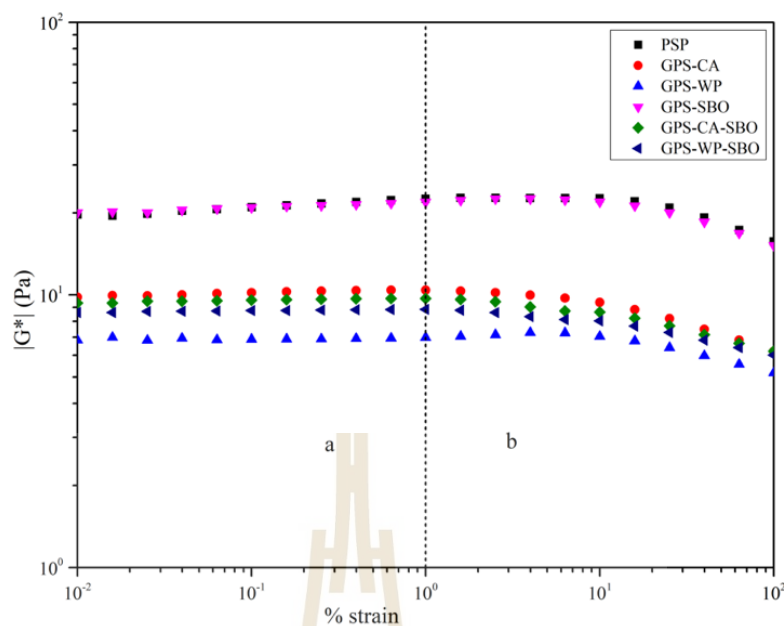
Figure 3.4 The linear viscoelastic regions of different pastes (a. linear viscoelastic region b. Nolinear viscoelastic region).

Clearly, for all samples, both moduli displayed strong frequency dependency, showing that when the frequency increased, the moduli also increased. The difference in the dynamic rheological properties was related to the ingredients of the sample. PSP and PSP-SBO exhibited a solid-like behavior with higher G' than G'' (tan δ<1) for the whole range of studied frequency. In contrast, other paste samples including GPS-CA, GPS-CA-SBO, GPS-WP, and GPS-WP-SBO, displayed a liquid-like behavior with the G' value lower than the G'' value (tan δ >1). In comparison with PSP, the addition of SBO into the GPS had a higher elastic and viscous modulus. This phenomenon was relevant to the viscosity results of PSP and GPS-SBO. With the addition CA or WP into GPS, the binary system displayed a significant decrease in modulus and an increase in loss tangent (tan δ) compared with PSP. The MP seemed to act as an inactive filler to prevent amylose rearrangement and weaken the GPS to

form a gel (Thaiudom and Pracham, 2018). The addition of CA and SBO together decreased modulus values and increased the tan δ of GPS-CA-SBO compared with GPS-CA. However, the modulus and tan δ values of the PSP with the addition WP and SBO had no significant difference with the PSP containing WP.
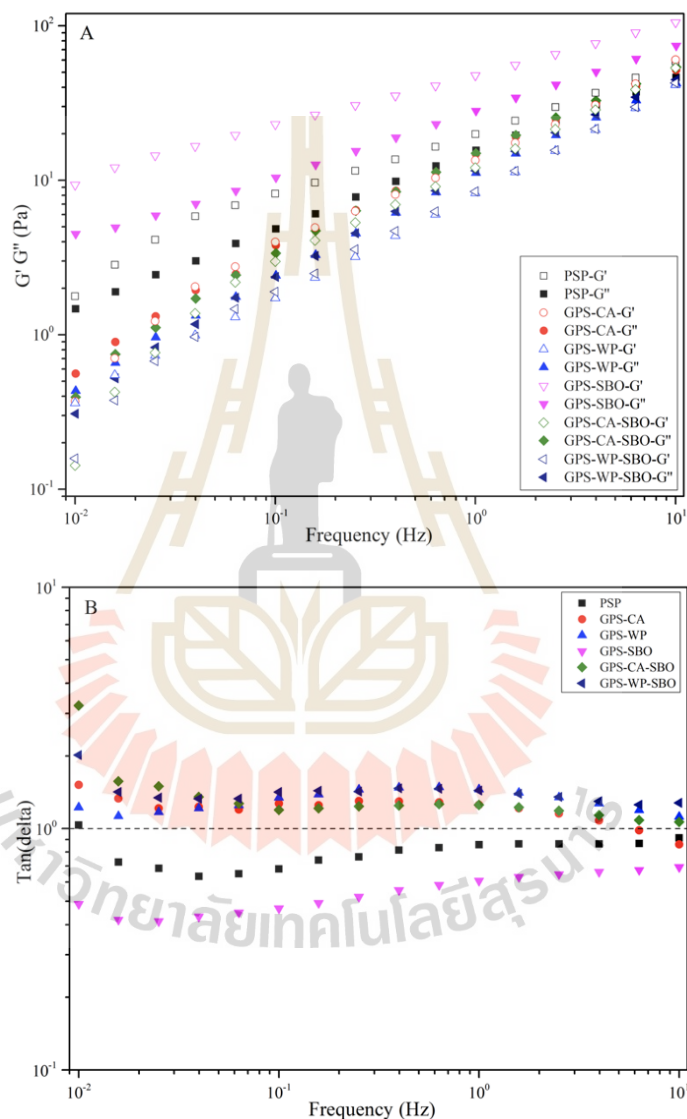
Figure 3.5 Frequency sweeps (A, B) of the pastes (37°C). Frequency-dependence of storage modulus (G', open symbols) and loss modulus (G'', filled symbols) was recorded at 0.1% strain and then loss tangent (tan δ) was derived.

Table 3.5 Data of dynamic oscillatory shear measurements fitting to $G' = k'\omega^{n'}$, $G'' = k''\omega^{n''}$, respectively.

Paste samples	k'	n'	R^2	k''	n''	R^2
PSP	20.15 ± 11.32^b	0.47 ± 0.10^{ab}	0.99	15.25 ± 3.92^b	0.48 ± 0.03^b	0.99
GPS-CA	13.04 ± 8.68^b	0.7 ± 0.16^a	0.99	14.38 ± 3.67^b	0.56 ± 0.03^a	0.99
GPS-WP	8.08 ± 2.62^b	0.72 ± 0.14^a	0.99	10.96 ± 0.92^b	0.59 ± 0.01^a	0.99
GPS-SBO	48.07 ± 19.58^a	0.35 ± 0.06^b	0.99	27.76 ± 8.84^a	0.43 ± 0.02^c	0.99
GPS-CA-SBO	11.57 ± 3.81^b	0.68 ± 0.19^a	0.99	14.52 ± 3.06^b	0.57 ± 0.02^a	0.99
GPS-WP-SBO	8.21 ± 2.06^b	0.69 ± 0.10^a	0.99	11.27 ± 0.80^b	0.60 ± 0.02^a	0.99

[a-c] The rheological parameters of dynamic oscillatory shear measurements include k' and k'' refer to the consistency coefficients (Pa.sn), while n', n'' are the behavior indexes. [a-c] Data bearing different superscript lowercase letters in the same column are significantly different ($p<0.05$).

3.5 Conclusions

The addition of MP and SBO to GPS would change the structure and physicochemical properties of the GPS. CA or WP and SBO were dispersed into the GPS's 3D networks, resulting in changes to the structure and viscosity of the GPS. MP had more impact on the rheological properties than the SBO. The addition of MP could reduce the viscosity of GPS significantly. Interaction between MP and SBO affected the viscosity of the GPS. This study provided a better understanding of binary and ternary interactions among GPS, MP, and SBO. In addition, it could provide future guidance for food products which contain starch, protein, and vegetable oil.

3.6 References

Alvarez, M., Canet, W., and Fernandez, C. (2008). Effect of addition of cryoprotectants on the mechanical properties, colour and sensory attributes of fresh and frozen/thawed mashed potatoes. **European Food Research and Technology.** 226(6): 1525-1544.

Alvarez, M. D., Fernandez, C., and Canet, W. (2010). Oscillatory rheological properties of fresh and frozen/thawed mashed potatoes as modified by different cryoprotectants. **Food and Bioprocess Technology**. 3(1): 55.

Alvarez, M. D., Fernandez, C., Olivares, M. D., Jimenez, M. J., and Canet, W. (2013). Sensory and texture properties of mashed potato incorporated with inulin and olive oil blends. **International Journal of Food Properties.** 16(8): 1839-1859.

Alzagtat, A. A., and Alli, I. (2002). Protein-lipid interactions in food systems: a review. **International Journal of Food Sciences and Nutrition**. 53(3): 249-260.

Bertoft, E., and Blennow, A. (2016). **Structure of potato starch.** Advances in potato chemistry and technology: Elsevier. 57-73.

Carvalho, C. W., Onwulata, C., and Tomasula, P. (2007). Rheological properties of starch and whey protein isolate gels. **Food Science and Technology International**. 13(3): 207-216.

Che, L.M., Wang, L.J., Li, D., Bhandari, B., Özkan, N., Chen, X. D., and Mao, Z.H. (2009). Starch pastes thinning during high-pressure homogenization. **Carbohydrate Polymers.** 75(1): 32-38.

Chen, He, X., Zhang, B., Fu, X., Li, L., and Huang, Q. (2018). Structure, physicochemical and in vitro digestion properties of ternary blends containing swollen maize starch, maize oil and zein protein. **Food Hydrocolloids.** 76: 88-95.

Chen, P., Yu, L., Simon, G. P., Liu, X., Dean, K., and Chen, L. (2011). Internal structures and phase-transitions of starch granules during gelatinization. **Carbohydrate Polymers.** 83(4): 1975-1983.

Chen, X., Du, X., Chen, P., Guo, L., Xu, Y., and Zhou, X. (2017). Morphologies and gelatinization behaviours of high-amylose maize starches during heat treatment. **Carbohydrate Polymers.** 157: 637-642.

Conforti, P. A., Lupano, C. E., and Yamul, D. K. (2013). Rheological, thermal and sensory properties of whey protein concentrate/pectin-fortified mashed potatoes made from dehydrated flakes. **International Journal of Food Science & Technology**. 48(5): 1035-1040.

Considine, T., Noisuwan, A., Hemar, Y., Wilkinson, B., Bronlund, J., and Kasapis, S. (2011). Rheological investigations of the interactions between starch and milk proteins in model dairy systems: A review. **Food Hydrocolloids.** 25(8): 2008-2017.

Crowe, T. C., Seligman, S. A., and Copeland, L. (2000). Inhibition of enzymic digestion of amylose by free fatty acids in vitro contributes to resistant starch formation. **The Journal of nutrition**. 130(8): 2006-2008.

Damodaran, S., Parkin, K. L., and Fennema, O. R. (2007). **Fennema's food chemistry**: CRC press.

De Kruif, C. G., Huppertz, T., Urban, V. S., and Petukhov, A. V. (2012). Casein micelles and their internal structure. **Advances in Colloid and Interface Science.** 171: 36-52.

Doublier, J.L., Garnier, C., Renard, D., and Sanchez, C. (2000). Protein-polysaccharide interactions. **Current opinion in Colloid & interface Science.** 5(3-4): 202-214.

Eliasson, A. C. (1994). Interactions between starch and lipids studied by DSC. **Thermochimica Acta.** 246(2): 343-356.

Fernandez, C., Alvarez, M., and Canet, W. (2008). Steady shear and yield stress data of fresh and frozen/thawed mashed potatoes: Effect of biopolymers addition. **Food Hydrocolloids.** 22(7): 1381-1395.

Fernandez, C., Canet, W., and Alvarez, M. (2009). Quality of mashed potatoes: effect of adding blends of kappa-carrageenan and xanthan gum. **European Food Research and Technology.** 229(2): 205.

Gandova, V., and Balev, D. (2016). Properties of emulsions based in soybean oil stabilized by different proteins. **Int J Inn Sci Eng Technol.** 3: 293-297.

Gao, R., Ye, F., Wang, Y., Lu, Z., Yuan, M., and Zhao, G. (2019). The spatial-temporal working pattern of cold ultrasound treatment in improving the sensory, nutritional and safe quality of unpasteurized raw tomato juice. **Ultrasonics sonochemistry.** 56: 240-253.

Gazi, I., and Huppertz, T. (2015). Influence of protein content and storage conditions on the solubility of caseins and whey proteins in milk protein concentrates. **International Dairy Journal.** 46: 22-30.

Goni, I., Garcia Alonso, A., and Saura Calixto, F. (1997). A starch hydrolysis procedure to estimate glycemic index. **Nutrition Research**. 17(3): 427-437.

Guraya, H. S., Kadan, R. S., and Champagne, E. T. (1997). Effect of rice starch-lipid complexes on in vitro digestibility, complexing index, and viscosity. **Cereal**

Chemistry. 74(5): 561-565.

Horne, D. S. (2017). **Characteristics of milk.** Fennema's Food Chemistry: CRC Press. 907-953

Ioffe, V. M., Gorbenko, G. P., Deligeorgiev, T., Gadjev, N., and Vasilev, A. (2007). Fluorescence study of protein-lipid complexes with a new symmetric squarylium probe. **Biophysical Chemistry.** 128(1): 75-86.

Kelly, R., Van Wagenberg, M., Latham, J., and Mitchell, J. (1995). A rheological comparison between the effects of sodium caseinate on potato and maize starch. **Carbohydrate Polymers.** 28(4): 347-350.

Kett, A. P., Chaurin, V., Fitzsimons, S. M., Morris, E. R., O'Mahony, J. A., and Fenelon, M. A. (2013). Influence of milk proteins on the pasting behaviour and microstructural characteristics of waxy maize starch. **Food Hydrocolloids.** 30(2): 661-671.

Li, S., Ye, F., Zhou, Y., Lei, L., and Zhao, G. (2019). Rheological and textural insights into the blending of sweet potato and cassava starches: In hot and cooled pastes as well as in fresh and dried gels. **Food Hydrocolloids.** 89: 901-911.

Liang, Y., M, L., Gillies, G., Patel, H., Ye, A., and Golding, M. (2017). The heat stability of milk protein-stabilized oil-in-water emulsions: A review. **Current Opinion in Colloid & Interface Science**. 28: 63-73.

Olkku, J., and Rha, C. (1978). Gelatinisation of starch and wheat flour starch-a review. **Food Chemistry.** 3(4): 293-317.

Patino, J. M. R. g., García, J. M. N., and Niño, M. R. R. g. (2001). Protein–lipid interactions at the oil-water interface. **Colloids and Surfaces B: Biointerfaces.** 21(1-3): 207-216.

Shim, J., and Mulvaney, S. J. (2001). Effect of heating temperature, pH, concentration and starch/whey protein ratio on the viscoelastic properties of corn starch/whey protein mixed gels. **Journal of the Science of Food and Agriculture.** 81(8): 706-717.

Sjoo, M., and Nilsson, L. (2017). Starch in food: Structure, function and applications: CRC Press.

Steffe, J. F. (1996). Rheological methods in food process engineering: Freeman press.

Swinkels, J. (1985). Composition and properties of commercial native starches. **Starch-Stärke.** 37(1): 1-5.

Taha, F., and Mohamed, S. (2004). Effect of different denaturating methods on lipid–protein complex formation. **LWT-Food Science and Technology**. 37(1): 99-104.

Tang, M. C., and Copeland, L. (2007). Analysis of complexes between lipids and wheat starch. **Carbohydrate Polymers**. 67(1): 80-85.

Thaiudom, S., and Pracham, S. (2018). The influence of rice protein content and mixed stabilizers on textural and rheological properties of jasmine rice pudding. **Food Hydrocolloids**. 76: 204-215.

Wang, L., Wang, W., Wang, Y., Xiong, G., Mei, X., Wu, W., Liao, L. (2018). Effects of fatty acid chain length on properties of potato starch–fatty acid complexes under partially gelatinization. **International Journal of Food Properties.** 21(1): 2121-2134.

Wang, S., Wang, J., Yu, J., and Wang, S. (2016). Effect of fatty acids on functional properties of normal wheat and waxy wheat starches: a structural basis. **Food Chemistry.** 190: 285-292.

Wang, S., Wang, S., Liu, L., Wang, S., and Copeland, L. (2017). Structural orders of wheat starch do not determine the in vitro enzymatic digestibility. **Journal of Agricultural and Food Chemistry**. 65(8): 1697-1706.

Wang, S., Zheng, M., Yu, J., Wang, S., and Copeland, L. (2017). Insights into the Formation and Structures of Starch-Protein-Lipid Complexes. **Journal of Agricultural and Food Chemistry.** 65(9): 1960-1966.

Wang, Y., Ye, F., Liu, J., Zhou, Y., Lei, L., and Zhao, G. (2018). Rheological nature and dropping performance of sweet potato starch dough as influenced by the binder pastes. **Food Hydrocolloids.** 85: 39-50.

Zabar, S., Lesmes, U., Katz, I., Shimoni, E., and Bianco-Peled, H. (2009). Studying different dimensions of amylose-long chain fatty acid complexes: Molecular, nano and micro level characteristics. **Food Hydrocolloids.** 23(7): 1918-1925.

Zhang, G., and Hamaker, B. R. (2003). A three component interaction among starch, protein, and free fatty acids revealed by pasting profiles. **Journal of Agricultural and Food Chemistry.** 51(9): 2797-2800.

Zhou, H., Wang, C., Shi, L., Chang, T., Yang, H., and Cui, M. (2014). Effects of salts on physicochemical, microstructural and thermal properties of potato starch. **Food Chemistry.** 156: 137-143.

CHAPTER IV

CHAPTER I THE STRUCTURE OF BINARY AND TERNARY MIXTURE SYSTEM OF GELATINIZED POTATO STARCH, MILK PROTEIN AND SOYBEAN OIL

4.1 Abstract

This study aimed to understand the effects of the addition of MP and SBO to GPS on the structural properties of the GPS. Binary and ternary mixtures were prepared using GPS mixed with 10% w/w (dry starch-based) MP (CA or WP) individually; with 15% w/w (dry starch based) SBO; or with both the MP and SBO. FTIR, Raman spectrometer, and XRD were used to study the interactions for different combinations in each mixture. The results of FTIR, Raman, and XRD analyses showed that there were no covalent interactions among GSP, MP, and SBO in this research, and no binary and ternary complex formation. After gelatinization of the potato starch and the homogenization of mixtures, the amorphous region of the potato starch increased while the short-range molecular order and the degree of crystallinity of the potato starch decreased. Compared to other samples, GPS-WP and GPS-WP-SBO possessed a bigger amorphous region and a less degree of crystallinity. The ternary systems of GPS-CA-SBO and GPS-WP-SBO showed lower FWHM values than the binary system of GPS-SBO, indicating a higher crystallinity of complexes formed in the presence of MP (CA or WP). However, the relative crystallinity (RC) of

the mixtures was lower than that for the PSP because the addition of MP, SBO, and both MP and SBO could retard the retrogradation of the PSP.

Keywords: Potato starch, Casein, Whey protein, Soybean oil, interaction.

4.2   Introduction

Starch, protein, and lipids are the three macronutrients which provide the body's energy in human diet. These three components are found in many food systems, especially starchy foods. These macronutrients undergo a series of changes and interactions during food processing. They have a significant impact on the quality attributes of the finished food, including taste, texture, shelf life and nutritional value (Ji, 2020; Parada and Santos, 2016; Ye et al., 2018). Understanding how these interactions occur in the food processing process will help optimize production and develop new food products with ideal microstructure and function. Mashed potatoes are a starchy food with MP and vegetable oil (Alvarez, Fernandez, and Canet, 2010; Álvarez, Fernández, Olivares, Jiménez, and Canet, 2013). In the Chapter III, a mashed potato model with PS, MP and vegetable oil as raw materials was established for simulation, and the simulated mashed potato model has been tested by confocal microscope and rheometer. In this chapter, the structure of the mashed potato model would be further analyzed by FTIR, Raman spectrometer, and XRD.

In recent decades, the complex of starch and lipids has been a focus of research, while the study of starch-protein-lipid complex is a relatively new field, and the current research results are still limited (Cai et al., 2021; Cervantes-Ramírez et al., 2020; Li, Shi, Du, Dong, and Yu, 2021). Many analytical methods have been used to characterize the formation and structure of binary and ternary complexes. These

methods include thermal, spectral, diffraction, imaging techniques, and so on (Wang et al., 2020).

FTIR has been used to detect the formation of starch-lipid complexes and starch-lipid-protein complexes because the interaction between starch and lipids changes the position of the lipid band (Wang et al., 2018; Wang, Zheng, Yu, Wang, and Copeland, 2017). FTIR was widely used for the structural characterization of proteins or peptides (Li, Li, Fox, Gidley, and Dhital, 2020; Tatulian, 2013). Although this method did not provide precise atomic resolution of the molecular structure, it was very sensitive to the conformational changes that occur in protein-functional transitions or intermolecular interactions. The interaction of the functional group of PS and CA also could be detected by infrared spectroscopy (Grega et al., 2003). As a non-destructive technique, Raman spectroscopy has been widely used to characterize the short-range molecular sequence of the double helix in starch samples (Zheng et al., 2020). The FWHM at 480 cm^{-1} could be used to predict the formation of starch-lipid complexes and characterize the degree of their ordered structure (Wang, Wang, Yu, and Wang, 2016). In recent years, Raman spectroscopy was used to detect short-range molecular order changes of starch-lipid complex and starch-lipid-protein complex (Chao et al., 2018; Wang et al., 2018; Wang et al., 2017). XRD techniques was widely used to characterize crystalline materials and provide information about crystal structure and cell size (Blazek and Gilbert, 2011). The distant structural sequence of natural starches was usually characterized using XRD, which resulted in three diffraction patterns, namely A-, B-, and C- (Sarko and Wu, 1978). In contrast, starch-lipid complexes exhibited a different XRD pattern, known as V-type. The long-range ordered structure of starch-lipid-protein complex by XRD showed the same V-shaped diffraction peak as starch-lipid complex (Hai and Yinxia, 2016).

In this chapter, the mashed potato model was prepared by the same method as the previous chapter. Binary and ternary mixtures were prepared by mixing GPS and MP or SBO separately and by mixing both MP and SBO with GPS via homogenization. FTIR, Raman spectrometer, and XRD were used to study the interactions for different combinations of the raw materials. Finally, this part of the study might give the information about ingredient interaction in binary and ternary systems composing potato starch, MP, and SBO.

4.3 Materials and methods

4.3.1 Materials

PS was purchased from Bangkok Inter Food Co.,Ltd. (Bangkok, Thailand). Micellar casein concentrates power with 82% (w/w) curd protein was received from Vicchi Enterprise Co., Ltd. (Bangkok, Thailand). WP was purchased from Shanghai Yuanye Biological Technology Co.,Ltd. SBO (Cook Brand) used in this study was purchased from a local supermarket in Nakhon Ratchasima province, Thailand. Potassium bromide (KBr) and all other chemicals used in this study were of analytical grade.

4.3.2 Sample preparation

The binary-component complex and ternary-component was prepared according to the method of 3.3.3. The composition of each sample is shown in Table 3.1. The 11 samples were then cooled down and frozen immediately (-80°C) in the freezer (Haier, Biomedical, Qingdao, China). The frozen samples were freeze-dried to avoid any further retrogradation. After freeze-drying, the dried samples were gently ground with a mortar and pestle, and then passed through a 60-mesh screen sieve. The

powder was stored in a laminated plastic bag at room temperature until further analysis (by FTIR, Raman spectroscopy, and XRD) but not exceed one week.

4.3.3 FTIR spectroscopy

The freeze-dried samples were mixed with KBr powder and pressed into transparent tablets. The spectrum of the tablets was recorded by a FTIR spectrometer (Spectrum 100, Perkin Elmer Inc., MA) after pretreatment at room temperature. The tablets were scanned at a resolution of $4 \ cm^{-1}$ in the wavelength range of 400-4000 cm^{-1}. To separate the peaks in the fingerprint region (about 900-1200 cm^{-1}) and to receive the area of each peak, the obtained spectrum obtained was treated by using baseline correction and then deconvoluted by using PeakFit software (version 4.12). The area of each peak was calculated (approximately 1049, 1022, and 995 cm^{-1}). Peak area ratios 1049 to 1022 cm^{-1} (1049/1022) and 1022 to 995 cm^{-1} (1022/995) were obtained.

4.3.4 Raman spectroscopy

An appropriate amount of freeze-dried powder was taken for analysis with a Raman spectrometer (DXR$_2$, Thermo Fisher Scientific, Massachusetts, USA). Using a microscope with a 20× lens, the excitation laser beam (785 nm excitation line of Ar-laser in Spectra-Physics) was focused on the sample placed on a glass slide. The laser power was set at $15 \ mW$. The recorded spectra ranged from $200 \ cm^{-1}$ to $3100 \ cm^{-1}$, with an average of 40 scans per spectrum and a resolution of $4 \ cm^{-1}$. The exposure time was 5 s and the slit width was 50 μm. Omnic software (version 9, Thermo Nicolet Inc., Waltham, MA, USA) was used to process Spectral data for automatic baseline correction, automatic smoothing, and standardization. The FWHM of 480 cm^{-1} was obtained by the software to characterize the short-range molecular

order of the starch samples. The spectral peaks of the wavenumbers between 900 cm^{-1} and 1800 cm^{-1} were resolved using Ominc software mentioned previously.

4.3.5 XRD

The freeze-dried samples were analyzed after 1-week of being in equilibrium in saturated NaCl solution at room temperature. The X-ray patterns were obtained from an X-ray 700 diffractometer (Shimadzu, Tokyo, Japan) with copper tubes (λ=1.5418 Å) at 40 kV and 40 mA. The samples were packed tightly but carefully avoid the sample deforming in a glass cell and scanned at a rate of 2 °/min with a step time of 0.95 s and a sampling width 0.02° over the range of 4° to 40° (2θ). The RC of the samples was calculated by using Jade 6.5 software (Materials Data Inc., Livermore, CA, USA).

4.3.6 Statistical analysis

Measurements of FTIR, and Raman spectrum were carried out in triplicate. The X-ray experiment was conducted in duplicate. The results were expressed as mean±standard deviation. Statistical analyses were conducted using SPSS 23.0. In all statistical analyses, $p<0.05$ was considered significant.

4.4 Results and Discussion

4.4.1 FTIR spectroscopy

FTIR spectra of oven dried PS, and the freeze-dried PSP, GPS-CA, GPS-WP, GPS-SBO, GPS-CA-SBO, GPS-WP-SBO, CA, WP, CA-SBO, and WP-SBO are presented in Fig. 4.1. The FTIR of the PSP were exactly similar with that of the PS, and there were no new absorption peaks. PS and PSP both had a characteristic FTIR absorption band at 3700-3000 cm^{-1}, which was associated with the hydroxyl

group. The absorption band at 2937 cm^{-1} was associated with the CH$_2$ deformation; at 1643 cm^{-1} with the adsorbed water of the starch amorphous region; and 1150 cm^{-1} with C-O and C-C stretching (Kizil, Irudayaraj, and Seetharaman, 2002). After the addition of MP to the samples: GPS-CA, GPS-WP, GPS-CA-SBO, GPS-WP-SBO, the binary and ternary mixtures had a characteristic peak about 1541 cm^{-1}, which was assigned to the deformation vibration of amino acids and the amide II absorption in samples of CA and WP (Wang et al., 2017; Zaleska, Ring, and Tomasik, 2001). After the addition of SBO to the samples: GPS-SBO, GPS-CA-SBO, GPS-WP-SBO, the binary and ternary mixtures had a characteristic peak at about 2850 cm^{-1}, which was attributed to the vibration of carbonyl groups. The characteristic peak at about 1750 cm^{-1} was attributed to the C-H asymmetric stretching vibration of the methylene groups of fatty acids (Yang, Irudayaraj, and Paradkar, 2005). Comparing the binary and ternary mixtures with PSP, the FTIR spectra of the binary and ternary mixtures had new characteristic peaks with the addition of new substances. However, the wavenumber of new characteristic peaks did not shift as compared with the corresponding new substances, indicating that there were no covalent interactions among GSP, MP, and SBO in this research.

The deconvoluted FTIR spectra between 1200 cm^{-1} and 900 cm^{-1} of PS, GPS-CA, GPS-WP, GPS-SBO, GPS-CA-SBO, GPS-WP-SBO are shown in Fig. 4.2. The PS had absorbency mainly at 1049, 1022, and 995 cm^{-1} in this region. The characteristic peak at 1049 cm^{-1} of the absorption band was assigned to the orderly area of PSP; the 1022 cm^{-1} peak was associated with the amorphous region; and the 995 cm^{-1} peak was derived from the bonding in the carbohydrate (Wang, Li, Copeland, Niu, and Wang, 2015). The absorbance intensity ratio of 1022/995 cm^{-1} was related to the amorphous region, while the strength ratio of 1049/1022cm^{-1} was related
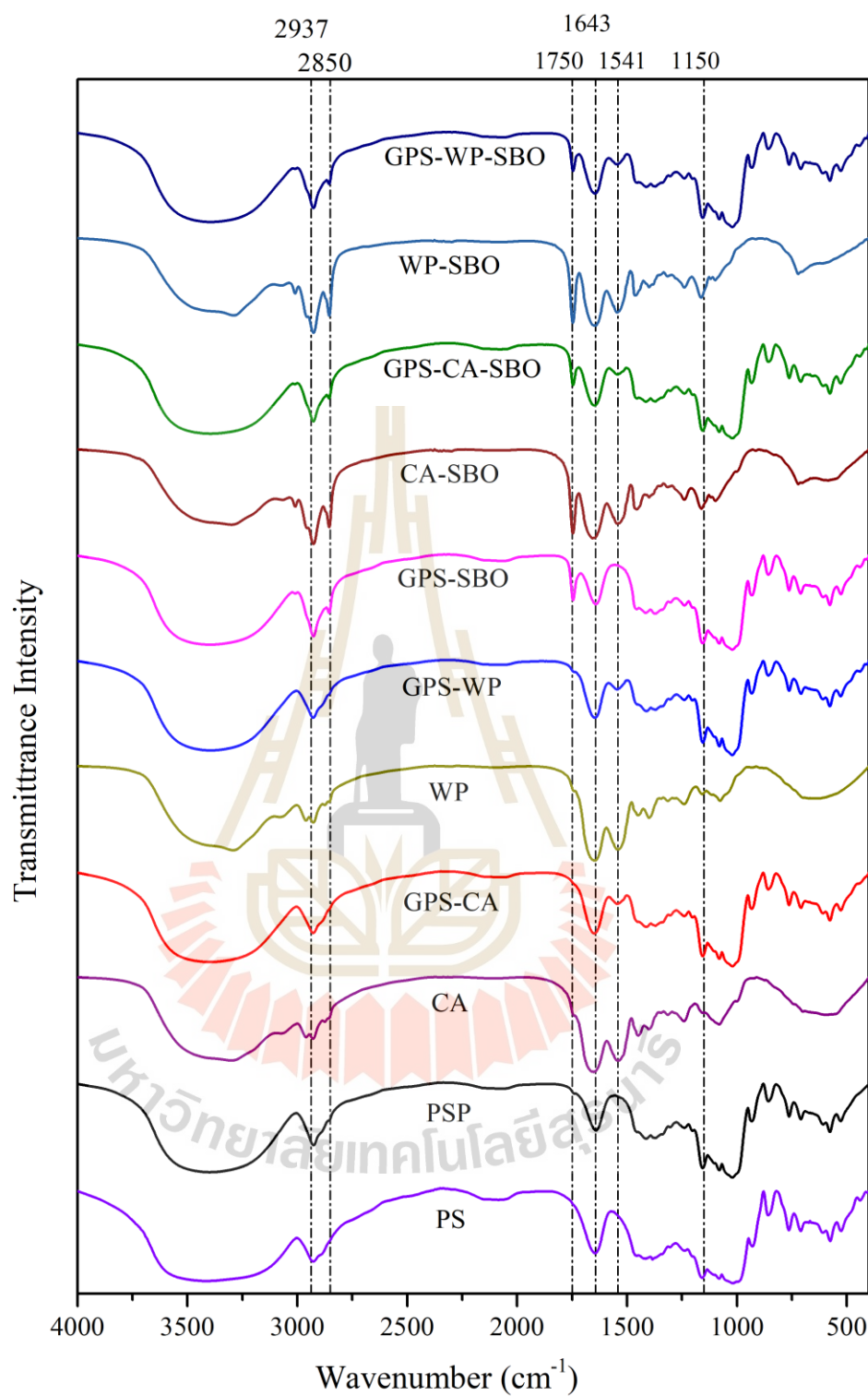
Figure 4.1 FTIR spectra of potato starch (PS) and freeze-dried powders including PSP, GPS-CA, GPS-WP, GPS-SBO, GPS-CA-SBO, GPS-WP-SBO, CA, WP, CA-SBO and WP-SBO.
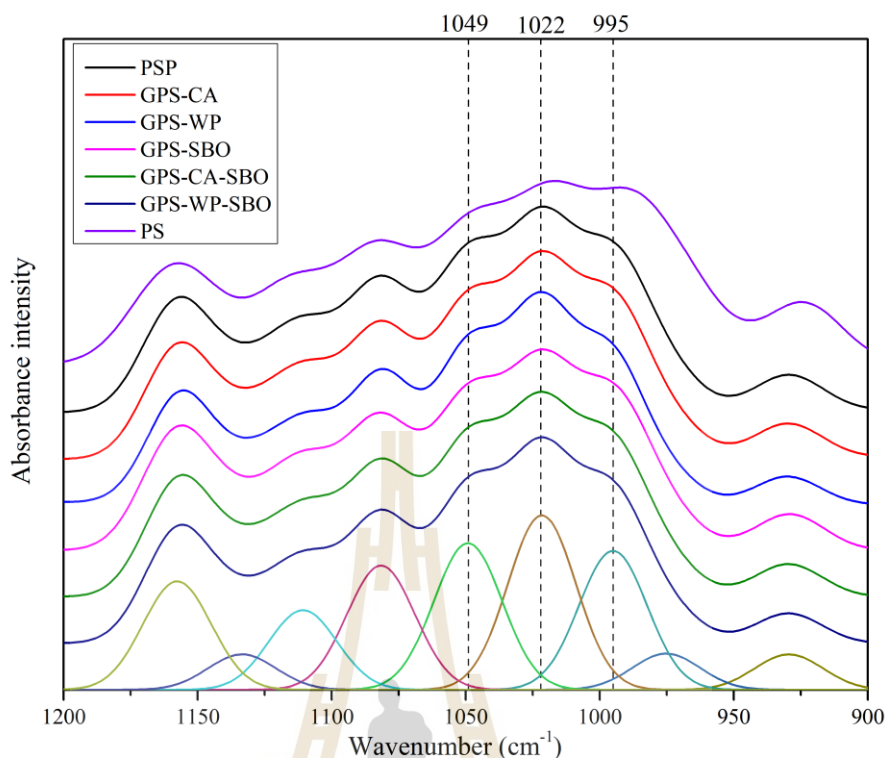
Figure 4.2 Deconvoluted FT-IR spectrum between $1200\,\mathrm{cm}^{-1}$ and $900\,\mathrm{cm}^{-1}$ of PS
and freeze-dried powder including PSP, GPS-CA, GPS-WP, GPS-SBO,
GPS-CA-SBO and GPS-WP-SBO. The peaks fitted of the PSP is shown
at the bottom.

to the degree of crystallinity of starch. The calculation results of the ratio of
$1049\,\mathrm{cm}^{-1}/1022\,\mathrm{cm}^{-1}$ and $1022\,\mathrm{cm}^{-1}/995\,\mathrm{cm}^{-1}$ of PS, PSP, GPS-CA, GPS-WP, GPS-
SBO, GPS-CA-SBO, and GPS-WP-SBO are illustrated in Table 4.1. The PS had the
least amorphous region and a higher degree of crystallinity because it was not
gelatinized and the structure was not destroyed (Liu, Charlet, Yelle, and Arul, 2002).
Compared to other samples, GPS-WP and GPS-WP-SBO had a bigger amorphous
region and a less degree of crystallinity. The reason was that WP had a smaller

particle size than that of the CA and SBO, which could better destroy the 3D structure of the GPS during the mixing processing (O'Mahony and Fox, 2014).

Table 4.1 Ratio of 1049 cm^{-1}/1022 cm^{-1} and 1022 cm^{-1}/995 cm^{-1} of PS, PSP, GPS-CA, GPS-WP, GPS-SBO, GPS-CA-SBO and GPS-WP-SBO.

Samples	1022/995	1049/1022
PS	1.11±0.01[d]	0.859±0.01[a]
PSP	1.26±0.01[c]	0.836±0.01[c]
GPS-CA	1.25±0.00[c]	0.832±0.00[cd]
GPS-WP	1.35±0.00[a]	0.814±0.01[e]
GPS-SBO	1.25±0.01[c]	0.847±0.00[b]
GPS-CA-SBO	1.24±0.03[c]	0.845±0.00[b]
GPS-WP-SBO	1.29±0.03[b]	0.825±0.01[d]

[a-e]Values are means±SD. Means with similar letters in a column do not differ significantly ($p > 0.05$).

4.4.2 Raman spectroscopy

Raman spectroscopy had been used as an analytical tool to determine the short-range molecular order of starch and to obtain the information on the structural changes of starch, protein, edible oils, and fats (Kizil et al., 2002; Rygula et al., 2013; Wang et al., 2015; Yang et al., 2005). This information gave a better understanding of the formation of binary and ternary mixtures. The Raman spectra of PS, and the freeze-dried PSP, GPS-CA, GPS-WP, GPS-SBO, GPS-CA-SBO, and GPS-WP-SBO are shown in Fig. 4.3. While the FWHM of the band at 480 cm^{-1} are listed in Table 4.2.
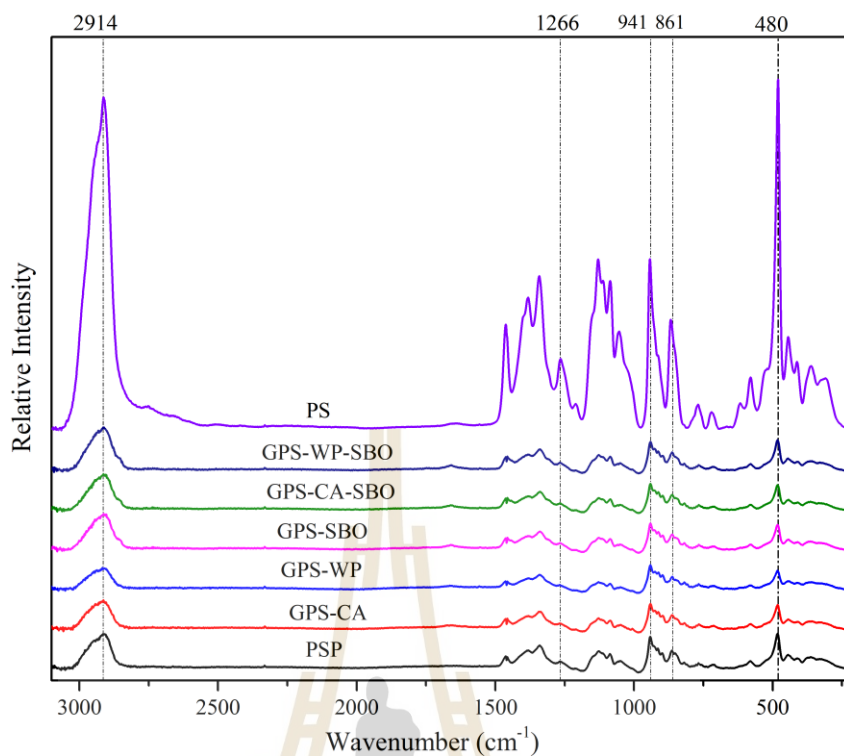
Figure 4.3 Raman spectra of PS and frozen dried powder including PSP, GPS-CA, GPS-WP, GPS-SBO, GPS-CA-SBO and GPS-WP-SBO.

PS showed the strongest bands at 480, 861, 941, 1266, and 2914 cm^{-1}, which are related to vibration in the pyranose ring of glucose, C (1)-H and CH_2 deformation, C-O-C skeletal mode vibrations of the α-1,4 glycosidic linkages, skeletal (C-C-O), and C-H stretching, respectively (Mutungi, Passauer, Onyango, Jaros, and Rohm, 2012; Wang et al., 2015). Compared with the weaker intensity for the spectrum of PS and PSP, PS had a greater structural order while the crystal structure of the GPS was destroyed. This result might be explained by the fact that the gelatinization and homogenization process changed the structure of the starch granules (Chen et al., 2017). The intensity within the region of 3000-2800 cm^{-1} could be associated with the changes of amylose and amylopectin contents in PS (Kizil et

al., 2002). Obviously, the intensity of the Raman spectrum in this scope was greatly reduced after gelatinization and homogenization. This might be due to the shear cut of the swollen amylopectin by homogenization, resulting in a corresponding increase in the amylose content (Li, Zhang, and Zheng, 2019). The Raman spectra of PS, freeze-dried CA, WP, CA-SBO, WP-SBO are presented in Fig. 4.4. Some peaks were related to SBO including 3013 cm^{-1} (=C–H stretching (asymmetry)), 2856 cm^{-1} (C–H stretching (asymmetry)), 1750 cm^{-1} (C=O stretching), 1660 cm^{-1} (C=C stretching) and 1447 cm^{-1} (C–H bending)) (Yang, Joseph, Manish, 2005).
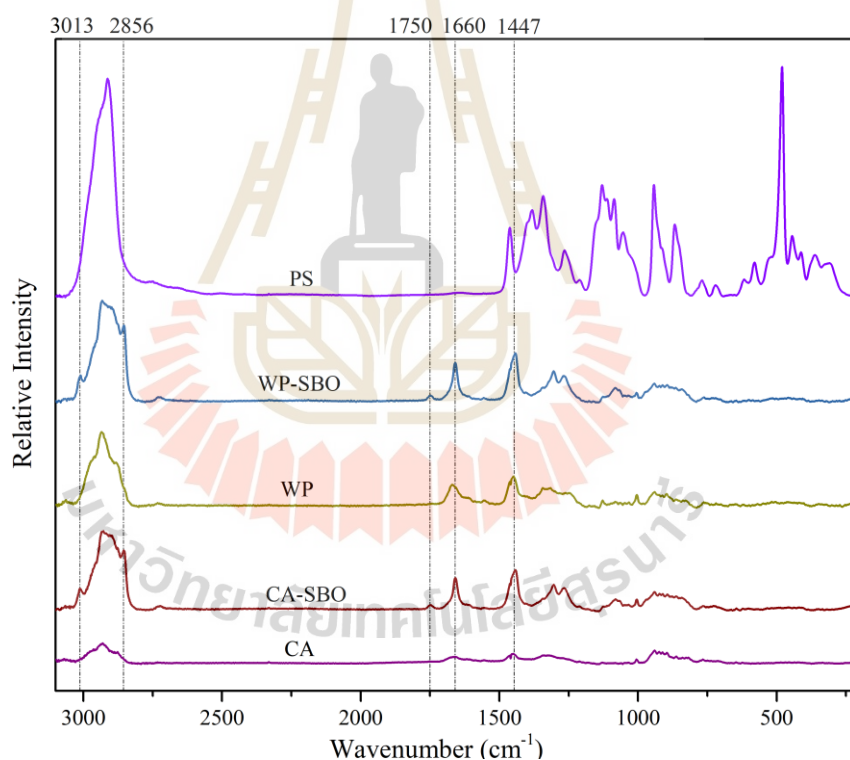
Figure 4.4 Raman spectra of RS and frozen dried powder including CA, WP-CA-SBO, WP-SBO.

The FWHM at 480 cm^{-1} of Raman spectra could be used to characterize the degree of ordered structure in starch, whereas the peaks located at

480 cm^{-1} were also characterized by the polymerization degree of polysaccharides (Li et al., 2019). A smaller FWHM value and a stronger absorption intensity at 480 cm^{-1} indicated a greater structural order. For all the pastes, PSP had the lowest FWHM value indicating that the PSP had a greater short-range molecular order. However, this result differed from Wang's studies (Wang et al., 2017) in which they found that the maize starch paste had a larger FWHM value than the maize starch pastes mixed with β-lactoglobulin, FAs, or β-lactoglobulin and FAs. There were two possible explanations for this result. One reason might be that the samples were processed in different ways. Wang's samples were mixed during the gelatinization process, while the samples of the current study were gelatinized first, then mixed again after it was chilled. During the cooling and freeze-drying process, the starch paste would retrograde which resulted in a smaller FWHM value (Fechner, Wartewig, Kleinebudde, and Neubert, 2005). The other reason might be the addition of protein and/or oil which could change the structure of GPS and inhibit its retrogradation (Hu et al., 2020; Wang, Zhang, Wang, Ai, and Xiong, 2020), so that the PSP had a stronger structure and a lower FWHM value compared with other samples. After the addition of MP (CA or WP) to GPS, the mixtures (GPS-CA or GPS-WP) had a relatively higher FWHM value than the other samples (PSP, GPS-SBO, GPS-CA-SBO, and GPS-WP-SBO), indicating that there were weak interactions between SP and MP (Li et al., 2019). The ternary samples (GPS-CA-SBO and GPS-WP-SBO) showed lower FWHM values than the GPS-SBO mixture, indicating there was higher crystallinity of complexes formed in the presence of MP. This might be because the addition of MP promoted the formation of a starch-oil complex, thus increasing the number of starch-lipid complexes (Chao et al., 2018).

Table 4.2 FWHM of the band at 480 cm^{-1} performed by Raman of PS, PSP, GPS-CA, GPS-WP, GPS-SBO, GPS-CA-SBO and GPS-WP-SBO.

Samples	FWHM at 480 cm^{-1}
PS	16.63±0.073[c]
PSP	19.06±0.364[b]
GPS-CA	20.57±0.845[a]
GPS-WP	20.50±0.057[a]
GPS-SBO	19.41±0.183[b]
GPS-CA-SBO	19.21±0.026[b]
GPS-WP-SBO	19.34±0.235[b]

[a-c]Values are means±SD. Means with similar letters in a column do not differ significantly ($p>0.05$).

4.4.3 X-ray Diffraction

The XRD patterns and relative crystallinity of the freeze-dried samples are shown in Fig. 4.5 and a notability analysis of the crystallinity values are illustrated in Table 4.3. PS exhibited a B-type crystalline structure along with strong reflections peaks at 5.7, 10.0, 11.2, 14, 15.0, 17.0, 18.2, 19.5, 24.0 and 26.2°(2θ) angles (Liu, Ming, Li, and Zhao, 2012). CA or WP and CA-SBO or WP-SBO did not show any diffraction peak (data do not show). This meant that there were no crystalline structures in these samples.
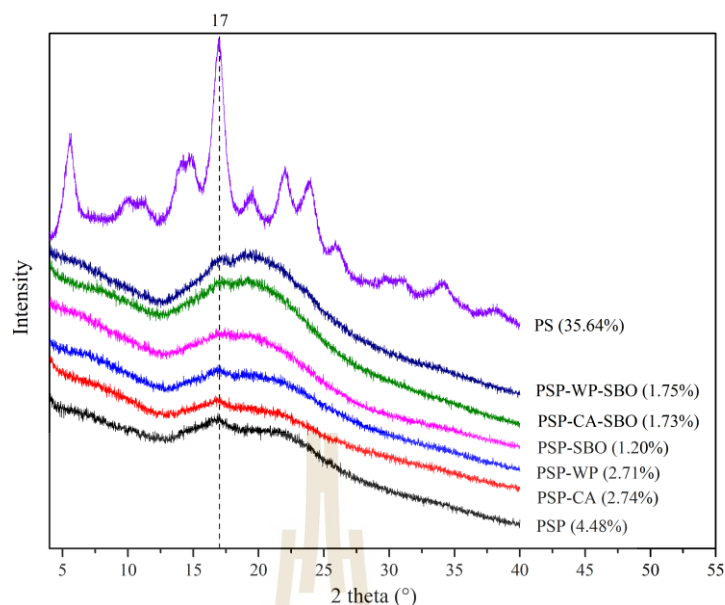
Figure 4.5 X-ray diffraction of the samples. Crystallinity (%) is given in parentheses.

In comparison with PS, the crystalline structure of the gelatinized and homogenous treated PS was seriously destroyed. All pastes showed only slight reflection peaks at 17.0°(2θ) angles. The RC of the other pastes was lower than that for the PSP. A possible explanation for this might be that the PSP had lost their crystal structure completely by the process of gelatinization, but some crystal structure could be detected because of the retrogradation of the samples during cooling and freezing-drying. However, the RC of the mixture pastes was lower than that for the PSP because the addition of MP, SBO, and both MP and SBO could retard the retrogradation of the GPS (Ji et al., 2017). Another possible explanation for this might be that the crystal structure of the GPS was seriously damaged in the process of gelatinization and homogenization (Lamberti, Geiselmann, Conde-Petit, and Escher, 2004). From the RCs of the paste samples, the addition of MP, SBO, and both MP and SBO could enhance the deformation of the crystal structure of GPS in this situation.

Table 4.3 Crystallinity values of PS, PSP, GPS-CA, GPS-WP, GPS-SBO, GPS-CA-
SBO and GPS-WP-SBO.

Samples	Crystallinity (%)
PS	35.64±0.18[a]
PSP	4.48±0.23[b]
GPS-CA	2.74±0.50[c]
GPS-WP	2.71±0.59[c]
GPS-SBO	1.2±0.11[d]
GPS-CA-SBO	1.73±0.35[d]
GPS-WP-SBO	1.75±0.33[d]

[a-d]Values are means±SD. Means with similar letters in a column do not differ significantly ($p>0.05$).

4.5 Conclusions

The addition of MP and SBO to GPS would change the structure of the GPS. There were no covalent interactions between starch, MP and SBO in this research. After the addition of MP and/or SBO, corresponding characteristic peaks was appeared in the obtained mixtures, such as deformation vibration of amino acids (1541 cm^{-1}) and methylene groups of FAs (1750 cm^{-1}). In addition, three structural parameters (the amorphous region, the short-range molecular order, and the relative crystallinity) of the samples changed after adding different substances (MP, SBO, and both MP and SBO) into GPS resulting in a change to the physicochemical properties of the mixture. This chapter provided a better understanding of binary and ternary

interactions among PS, MP, and SBO. In addition, it could provide future guidance

for food design which contain starch, protein, and vegetable oil.

4.6 References

Alvarez, M. D., Fernandez, C., and Canet, W. (2010). Oscillatory rheological properties of fresh and frozen/thawed mashed potatoes as modified by different cryoprotectants. **Food and Bioprocess Technology.** 3(1): 55.

Álvarez, M. D., Fernández, C., Olivares, M. D., Jiménez, M. J., and Canet, W. (2013). Sensory and texture properties of mashed potato incorporated with inulin and olive oil blends. **International Journal of Food Properties.** 16(8): 1839-1859.

Blazek, J., and Gilbert, E. P. (2011). Application of small-angle X-ray and neutron scattering techniques to the characterisation of starch structure: A review. **Carbohydrate Polymers.** 85(2): 281-293.

Cai, J., Chao, C., Niu, B., Copeland, L., Yu, J., Wang, S., and Wang, S. (2021). New insight into the interactions among starch, lipid and protein in model systems with different starches. **Food Hydrocolloids.** 112: 106323.

Cervantes-Ramírez, J. E., Cabrera-Ramirez, A. H., Morales-Sánchez, E., Rodriguez-García, M. E., de la Luz Reyes-Vega, M., Ramírez-Jiménez, A. K., Gaytán-Martínez, M. (2020). Amylose-lipid complex formation from extruded maize starch mixed with fatty acids. **Carbohydrate Polymers.** 246: 116555.

Chao, C., Cai, J., Yu, J., Copeland, L., Wang, S., and Wang, S. (2018). Toward a better understanding of starch-monoglyceride–protein interactions. **Journal of Agricultural and Food Chemistry.** 66(50): 13253-13259.

Chen, X., He, X., Zhang, B., Fu, X., Jane, J., and Huang, Q. (2017). Effects of adding corn oil and soy protein to corn starch on the physicochemical and digestive properties of the starch. **International Journal of Biological Macromolecules**. 104: 481-486.

Fechner, P. M., Wartewig, S., Kleinebudde, P., and Neubert, R. H. (2005). Studies of the retrogradation process for various starch gels using Raman spectroscopy. **Carbohydrate Research.** 340(16): 2563-2568.

Grega, T., Najgebauer, D., Sady, M., Baczkowicz, M., Tomasik, P., and Faryna, M. (2003). Biodegradable complex polymers from casein and potato starch. **Journal of Polymers and the Environment.** 11(2): 75-83.

Hai, L., and Yinxia, C. (2016). Review on Theory and Technology Research of Starch-lipid Complex. **Agricultural Science & Technology.** 17(8).

Hu, Y., He, C., Zhang, M., Zhang, L., Xiong, H., and Zhao, Q. (2020). Inhibition from whey protein hydrolysate on the retrogradation of gelatinized rice starch. **Food Hydrocolloids**. 105840.

Ji, N., Liu, C., Zhang, S., Yu, J., Xiong, L., and Sun, Q. (2017). Effects of chitin nano-whiskers on the gelatinization and retrogradation of maize and potato starches. **Food Chemistry.** 214: 543-549.

Ji, Y. (2020). Effect of annealing on the functional properties of corn starch/corn oil/lysine blends. **International Journal of Biological Macromolecules**. 144: 553-559.

Kizil, R., Irudayaraj, J., and Seetharaman, K. (2002). Characterization of irradiated starches by using FT-Raman and FTIR spectroscopy. **Journal of Agricultural and Food Chemistry.** 50(14): 3912-3918.

Lamberti, M., Geiselmann, A., Conde-Petit, B., and Escher, F. (2004). Starch transformation and structure development in production and reconstitution of potato flakes. **LWT-Food Science and Technology.** 37(4): 417-427.

Li, H.T., Li, Z., Fox, G. P., Gidley, M. J., and Dhital, S. (2020). Protein-starch matrix plays a key role in enzymic digestion of high-amylose wheat noodle. **Food Chemistry.** 336: 127719.

Li, Q., Shi, S., Du, S.k., Dong, Y., and Yu, X. (2021). Starch-palmitic acid complex formation and characterization at different frying temperature and treatment time. **LWT.** 136: 110328.

Li, W., Zhang, F., and Zheng, J. (2019). Influence of Ultrasonic Treatment on the Physiochemical Properties and Feature Structure of Pea Starch in Acid and Salt Systems. **Starch-Stärke**. 71(9-10): 1900064.

Liu, J., Ming, J., Li, W., and Zhao, G. (2012). Synthesis, characterisation and in vitro digestibility of carboxymethyl potato starch rapidly prepared with microwave-assistance. **Food Chemistry.** 133(4): 1196-1205.

Liu, Q., Charlet, G., Yelle, S., and Arul, J. (2002). Phase transition in potato starch-water system I. Starch gelatinization at high moisture level. **Food Research International.** 35(4): 397-407.

Mutungi, C., Passauer, L., Onyango, C., Jaros, D., and Rohm, H. (2012). Debranched cassava starch crystallinity determination by Raman spectroscopy: Correlation of features in Raman spectra with X-ray diffraction and 13C CP/MAS NMR spectroscopy. **Carbohydrate polymers.** 87(1): 598-606.

O'Mahony, J., and Fox, P. (2014). **Milk: an overview.** Milk proteins: Elsevier. 19-73.

Parada, J., and Santos, J. L. (2016). Interactions between starch, lipids, and proteins in foods: Microstructure control for glycemic response modulation. **Critical Reviews**

in Food Science and Nutrition. 56(14): 2362-2369.

Rygula, A., Majzner, K., Marzec, K. M., Kaczor, A., Pilarczyk, M., and Baranska, M. (2013). Raman spectroscopy of proteins: a review. **Journal of Raman Spectroscopy**. 44(8): 1061-1076.

Sarko, A., and Wu, H. C. (1978). The crystal structures of A-, B-and C-polymorphs of amylose and starch. **Starch-Stärke.** 30(3): 73-78.

Tatulian, S. A. (2013). Structural characterization of membrane proteins and peptides by FTIR and ATR-FTIR spectroscopy. Lipid-protein interactions: Springer. 177-218.

Wang, L., Wang, W., Wang, Y., Xiong, G., Mei, X., Wu, W., Liao, L. (2018). Effects of fatty acid chain length on properties of potato starch–fatty acid complexes under partially gelatinization. **International Journal of Food Properties**. 21(1): 2121-2134.

Wang, L.f., Zhang, L., Wang, H., Ai, L., and Xiong, W. (2020). Insight into protein-starch ratio on the gelatinization and retrogradation characteristics of reconstituted rice flour. **International Journal of Biological Macromolecules**. 146: 524-529.

Wang, S., Li, C., Copeland, L., Niu, Q., and Wang, S. (2015). Starch retrogradation: A comprehensive review. **Comprehensive Reviews in Food Science and Food Safety**. 14(5): 568-585.

Wang, S., Wang, J., Yu, J., and Wang, S. (2016). Effect of fatty acids on functional properties of normal wheat and waxy wheat starches: a structural basis. **Food Chemistry.** 190: 285-292.

Wang, S., Chao, C., Cai, J., Niu, B., Copeland, L., and Wang, S. (2020). Starch-lipid and

starch-lipid-protein complexes: A comprehensive review. **Comprehensive Reviews in Food Science and Food Safety.** 19(3): 1056-1079.

Wang, S., Zheng, M., Yu, J., Wang, S., and Copeland, L. (2017). Insights into the Formation and Structures of Starch-Protein-Lipid Complexes. **Journal of Agricultural and Food Chemistry**. 65(9): 1960-1966.

Yang, H., Irudayaraj, J., and Paradkar, M. M. (2005). Discriminant analysis of edible oils and fats by FTIR, FT-NIR and FT-Raman spectroscopy. **Food Chemistry.** 93(1): 25-32.

Ye, J., Hu, X., Luo, S., McClements, D. J., Liang, L., and Liu, C. (2018). Effect of endogenous proteins and lipids on starch digestibility in rice flour. **Food Research International.** 106: 404-409.

Yang, H., Joseph I., and Manish M. P. (2005). Discriminant analysis of edible oils and fats by FTIR, FT-NIR and FT-Raman spectroscopy. **Food Chemistry.** 93: 25-32.

Zaleska, H., Ring, S., and Tomasik, P. (2001). Electrosynthesis of potato starch-casein complexes. **International Journal of Food Science & Technology**. 36(5): 509-515.

Zheng, M., Lin, Y., Wu, H., Zeng, S., Zheng, B., Zhang, Y., and Zeng, H. (2020). Water migration depicts the effect of hydrocolloids on the structural and textural properties of lotus seed starch. **Food Chemistry.** 315: 126240.

CHAPTER V

CHAPTER I THE MICROSTRUCTURE, RHEOLOGICAL CHARACTERISTICS AND DIGESTIBILITY PROPERTIES OF BINARY AND TERNARY MIXTURE SYSTEM OF GELATINIZED POTATO STARCH, MILK PROTEIN AND SOYBEAN OIL DURING *IN VITRO* DIGESTION PROCESS

5.1 Abstract

This chapter was conducted to study the effects of MP and SBO on the digestibility of GPS. The samples were digested and observed with a CLSM. The viscosity of the digestates was determined by a rheometer. In addition, starch digestibility, protein digestibility, and FFA release of binary and ternary mixed samples were determined using *in vitro* simulation. Results showed that the addition of MP and SBO had little effect on GPS viscosity during digestion. However, with the addition of enzymes, the viscosity of the digestive juice decreased significantly. Specifically, MP addition could promote PSP digestion, while SBO slowed down PSP digestion. However, PSP digestion was promoted by the addition of protein and oil. The mix and homogenization of SBO and MP could promote protein digestibility of MP, while the mix and homogenization of GPS and MP could inhibit the protein

digestibility of MP. The mixture of MP and/or GPS with SBO promoted the release of FFA in SBO. The highest release rate of FFA was attained by a mix of MP and SBO. Therefore, this study could provide a guide to the composition and intake of food materials in daily life by providing the effects of dairy protein and vegetable oil additions on the digestibility of the potato starch, which benefit the starch-based food product manufacturing and also assist the knowledge of digestibility of starch when mixed with such protein and oil.

Keywords: Potato starch, Casein, Whey protein, Soybean oil, digestibility.

5.2 Introduction

Starch is a major food source for humans, accounting for about 70 percent of the calories in the human diet. Starchy foods are products that contain high amounts of starch, but these foods often also contain a certain number of proteins and fats. There are many studies on the binary interaction between starch and protein or lipid (Ai, Hasjim, and Jane, 2013; Eliasson, Finstad, and Ljunger, 1988; Eliasson and Wahlgren, 2004; Jamilah et al., 2009). Mixing starch with proteins or lipids could affect the digestibility of starch (Farooq, Dhital, Li, Zhang, and Huang, 2018; Jenkins et al., 1987; Kawai, Takato, Sasaki, and Kajiwara, 2012). Amylose was known to form a single spiral complex with lipids (Zabar, Lesmes, Katz, Shimoni, and Bianco-Peled, 2009). Moreover, amylose, when combined with lipids and other similar compounds, became resistant to α-amylase (Putseys, Lamberts, and Delcour, 2010). Then the addition of protein to starch might hinder or promote the starch digestion (Lu, Donner, Yada, and Liu, 2016; Sopade and Gidley, 2009). However, in practical terms, these three ingredients have been often present in food at the same time, and

their interactions further affect certain physiological responses, such as the postprandial blood sugar response (Lin, Yang, Chi, and Ma, 2020; Ye et al., 2018).

In recent years, there have been some studies on the interactions among starch, protein, lipid and their effects on starch digestibility (Chen et al., 2018; Wang et al., 2014). The effect of endogenous proteins and lipids on starch digestibility of kodo millte flour and rice flour was investigated (Annor, Marcone, Bertoft, and Seetharaman, 2013). The results showed that endogenous lipids and proteins could inhibit starch digestion. Proteins and lipids might slow down the hydrolysis of starch by forming a coating around the starch granules, which could inhibit their swelling and restricts the entry of digestive enzymes into the underlying starch molecules. Chen et al. (2017) carried out a study on adding soy protein and corn oil to corn starch. The complex reduced the content of RDS and increased the sum of SDS and RS contents. The effect of soy protein on the digestibility of the ternary blends was greater than that of corn oil. The physical barrier of corn oil, protein-starch matrix and amylose-lipid complex could provide resistance to starch digestion (Chen et al., 2017). The degree of unsaturation of FAs and chain length affected *in vitro* digestibility of starch-protein-fatty acid complexes (Zheng et al., 2018).

Starchy foods include bread, baked goods, mashed potato, among others, all of which are a matrix of starches, proteins and lipids, but the type of raw materials and processing conditions affect their microstructure and ultimately their performance. Food processing influenced the GI of potato products (Ek, Brand-Miller, and Copeland, 2012). *In vitro* and *in vivo* studies of several cultivars of potato demonstrated that cooked potato exhibited the fastest starch digestion rate and absorption rate in humans, making the levels of postprandial blood glucose increase

(Tian, Chen, Ye, and Chen, 2016). Highly digestible carbohydrate-rich foods lost their popularity due to their effect on the postprandial blood glucose level elevation when consumed, which could cause physiological complications associated with obesity and diabetes. Hence, there is a need for a greater understanding the effects of adding proteins and lipids to cooked potato as well as its digesta properties.

In order to study the interaction of three nutrients in mashed potato, a mashed potato model was established using GPS, MP and SBO as raw materials. The interaction of GPS, MP and SBO were studied by using CLSM, Rheometer, FTIR, and Raman Spectrometer. This chapter was conducted to observe changes in microstructure, viscosity and the digestibility of each component in the whole mixture during the digestion process based on previous studies, and the effect of protein and lipid on starch hydrolysis in GPS was studied along with its mechanism.

5.3   Materials and methods

5.3.1   Materials

Potato starch was purchased from Bangkok Inter Food Co., Ltd. (Bangkok, Thailand). Micellar casein concentrates powder with 82% (w/w) total protein was received from Vicchi Enterprise Co., Ltd. (Bangkok, Thailand). WP was purchased from Shanghai Yuanye Biological Technology Co., Ltd. (Shanghai, China). SBO (Cook Brand) used in this study were purchased from a local supermarket in Nakhon Ratchasima province, Thailand. α-Amylase from porcine pancreas (A-3176), Pepsin from porcine gastric mucosa (P7000) and pancreatin from porcine pancreas (P7545, activity 4×USP), were purchased from Sigma-Aldrich Chemical Co. (St. Louis, MO, USA). Amyloglucosidase (3200 U/ml) was supplied by Megazyme

International Ireland Ltd. (Ireland). The glucose oxidase-peroxidase (GOPOD) assay kit was purchased from Megazyme International Ltd. (Co. Wicklow, Ireland). APTS, FITC, Nile Red, ethyl alcohol, acetone, and other chemicals used in this study were of analytical grade.

5.3.2 Sample preparation

The binary-component complex and ternary-component was prepared according to the method of 3.3.1. There were 11 fresh samples. The composition of each sample is shown in Table 3.1.

5.3.3 *In-vitro* starch digestion

A rapid *in vitro* starch digestion assay according to the methods of Sopade and Gidley was used (Mahasukhonthachat, Sopade, and Gidley, 2010). Samples were weighed for 2.5 g and treated with 1 ml of artificial saliva, which contained porcine α-amylase (Sigma A-3176 Type VI-B; 250 U per ml of carbonate buffer) for 15-20 s. Thereafter, 5 ml of pepsin (Sigma P-6887, from gastric porcine mucosa; 1 ml per ml of 0.02 M aq. HCl) was added to the mixture and was incubated at 37°C for 30 min in a water bath rotating at 85 rpm. The digested mix was neutralized with 5 ml of 0.02 M aq. NaOH. Then its pH was adjusted to 6 using 25 ml of 0.2 M sodium acetate buffer. Then 5 mL of pancreatin (Sigma P1750 from porcine pancreas; 2 mg per ml of acetate buffer) and amyloglucosidase (Megazyme International Ireland Ltd., Ireland; 28 U per ml of acetate buffer) solution was added into the digestion tube. The mixture was incubated for 4 h.

Aliquots (0.5 ml) were withdrawn at 0, 10, 20, 30, 45,60, 90, 120, 150, 180, 210, 240 min of digestion at the intestinal stage, followed by mixing with absolute ethanol (3 ml). The samples were then analyzed for glucose using D-glucose assay

(GOPOD-FORMAT, K-GLUC 05/2008, Megazyme International Ireland Ltd.,

Ireland) as shown in the appendix A. Results were expressed as percent starch

hydrolysis with the following equations (Tamura, Singh, Kaur, and Ogawa, 2016):

$$\%S_H = \frac{S_h}{S_i} = 0.9 \times \frac{G_p}{S_i} \tag{5.1}$$

where $\%S_H$ is the percent starch hydrolysis (total), S_h is the amount of starch

hydrolyzed, S_i is the initial amount of starch (g), and G_p is the amount of glucose

produced (g). A conversion factor (from starch to glucose) of 0.9 which is generally

calculated from the molecular weight of starch monomer/molecular weight of glucose

(162/180 = 0.9) was be used. The total starch content of the samples (initial amount of

starch) was analyzed using the method following 3.3.2.

5.3.4 Estimation of glycemic index (GI)

The digestogram (digested starch at a specific time period) of each

sample was modelled using a modified first-order kinetic model, Eqn. (5.2), as

described below (Mahasukhonthachat et al., 2010).

$$D_t = D_{\infty-0} \left(1 - \exp[-Kt] \right) \tag{5.2}$$

where D_t (g/100 g dry starch) is the digested starch at time t, D_0 is the digested starch

at time t = 0, $D\infty$ is the digestion at infinite time $(D_0 + D_{\infty-0})$, and K is the rate

constant (min^{-1}). $D_{\infty-0}$ is the values estimated from $t = 0$–240 min.

In order to calculate the estimated GIs of the samples, the areas under the

digestograms ($AUCexp$) were computed with Eqn. (5.3) (Mahasukhonthachat et al.,

2010):

$$AUC_{exp} = [D_{\infty}t + \frac{D_{\infty-0}}{K} \exp(-Kt)]_{t_1}^{t_2} \tag{5.3}$$

$$\frac{dD_t}{dx}\Big|_{t=0} = D_{\infty-0}K \tag{5.4}$$

Estimated GI values were determined using the method proposed by Goñi with some modifications (Goñi, Garcia-Alonso, and Saura-Calixto, 1997; Srikaeo and Sangkhiaw, 2014). Single-point measurements of starch digestion at 90 min in samples was used to *estimate GI*. The hydrolysis index (*HI*) of each sample was calculated by dividing the area under its digestogram with the area under the digestogram of a fresh white bread, which was calculated in this study to be about 17,000 min g/100 g dry sample (from 0 to 240 min). Using the parameters of the modified first-order kinetic model for both the samples and fresh white bread, estimated GI (average) (GIAVG) for each sample was calculated using Eqn. (5.5) (Srikaeo and Sangkhiaw, 2014):

$$Estimated\ GI = \left[\frac{\left((39.71+0.803H_{90})+(39.51+0.573HI)\right)}{2}\right] \tag{5.5}$$

5.3.5 Protein digestion

The *in vitro* protein digestibility of the formulations was carried out according to the method of Srigiripura and Kotebagilu et al. (2019). The samples which contain protein were taken in quantities equivalent to 100 mg of protein (about 10.0 g) for analysis. Kjeldahl method was employed to measure protein content of the samples. The samples were taken in 50 ml centrifuge tubes and 15 ml of 0.1 N HCl containing 1.5 mg of pepsin was added to all the samples and incubated at 37°C for 3 hours. Then 1.5 ml of 0.5 N NaOH and 7.5 ml of 0.2 M phosphate buffer containing 4 mg of pancreatin was added to the samples before incubation at 37°C for 24 hours. Thereafter, 10% TCA was added to stop the incubation, as the mixture was allowed to

stand for two hours. The samples were afterwards centrifuged at 4000 rpm for 15 mins while Kjeldahl method was used to analyze the protein content present in the supernatant. The protein digestibility was calculated using the following formula (5.6) (Srigiripura, Kotebagilu, and Urooj, 2019):

$$\textbf{\textit{Protein Digestibility}}(\%) = \frac{\textit{Protein content in the supernatant}}{\textit{Total protein content of the samples}} \times \textbf{100} \qquad (5.6)$$

5.3.6 FFA release

The single-stage digestion model used in this study was modified slightly from those described previously (Hu, Li, Decker, and McClements, 2010; Qin, Yang, Gao, Yao, and McClements, 2017; Wan et al., 2020). The basic procedure used is described as follows: 20.0 g of sample (which contain SBO) was weighed into a glass beaker and placed into a water bath at 37°C for 10 mins. The sample was adjusted to pH 7.0 using NaOH (0.5 N) or HCl (0.1N) solutions. Then 3.5 ml of preheated bile extract solution (187.5 mg bile extract dissolved in phosphate buffer, pH 7, 37°C) and 1.5 ml of mineral ion solution (containing 0.25 M Ca^{2+} and 3.75 M Na^+, 37°C) were added to the sample under continuous stirring, followed by readjustment of the mixture back to pH 7.0. Two and a half milliliters of freshly prepared porcine pancreatin suspension (60 mg pancreatin powder dispersed in 5 mM phosphate buffer, pH 7, 37°C) was added to the mixture in order to initialize the titration. During the intestinal digestion, the pH was monitored using a pH meter (SevenCompact™ S210-S, Mettler Toledo International Trade Co., Ltd., China, Shanghai) at every 2 mins until 120 min after digestion and maintained at 7.000± 0.005 by adding 0.5M NaOH through a burette. The percentage of FFA released was calculated by recording the volume of 1 M NaOH used to neutralize the FFA

produced by the triglycerides (assuming two FFAs were released per triglyceride) (Guo, Bellissimo, and Rousseau, 2017; Wan et al., 2020):

$$FFA\% = 100 \times \frac{(V_{NaOH\ for\ sample} - V_{NaOH\ for\ blank}) \times C_{NaOH} \times MW_{lipid}}{2W_{lipid}} \qquad (5.7)$$

Here, $V_{NaOH\ for\ sample}$ is the volume of NaOH (L) titrated into the reaction vessel to neutralize the FFAs released; $V_{NaOH\ for\ blank}$ is the volume of NaOH (L) titrated into the reaction vessel to neutralize the FFAs released in the absence of corn oil. C_{NaOH} is the concentration of NaOH (0.1 M); W_{Lipid} is the average molecular weight of corn oil (872 g mol^{-1}), W_{lipid} is the initial mass of SBO (g) in the intestinal phase.

5.3.7 Microstructure analysis

Samples prepared in 5.3.2 were taken during the simulated digestion process, in which fresh samples were digested in the stomach for 15 min and in the small intestine for 5 min. The samples were observed with CLSM using the fluorescent mode (Nikon A1R, Nikon Crop., Tokyo, Japan) according to the method of Thaiudom and Pracham (2018). APTS in distilled water was used to dye PS while Nile Red was applied to dye SBO. FITC in acetone was used to dye both PS and CA. APTS developed blue color while FITC and Nile red developed green and red colors, respectively. The samples (around 0.2 ml) were placed in the tubes, followed by adding a drop of APTS (around 10µl) to each tube, with thorough mixing and staining before storage at ambient temperature for 10 min. Similarly, FITC and Nile red staining were carried out at 10 min intervals. The stained samples were placed on slides while placing the cover glasses on the slides.

5.3.8 Rheology

The viscosity of the paste samples during simulated *in vitro* digestibility (Mahasukhonthachat et al., 2010) was studied using the modified method of Bordoloi, Singh and Kaur (2012). Time sweep experiments were conducted with a dynamic rheometer (AR-G2 Rheometer, TA Instruments, New Castle, DE) equipped with a Peltier cylinder system. The measurements were achieved with a measuring cup and vaned rotor geometry. One and a half gram of sample was weighed into a 50 ml centrifuge tube and 0.4 ml of artificial saliva containing porcine α-amylase (250 U per ml of carbonate buffer, pH 7) was add into the tube and mixed for 20 seconds. Then 3 ml pepsin solution (1 ml per ml of 0.02 M HCl, pH 2) was also added into the tube. The mixture of the paste and enzyme solution were immediately loaded into the rheometer's cup. The experiment was carried out at 37°C using a multi-step flow procedure. Prior to the second step, the shear rate was increased to 300 s^{-1} for 60 s for a thorough mixing, after which it was maintained at 100 s^{-1} for 1800 s. Prior to the final step, the mixture was neutralized (3 ml, 0.02 M NaOH), and the pH was adjusted with 15 ml of 0.2 M sodium acetate buffer (pH 6). Afterwards, the 3 ml of pancreatin mixture (2 mg per ml of acetate buffer) and amyloglucosidase (28 U per ml of acetate buffer) was added and mixed using the shear rate of 300 s^{-1} for 30 s. During the final step, a shear rate of 100 s^{-1} was maintained for 3600 s. Control PSP was prepared in the same way without the addition of enzymes and set as the control.

5.3.9 Statistical analysis

Measurements of all experiments were carried out in triplicate. The results were expressed as mean±standard deviation. Statistical analyses were conducted using SPSS 23.0. In all statistical analyses, $p < 0.05$ was considered significant.

5.4 Results and Discussion

5.4.1 *In vitro* starch digestibility

The effect of MP addition (CA or WP) and/or SBO on starch digestibility of GPS is shown in Fig.5.1. In the simulated oral phase (first stage, 15-20s), α-amylase hydrolysis of a small number of PS occurred, but glucose was rarely produced. In the gastric phase (second stage-30 mins), no glucose was released from the samples. This is due to the low pH environment at this stage, leading to α-amylase enzyme inactivation (Bordoloi et al., 2012). The detection of glucose content in the whole *in vitro* digestion process began at the end of gastric phase. However, glucose could be found at the end of the gastric phase with a small amount. This was attributed to starch hydrolysis during the simulated oral cavity (Raigond et al., 2020).

When the pancreatin and amyloglucosidase were added to the reaction mixture, all the samples were digested rapidly. GPS-CA, GSP-WP, GSP-CA-SBO, and GSP-WP-SBO were rapidly digested within the first 30 mins. At 30 min, starch digestibility could reach 30-40%. The digestion rate of PSP and gelatinized GPS-SBO during this period was relatively slow, and the digestibility was less than 10% after half an hour. These differences might be due to the composition of the individual samples (Na-Nakorn, Kulrattanarak, Hamaker, and Tongta, 2019; Wang et al., 2018). These components were digested by corresponding enzymes throughout the simulated digestion process. Previous studies showed that the viscosity of GPS decreased significantly after the addition of MP and homogenization (chapter III). Pepsin could digest MP and change the structures of GPS-CA, GPS-WP, GPS-CA-SBO, and GPS-WP-SBO during the gastric phase. After the MP was digested during the gastric phase, the structure of samples became looser, so when pancreatin and amyloglucosidase were added, the digestion rate became significantly
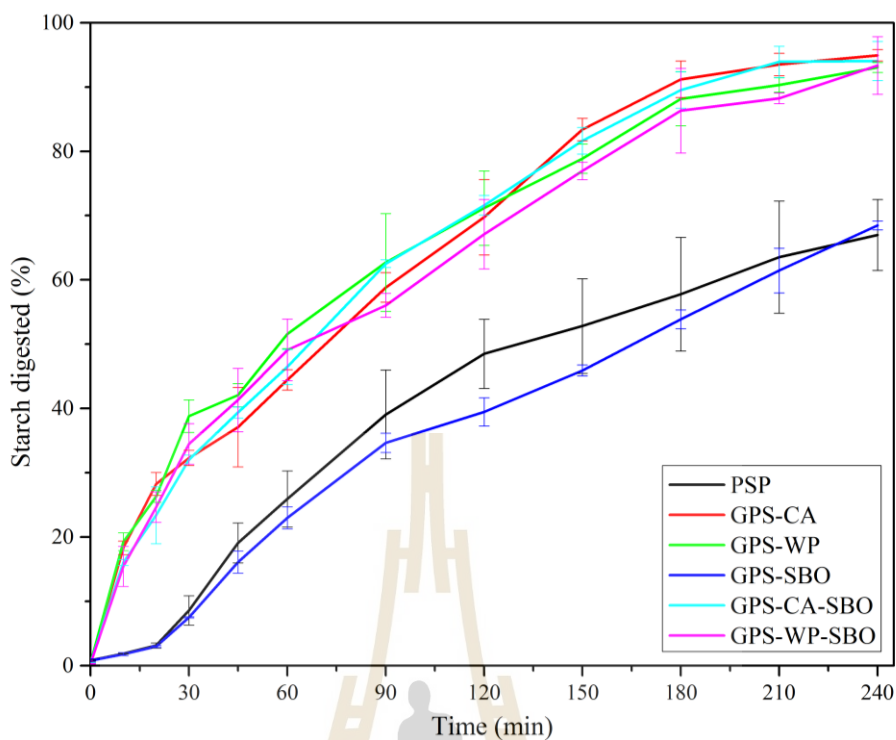
Figure 5.1 Digestograms of PSP, GPS-CA, GPS-WP, GPS-SBO, GPS-CA-SBO, and GPS-WP-SBO during intestinal phase.

faster than that of PSP and GPS-SBO. Half an hour later, the starch hydrolysis rate of the whole sample was slower until the end of digestion. At 240 mins, the digestibility of GPS-CA, GPS-WP, GPS-CA-SBO, and GPS-WP-SBO reached 90%-95%. The final digestibility of PSP, GPS-SBO was between 60-65%. Qualitatively, the digested starch obtained in GPS-CA, GPS-WP, GPS-CA-SBO, GPS-WP-SBO was more than that obtained in PSP, while digested starch obtained in GPS-SBO was less than that of PSP. Thus, MP played an important role in enhancing starch hydrolysis. There were several possible reasons for the fact that the presence of MP might increase the enzymatic digestion on starch. Firstly, the decrease of the viscosity of PSP after adding MP might enhance enzyme susceptibility and hydrolysis (Sopade and Gidley,

2009). Secondly, the MP as a small practical state in the binary or ternary system could disrupt GPS gelling 3D network, making it easy for the enzyme to contact the starch (Fig. 5.5). Inhibitory effect of SBO on starch could be attributed to the interaction between starch and oil that hindered the starch digestion (Chen et al., 2018).

5.4.2 Hydrolysis kinetics and estimated glycemic index

The rate of starch loosening is an important factor of the glycemic response. *In vitro* studies provided high efficiency of predicting postprandial outcomes. Regardless of composition, each sample exhibited uniphase digestion. The *in vitro* digestion results, including equilibrium concentration (C1) at 180 min, kinetic constant (k), hydrolysis index (HI), and estimated GI, are listed in Table 5.1.

The equilibrium concentration (C1) represented the proportion of the amount of hydrolysis of starch in 180 mins to total starch. The addition of SBO had no significant effect on the kinetic constants of GPS. The addition of MP and/or SBO into GPS significantly increased the kinetic constants of GPS. In addition, the type and degree of processing were additional factors, as well as the resulting physical and chemical transformations that affected structural, molecular and functional properties of the gelatinized starch. The viscosity of the fresh sample was measured. It could be seen from the results that the smaller the viscosity, the larger the kinetic constant, the easier the GPS was digested, and the higher the predicted blood glucose value occurred. MP was added to the GPS, making the 3D structure of GPS more dispersed, and α-amylase was easier to penetrate into the GPS. SBO infiltrated into GPS might have interaction. Starch was more tightly bound to SBO, which making it harder for α-amylase to get into the starch (Fig. 5.5-1, 2, and4).

Table 5.1 Model parameters, hydrolysis index (*HI*) and estimated glycaemic index (*GI*) of the fresh paste samples (*in vitro* method).

	D_0	D_∞	$K \times 10^{-3}$	$AUC \times 10^3$	HI	Estimated H_{90}	Estimated GI
PSP	0.82 ± 0.14^a	99.18 ± 0.14^a	4.82 ± 0.97^b	9.85 ± 1.32^b	58.07 ± 7.8^b	35.66 ± 5.56^b	70.31 ± 4.47^b
GPS-CA	0.43 ± 0.07^b	99.57 ± 0.07^a	10.98 ± 0.21^a	15.58 ± 0.14^a	91.83 ± 0.80^a	62.98 ± 0.74^a	90.95 ± 0.52^a
GPS-WP	0.40 ± 0.06^b	93.75 ± 0.51^c	13.67 ± 1.85^a	15.95 ± 0.71^a	94.01 ± 4.18^a	66.58 ± 4.26^a	93.02 ± 2.91^a
GPS-SBO	0.79 ± 0.27^a	99.21 ± 0.27^a	3.97 ± 0.18^c	8.65 ± 0.24^b	50.96 ± 1.41^b	30.63 ± 0.94^b	66.26 ± 0.78^b
GPS-CA-SBO	0.42 ± 0.07^b	99.31 ± 0.122^a	10.81 ± 0.27^b	15.47 ± 0.17^a	91.17 ± 1.01^a	62.52 ± 0.73^a	90.58 ± 0.58^a
GPS-WP-SBO	0.31 ± 0.06^b	95.47 ± 1.27^b	11.72 ± 0.86^{ab}	15.37 ± 0.21^a	90.55 ± 1.21^a	62.49 ± 1.82^a	90.39 ± 1.08^a

[a-c] Values are means ± standard deviations (*n*=2).

[d] For each parameter (column), values with the same letters are not significantly different (*p*>0.05).
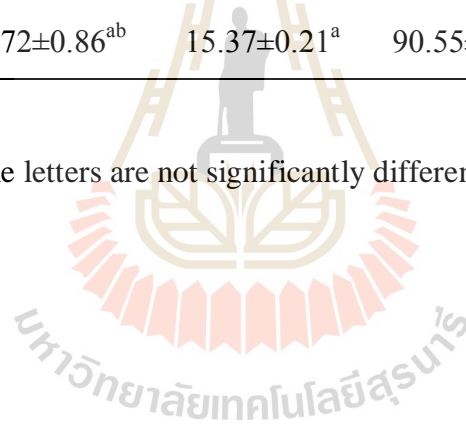
5.4.3   Protein digestion

The protein content for all samples containing MP are shown in Figure 5.2. The protein content in the measured samples was close to 1.0 %, and there is no significant difference among those samples. Protein digestibility of the test samples are shown in Fig.5.3. For single-phase samples, WP possessed higher protein digestibility than CA. The results were consistent with previous studies (Boirie et al., 1997; Mahe et al., 1996). This is due to the average diameter of casein micelles was 120 nm, which was larger than that of whey protein. For binary systems, the digestibility of CA-SBO and WP-SBO was higher than that of CA and WP. This was due to the fact that β-lactoglobulin and β-casein were more easily broken down by pepsin when adsorbed at the oil-water interface than in solution (Macierzanka, Sancho, Mills, Rigby, and Mackie, 2009; Sarkar, Goh, Singh, and Singh, 2009). The proteins unfold on the surface of the droplet, improving their accessibility to pepsin (Tunick et al., 2016). On the contrary, the digestibility of GPS-CA and GPS-WP were lower than that of CA and WP, which might refer to the result in a part of rheology further too. The integration of the MP into the 3D network of GPS when MP was added to gelatinized starch, hindered the contact between protein and enzymes (Oñate Narciso and Brennan, 2018). For the ternary system, the protein digestibility of GPS-CA-SBO and GPS-WP-SBO were lower than that of GPS-CA and GPS-WP, respectively. This was due to the protein being more stable in this ternary system. CA and WP could adsorb on the surface of the SBO.
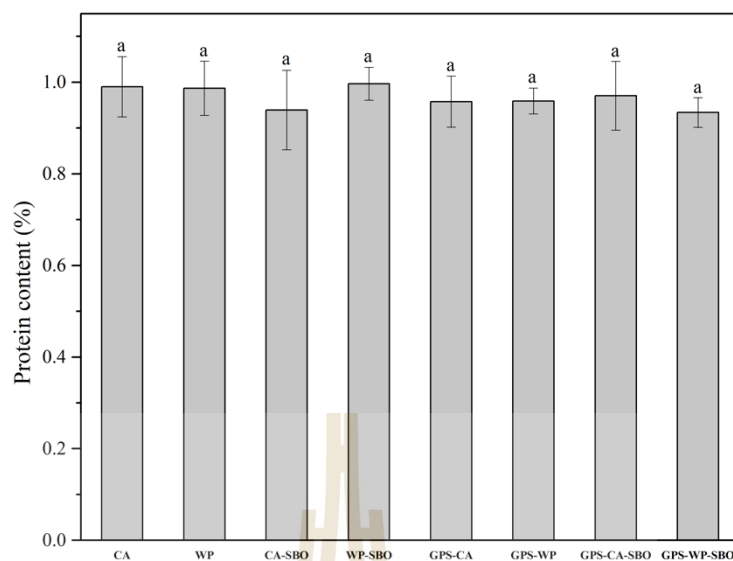
Figure 5.2 The protein content (%) of fresh samples calculated from total nitrogen content.
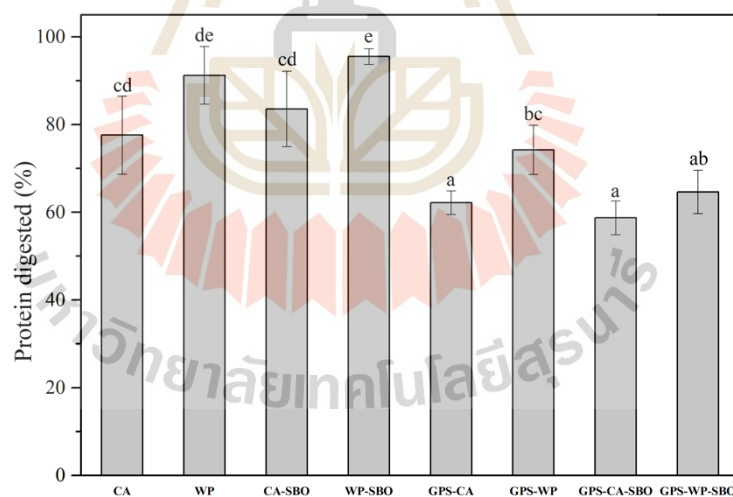
Figure 5.3 Protein digestibility of CA, WP, CA-SBO, WP-SBO, GPS-CA, GPS-WP, GPS-CA-SBO, and GPS-WP-SBO.

5.4.4 FFA release

The fat digestibility of all the samples containing SBO was determined. The total FFAs released from the oil phase are shown in Fig. 5.4. With the increase in digestion time, the released amounts of FFA in each sample gradually increased, especially rapidly in the first 30 min, and then flattened out after 60 min. This was due to the accumulation of lipolytic products at the interface that prevented pancreatic lipase from entering the triglyceride core (Gallier and Singh, 2012). After 2 h of artificial intestinal fluid digestion, the FFAs release ratio of samples with different components was different. The final release of FFA from SBO was the lowest, at about 50%. This might be because oil was incompatible with water, and the oil clumped together during the digestion model, reducing the reaction surface. The fat digestibility of GPS-SBO was higher than that of oil alone. After starch granules was gelatinized, starch could undergo a relatively slow process of reassociation after cooling (Wang, Li, Copeland, Niu, and Wang, 2015). So, the mixing of GPS and SBO made SBO less likely to aggregate than SBO in water and so that it could be more released into the intestinal fluid (Mun, Kim, Shin, and McClements, 2015). However, in binary systems, CA-SBO and WP-SBO possessed higher final FFA. This might be attributed to the emulsification property of CA and WP after homogenization, which increased the surface available to the lipase (Tunick et al., 2016). In the ternary system, the sample mixed with GPS made the final FFA lower than that in the binary system CA-SBO and WP-SBO. This was due to the effect of GPS which could reduce the activity of enzymes digesting the lipids at the interfacial layer and delayed the release of FFA (Xu et al., 2014). But the ternary system of GPS-CA-SBO and GPS-WP-SBO had higher FFA release than GPS-SBO. This might be because the

emulsifying property of CA and WP. This made oil more dispersed in the ternary system of GPS-CA-SBO and GPS-WP-SBO than in the binary system of GPS-SBO. So, the enzyme could intrude to the oil particles easier.
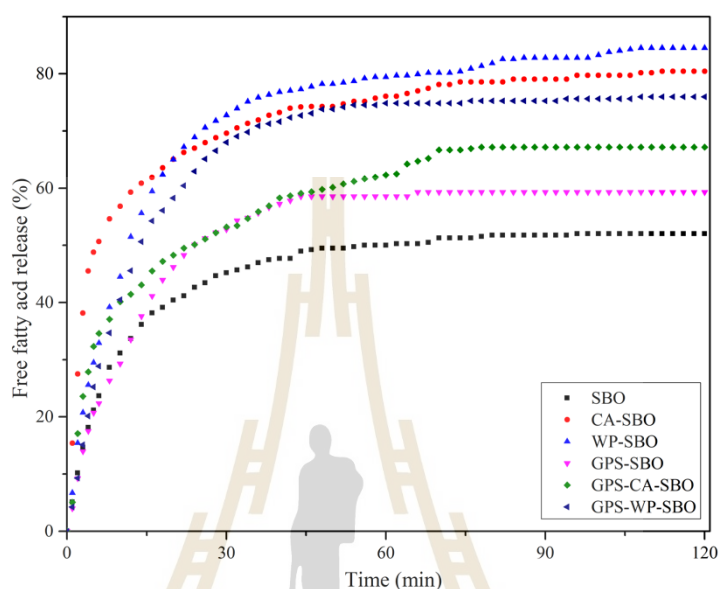
Figure 5.4 Free fatty acid release profiles from oil-water mixture (SBO), CA-SBO, WP-SBO, GPS-SBO, GPS-CA-SBO, and GPS-WP-SBO during *in vitro* intestinal digestion (*n*=3).

5.4.5 Microstructures

All the samples containing GPS and the state of each sample in the process of simulated intestinal conditions were observed by CLSM. The observation results are shown in Figure 5.5. Their images from different channels (405 nm, 488 nm, or 561 nm) are shown in Appendix E 1-6. The bule color of ATP-stained PSP and the green color of FTIC-stained PSP were clearly seen in that Figure. A superposition of two colors appeared cyan (as shown in Figure 5.5-1). As could be seen from the

143

figure, the fresh PSP sample had a uniform texture with no granular matter, indicating

that the GPS
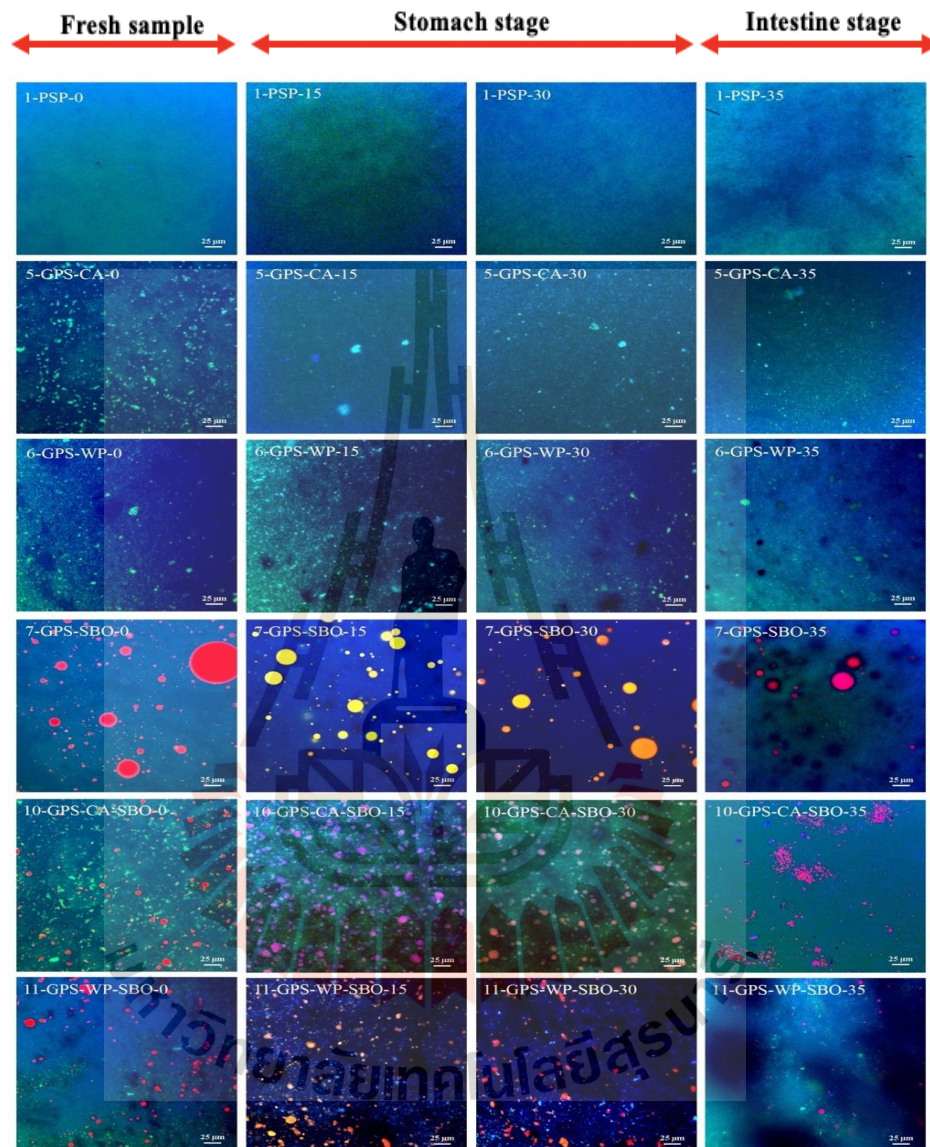
Figure 5.5 CLSM images of the fresh samples and the samples during *in vitro* digestion (Stomach phase 15 min and 30 min; Small intestine phase 5 min) process. Sample code:1-PSP-0, 1 means sample number 1, PSP means potato starch paste, 0, 15, 30,35 means fresh sample, stomach phase 15 min, stomach phase 30 min and small intestine phase 5 min respectively).

was completely gelatinized and the particle structure of the sample was completely destroyed after homogenization. The images obtained from the simulated digestion process showed that their green coloration reduced in luminosity when the digestion time increased, just as the blue color of the image became darker when the digestion time reached 35 min. This could be ascribed to the decrease in sample concentration upon the addition of enzyme solution in the gastric and intestinal phases (Singh, Dartois, and Kaur, 2010). In addition, the PS was hydrolyzed after the addition of pancreatin and amyloglucosidase.

As proteins, CA and WP were stained bright green by FITC. In the binary system, for GPS-CA and GPS-WP samples, it could be seen from Figure 5.5 (5-GPS-CA-0, 6-GPS-WP-0) that CA and WP were scattered in the 3D network of GSP. This phenomenon was similar to the separation of polysaccharides from proteins (Doublier, Garnier, Renard, and Sanchez, 2000; Kett et al., 2013; Thaiudom and Goff, 2003; Thaiudom and Pracham, 2018). For Figure 5.5-GPS-CA, the concentration of CA was significantly reduced during gastric simulated digestion (15 min, 30 min), due to the addition of pepsin during this process, which caused partial digestion of CA. For Figure 5.5 (6-GPS-WP), partial digestion of WP was observed after 30 min of gastric phase. However, the image of the small intestine simulated digestion for 5 min showed a cavity, which was also caused by the dilution of the sample and hydrolysis of PS.

SBO was dyed red with Nile red. The observation result of GPS-SBO is shown in Figure 5.5 (7-GPS-SBO-0). The SBO droplets could be seen the infiltrating into the GPS 3D structure. GPS overlapped with SBO in pink color. This indicated that there was an interaction between SBO and GPS in the sample, which might form

starch-lipid complex (Chen et al., 2018). During simulated digestion in the gastric phase (15 min and 30 min), the oil droplets were also stained by FITC green, which overlapped with Nile red, and finally showed yellow color. After simulated digestion of the small intestine for 5 min (35 min), the digested sample was diluted with the addition of enzyme solution, and part of GPS was digested quickly. Some void space could be seen in the image. Pancreatin in digestive juices containing lipases could digest oil and the hydrolysis of oil causes the appearance of cavities (Gurr, 1999).

For the ternary system samples, the images of GPS-CA-SBO (Fig. 5.5-10) and GPS-WP-SBO, (Fig.5.5-11) indicated that CA, WP, and SBO were dispersed in the GSP 3D network. Compared with the GPS-SBO binary system, the dispersion of SBO in the ternary system was better and the distribution of oil droplets was more uniform. This was because MP could emulsify the ternary mixture in the homogenizing process (Gandova and Balev, 2016). During simulated digestion, the protein was partially digested in the samples of the ternary system. GPS and SBO were diluted and digested during intestinal phase (35 min).

5.4.6 Rheology-Flow behavior

The viscosity of the samples containing GPS in the composition during the simulation of *in vitro* digestibility is shown in Figure 5.6. The viscosity of a fresh samples depended on the composition and interaction between the dispersed phase and the substrate (Ribotta and Rosell, 2010; C. Yang, Zhong, Goff, and Li, 2019; H. Yang, Irudayaraj, Otgonchimeg, and Walsh, 2004). The *in vitro* digestion viscosity of PSP-control was significantly higher than that of PSP, GPS-CA, GPS-WP, GPS-SBO, GPS-CA-SBO and GPS-WP-SBO added with corresponding enzymes. In the simulated gastric phase without the addition of enzymes, the viscosity of PSP first

increased, then slightly decreased, and then remained basically unchanged (Figure 5.6). The viscosity of PSP increased slowly in the simulated intestinal phase with the addition of enzyme, and then remained basically stable. However, the viscosity of PSP was much lower than that of PSP-Control. In the gastric phase, the viscosity of GPS-SBO was the highest, followed by PSP. This was similar to the results of previous experiments on the measurement of fresh samples viscosity (see 3.3.3). Binary or ternary mixtures with MP (GPS-CA, GPS-WP, GPS-CA-SBO and GPS-WP-SBO) showed slightly lower viscosity during the gastric phase. In addition to the slightly lower viscosity of the samples themselves, part of the MP was hydrolyzed by pepsin in the gastric phase, which also changed the viscosity of the sample (A. Ye, Cui, Dalgleish, and Singh, 2016). The structure of the MP was destroyed after hydrolysis, which also caused the 3D network of the GPS in the sample to become loose, thus reducing the viscosity of the whole system.

With the addition of the enzyme solution prior to the intestinal stage, the viscosity of the mixture in the reaction tube decreased, not only because the sample was diluted by the addition of the enzyme solution but also because of the rapid hydrolysis of the sample by the addition of enzymes. However, the results showed that viscosity of samples was higher during intestine stage than stomach stage. This was due to the addition of enzyme solution, making the liquid level increase, resulting in the larger contact area between the liquid and the instrument, consequentially in the increase of resistance in the instrumental rotation. Compared with PSP-control, the viscosity of each sample added with enzyme solution was significantly lower, due to the hydrolysis of GPS, SBO, and MP by the addition of enzymes. However, there was no significant difference in the viscosity of enzyme preparations. High viscosity

of GPS was hydrolyzed by α-amylase and amyloglucosidase to sugar, dextrins and maltooligosaccharides, which possessed a low viscosity (Woods and Swinton, 1995). SBO was hydrolyzed by lipase to FFA (Akoh, 2017). Protease hydrolyzes MP into small molecular polypeptides (Dupont and Tome, 2014). So, the viscosity of samples which were added the enzyme solution was significantly lower than PSP-control.
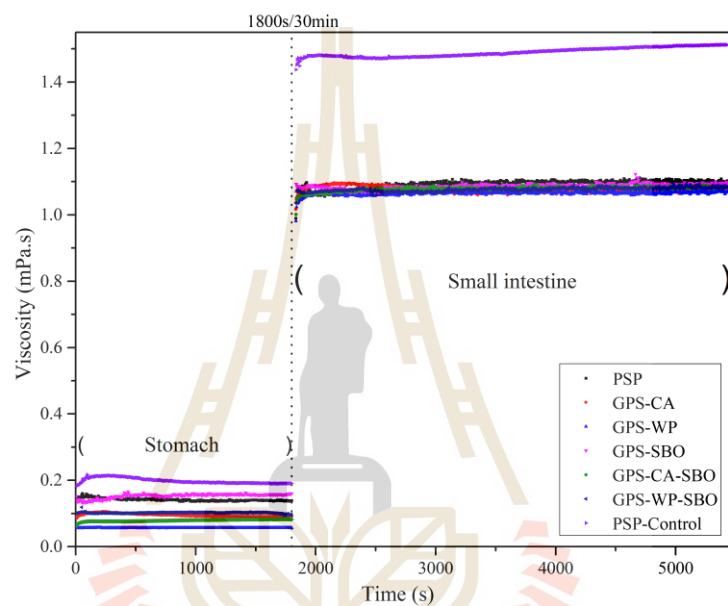
Figure 5.6 Effect of *in vitro* digestion on viscosity of PSP-Control, PSP, GPS-CA, GPS-WP, GOS-SBO, GPS-CA-SBO and GPS-WP-SBO. The PSP-Control was that PSP didn't add the corresponding enzyme during *in vitro* digestion.

5.5 Conclusions

The addition of MP and/or SBO to GPS could change the digestibility properties of the GPS. SBO could inhibit the digestion of GPS, while the addition of MP could promote the digestion of GPS. The homogenization of SBO and MP (CA or WP) promoted the digestion of protein, while the homogenization of GPS and MP

inhibited protein digestion. The mixtures of GPS-MP-SBO inhibited protein digestion. However, this inhibition was found in a higher rate in the mixture of GPS-SBO than in GPS-MP-SBO. Mixture of MP and/or GPS with SBO promoted the release of FFA in SBO. Mixture of MP with SBO resulted in the best release of FFA in SBO. CLSM was an effective tool for revealing the changes of binary and ternary systems during a simulated digestion. SBO increased the viscosity of the sample, while the mixture of MP and GPS decreased the viscosity. Finally, the evidences found in this study could be benefit as a guidance of food processing and food product development, especially in a field of food ingredient interaction in dairy and starch technology.

5.6   References

Ai, Y., Hasjim, J., and Jane, J. (2013). Effects of lipids on enzymatic hydrolysis and physical properties of starch. **Carbohydrate Polymers.** 92(1): 120-127.

Akoh, C. C. (2017). Food lipids: chemistry, nutrition, and biotechnology: CRC press.

Annor, G. A., Marcone, M., Bertoft, E., and Seetharaman, K. (2013). In vitro starch digestibility and expected glycemic index of kodo millet (Paspalum scrobiculatum) as affected by starch–protein–lipid interactions. **Cereal Chemistry.** 90(3): 211-217.

Boirie, Y., Dangin, M., Gachon, P., Vasson, M. P., Maubois, J.L., and Beaufrère, B. (1997). Slow and fast dietary proteins differently modulate postprandial protein accretion. **Proceedings of the National Academy of Sciences.** 94(26): 14930-14935.

Bordoloi, A., Singh, J., and Kaur, L. (2012). In vitro digestibility of starch in cooked potatoes

as affected by guar gum: Microstructural and rheological characteristics. **Food Chemistry.** 133(4): 1206-1213.

Chen, He, X., Zhang, B., Fu, X., Li, L., and Huang, Q. (2018). Structure, physicochemical and in vitro digestion properties of ternary blends containing swollen maize starch, maize oil and zein protein. **Food Hydrocolloids.** 76: 88-95.

Chen, X., He, X., Zhang, B., Fu, X., Jane, J., and Huang, Q. (2017). Effects of adding corn oil and soy protein to corn starch on the physicochemical and digestive properties of the starch. **International Journal of Biological Macromolecules.** 104: 481-486.

Doublier, J.L., Garnier, C., Renard, D., and Sanchez, C. (2000). Protein-polysaccharide interactions. **Current opinion in Colloid & interface Science.** 5(3-4): 202-214.

Dupont, D., and Tome, D. (2014). **Milk proteins: digestion and absorption in the gastrointestinal tract**. Milk Proteins: Elsevier. 557-569.

Ek, K. L., Brand-Miller, J., and Copeland, L. (2012). Glycemic effect of potatoes. **Food Chemistry.** 133(4): 1230-1240.

Eliasson, A., Finstad, H., and Ljunger, G. (1988). A Study of Starch-Lipid Interactions for Some Native and Modified Maize Starches. **Starch-Stärke**. 40(3): 95-100.

Eliasson, A. C., and Wahlgren, M. (2004). Starch-lipid interactions and their relevance in food products. **Starch in food: Structure, function and applications**: 441-460.

Farooq, A. M., Dhital, S., Li, C., Zhang, B., and Huang, Q. (2018). Effects of palm oil on structural and in vitro digestion properties of cooked rice starches. **International**

Journal of Biological Macromolecules. 107: 1080-1085.

Gallier, S., and Singh, H. (2012). Behavior of almond oil bodies during in vitro gastric and intestinal digestion. **Food & function**. 3(5): 547-555.

Gandova, V., and Balev, D. (2016). Properties of emulsions based in soybean oil stabilized by different proteins. **Int J Inn Sci Eng Technol**. 3: 293-297.

Goñi, I., Garcia-Alonso, A., and Saura-Calixto, F. (1997). A starch hydrolysis procedure to estimate glycemic index. **Nutrition Research**. 17(3): 427-437.

Guo, Q., Bellissimo, N., and Rousseau, D. (2017). Role of gel structure in controlling in vitro intestinal lipid digestion in whey protein emulsion gels. **Food Hydrocolloids.** 69: 264-272.

Gurr, M. I. (1999). Lipids in nutrition and health: A reappraisal: Elsevier.

Hu, M., Li, Y., Decker, E. A., and McClements, D. J. (2010). Role of calcium and calcium-binding agents on the lipase digestibility of emulsified lipids using an in vitro digestion model. **Food Hydrocolloids.** 24(8): 719-725.

Jamilah, B., Mohamed, A., Abbas, K., Rahman, R. A., Karim, R., and Hashim, D. (2009). Protein-starch interaction and their effect on thermal and rheological characteristics of a food system: A review. **J. Food Agric. Env.** 7: 169-174.

Jenkins, D., Thorne, M. J., Wolever, T., Jenkins, A. L., Rao, A. V., and Thompson, L. U. (1987). The effect of starch-protein interaction in wheat on the glycemic response and rate of in vitro digestion. **The American journal of clinical nutrition**. 45(5): 946-951.

Kawai, K., Takato, S., Sasaki, T., and Kajiwara, K. (2012). Complex formation, thermal properties, and in-vitro digestibility of gelatinized potato starch–fatty acid mixtures. **Food Hydrocolloids.** 27(1): 228-234.

Kett, A. P., Chaurin, V., Fitzsimons, S. M., Morris, E. R., O'Mahony, J. A., and Fenelon, M. A. (2013). Influence of milk proteins on the pasting behaviour and microstructural characteristics of waxy maize starch. **Food Hydrocolloids.** 30(2): 661-671.

Lin, L., Yang, H., Chi, C., and Ma, X. (2020). Effect of protein types on structure and digestibility of starch-protein-lipids complexes. **LWT.** 134: 110175.

Lu, Z., Donner, E., Yada, R. Y., and Liu, Q. (2016). Physicochemical properties and in vitro starch digestibility of potato starch/protein blends. **Carbohydrate Polymers.** 154: 214-222.

Macierzanka, A., Sancho, A. I., Mills, E. C., Rigby, N. M., and Mackie, A. R. (2009). Emulsification alters simulated gastrointestinal proteolysis of β-casein and β-lactoglobulin. **Soft Matter.** 5(3): 538-550.

Mahasukhonthachat, K., Sopade, P., and Gidley, M. (2010). Kinetics of starch digestion in sorghum as affected by particle size. **Journal of Food Engineering.** 96(1): 18-28.

Mahe, S., Roos, N., Benamouzig, R., Davin, L., Luengo, C., Gagnon, L., Tomé, D. (1996). Gastrojejunal kinetics and the digestion of [15N] beta-lactoglobulin and casein in humans: the influence of the nature and quantity of the protein. **The American journal of clinical nutrition.** 63(4): 546-552.

Mun, S., Kim, Y. R., Shin, M., and McClements, D. J. (2015). Control of lipid digestion and nutraceutical bioaccessibility using starch-based filled hydrogels: Influence of starch and surfactant type. **Food Hydrocolloids**. 44: 380-389.

Na-Nakorn, K., Kulrattanarak, T., Hamaker, B. R., and Tongta, S. (2019). Starch digestion kinetics of extruded reformed rice is changed in different ways with

added protein or fiber. **Food & function.** 10(8): 4577-4583.

Oñate Narciso, J., and Brennan, C. (2018). Whey and pea protein fortification of rice starches: Effects on protein and starch digestibility and starch pasting properties. **Starch-Stärke.** 70(9-10): 1700315.

Putseys, J., Lamberts, L., and Delcour, J. (2010). Amylose-inclusion complexes: Formation, identity and physico-chemical properties. **Journal of Cereal Science.** 51(3): 238-247.

Qin, D., Yang, X., Gao, S., Yao, J., and McClements, D. J. (2017). Influence of dietary fibers on lipid digestion: Comparison of single-stage and multiple-stage gastrointestinal models. **Food Hydrocolloids.** 69: 382-392.

Raigond, P., Atkinson, F. S., Lal, M. K., Thakur, N., Singh, B., and Mishra, T. (2020). **Potato Carbohydrates.** Potato: Springer. 13-36.

Ribotta, P. D., and Rosell, C. M. (2010). Effects of enzymatic modification of soybean protein on the pasting and rheological profile of starch–protein systems. **Starch-Stärke.** 62(7): 373-383.

Sarkar, A., Goh, K. K., Singh, R. P., and Singh, H. (2009). Behaviour of an oil-in-water emulsion stabilized by β-lactoglobulin in an in vitro gastric model. **Food Hydrocolloids.** 23(6): 1563-1569.

Singh, J., Dartois, A., and Kaur, L. (2010). Starch digestibility in food matrix: a review. **Trends in Food Science & Technology.** 21(4): 168-180.

Sopade, P. A., and Gidley, M. J. (2009). A rapid in-vitro digestibility assay based on glucometry for investigating kinetics of starch digestion. **Starch-Stärke.** 61(5): 245-255.

Srigiripura, C. V., Kotebagilu, N. P., and Urooj, A. (2019). In Vitro Starch and Protein

Digestibility of Disease Specific Nutrition Formulations. **Current Research in Nutrition and Food Science Journal.** 7(1): 66-74.

Srikaeo, K., and Sangkhiaw, J. (2014). Effects of amylose and resistant starch on glycaemic index of rice noodles. **LWT-Food Science and Technology.** 59(2): 1129-1135.

Tamura, M., Singh, J., Kaur, L., and Ogawa, Y. (2016). Impact of the degree of cooking on starch digestibility of rice–An in vitro study. **Food Chemistry.** 191: 98-104.

Thaiudom, S., and Goff, H. (2003). Effect of κ-carrageenan on milk protein polysaccharide mixtures. **International Dairy Journal.** 13(9): 763-771.

Thaiudom, S., and Pracham, S. (2018). The influence of rice protein content and mixed stabilizers on textural and rheological properties of jasmine rice pudding. **Food Hydrocolloids.** 76: 204-215.

Tian, J., Chen, J., Ye, X., and Chen, S. (2016). Health benefits of the potato affected by domestic cooking: A review. **Food Chemistry.** 202: 165-175.

Tunick, M. H., Ren, D. X., Van Hekken, D. L., Bonnaillie, L., Paul, M., Kwoczak, R., and Tomasula, P. M. (2016). Effect of heat and homogenization on in vitro digestion of milk. **Journal of Dairy Science.** 99(6): 4124-4139.

Wan, L., Li, L., Harro, J. M., Hoag, S. W., Li, B., Zhang, X., and Shirtliff, M. E. (2020). In Vitro Gastrointestinal Digestion of Palm Olein and Palm Stearin-in-Water Emulsions with Different Physical States and Fat Contents. **Journal of Agricultural and Food Chemistry.** 68(26): 7062-7071.

Wang, L., Wang, W., Wang, Y., Xiong, G., Mei, X., Wu, W., Liao, L. (2018). Effects of fatty acid chain length on properties of potato starch–fatty acid complexes

under partially gelatinization. **International Journal of Food Properties.** 21(1): 2121-2134.

Wang, S., Li, C., Copeland, L., Niu, Q., and Wang, S. (2015). Starch retrogradation: A comprehensive review. **Comprehensive Reviews in Food Science and Food Safety.** 14(5): 568-585.

Wang, S., Luo, H., Zhang, J., Zhang, Y., He, Z., and Wang, S. (2014). Alkali-induced changes in functional properties and in vitro digestibility of wheat starch: the role of surface proteins and lipids. **Journal of Agricultural and Food Chemistry.** 62(16): 3636-3643.

Woods, L., and Swinton, S. (1995). **Enzymes in the starch and sugar industries.** Enzymes in food processing: Springer. 250-267.

Xu, D., Yuan, F., Gao, Y., Panya, A., McClements, D. J., and Decker, E. A. (2014). Influence of whey protein–beet pectin conjugate on the properties and digestibility of β-carotene emulsion during in vitro digestion. **Food Chemistry.** 156: 374-379.

Yang, C., Zhong, F., Goff, H. D., and Li, Y. (2019). Study on starch-protein interactions and their effects on physicochemical and digestible properties of the blends. **Food Chemistry.** 280: 51-58.

Yang, H., Irudayaraj, J., Otgonchimeg, S., and Walsh, M. (2004). Rheological study of starch and dairy ingredient-based food systems. **Food Chemistry.** 86(4): 571-578.

Ye, A., Cui, J., Dalgleish, D., and Singh, H. (2016). The formation and breakdown of structured clots from whole milk during gastric digestion. **Food & function.** 7(10): 4259-4266.

Ye, J., Hu, X., Luo, S., McClements, D. J., Liang, L., and Liu, C. (2018). Effect of endogenous proteins and lipids on starch digestibility in rice flour. **Food Research International.** 106: 404-409.

Zabar, S., Lesmes, U., Katz, I., Shimoni, E., and Bianco-Peled, H. (2009). Studying different dimensions of amylose–long chain fatty acid complexes: Molecular, nano and micro level characteristics. **Food Hydrocolloids**. 23(7): 1918-1925.

Zheng, M., Chao, C., Yu, J., Copeland, L., Wang, S., and Wang, S. (2018). Effects of Chain Length and Degree of Unsaturation of Fatty Acids on Structure and in Vitro Digestibility of Starch-Protein-Fatty Acid Complexes. **Journal of Agricultural and Food Chemistry.** 66(8): 1872-1880.
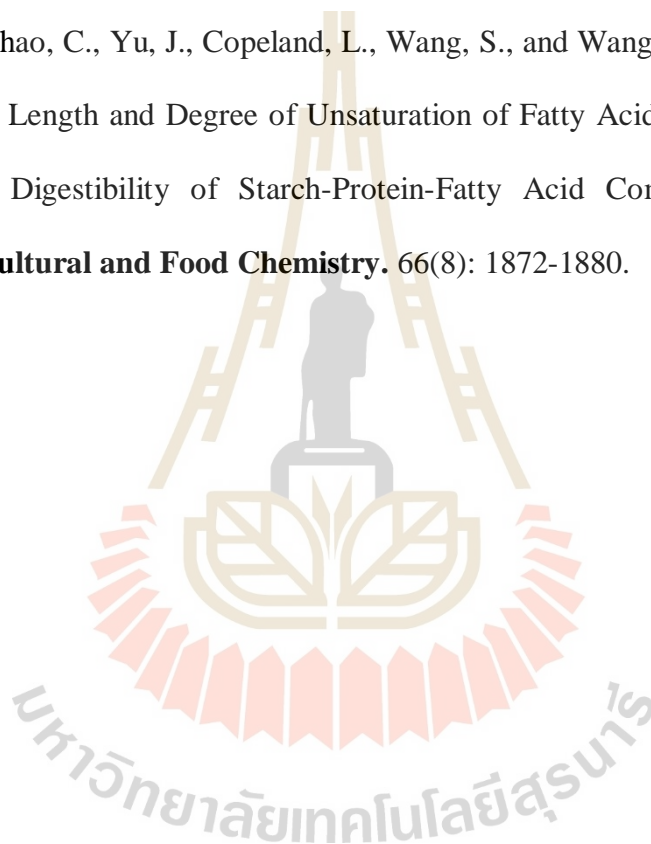
CHAPTER VI

SUMMARY

The addition of MP and SBO to GPS could change the structure and physicochemical properties of the GPS. CA or WP and SBO were dispersed into the GPS's 3D networks, resulting in changes to the structure and viscosity of the GPS. MP had more impact on the rheological properties than the SBO. The addition of MP could reduce the viscosity of GPS significantly. Interaction between MP and SBO affected the viscosity of the potato paste.

There were no covalent interactions between potato starch, MP and SBO in this research. After the addition of MP and/or SBO into GPS, corresponding characteristic peaks was appeared in the obtained mixtures. In addition, the amorphous region, the short-range molecular order, and the relative crystallinity of the GPS were changed after MP, SBO, or both adding into GPS. This leads to changes in the physicochemical properties of the mixtures.

The addition of MP and/or SBO to GPS also affected the digestibility properties of the GPS. The addition of SBO could inhibit the digestion of GPS, while the addition of MP could improve the digestion of GPS. The homogenization of SBO and MP enhanced the digestion of protein, while the homogenization of GPS and MP inhibited protein digestion. The simultaneous mixing of SBO with GPS and MP inhibited protein digestion, but this had a less inhibition effect than the GPS-MP. Mixture of MP and/or GPS with SBO promoted the release of FFA in SBO. Mixture

of MP with SBO resulted in the best release of FFA in SBO. CLSM showed the changes in the binary and tertiary during simulated digestion. The viscosity measurement showed that the addition of SBO could increase the viscosity of the PSP, while the mixture of MP and GPS contributed to the decrease of the PSP viscosity. Thus, this information should benefit the food manufacturing and gastronomy in terms of the development of food products composing of potato starch.
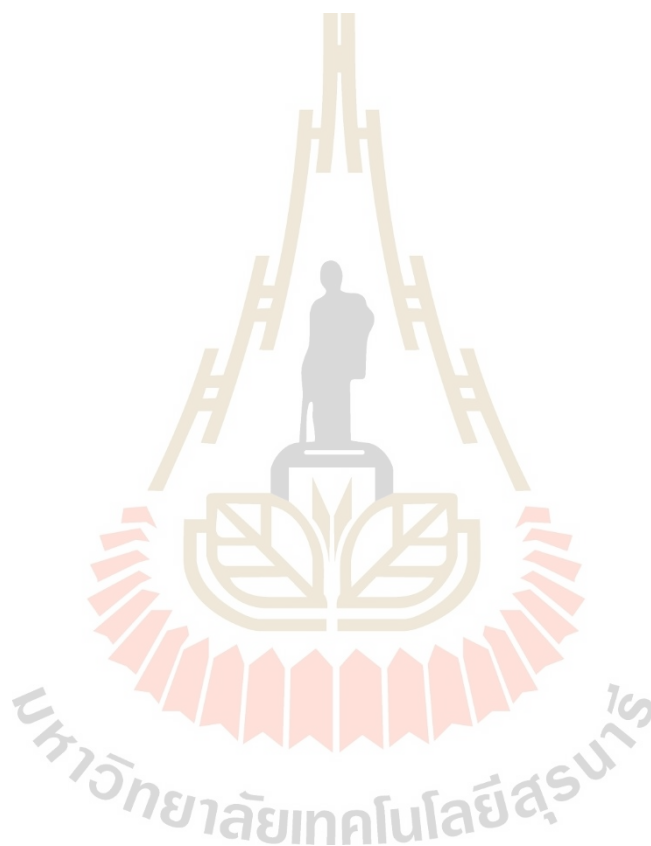
APPENDIXES

SUPPLEMENTARY DATA
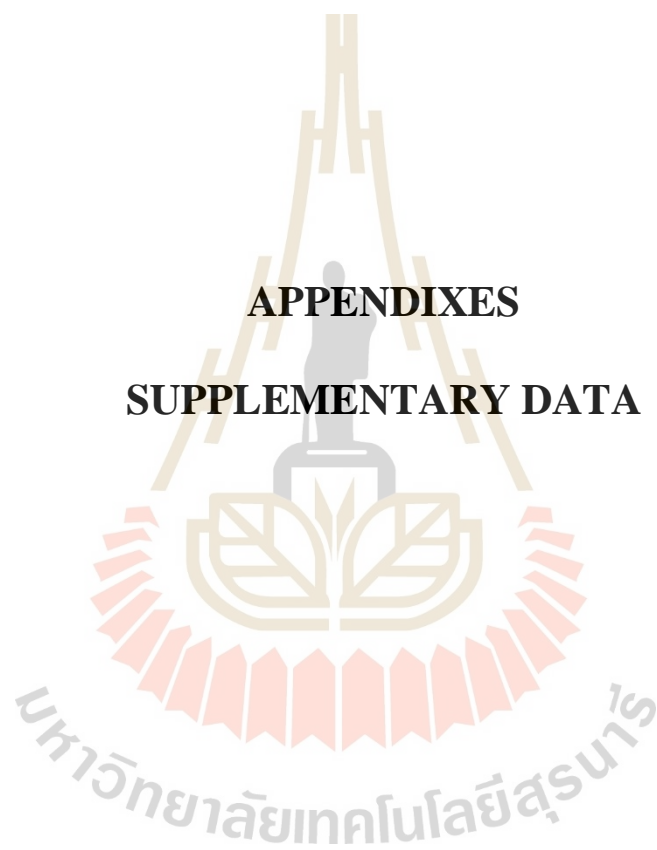
APPENDIX A

D-glucose assay procedure:

Add 3.0 ml of GOPOD Reagent to 0.1 ml of sample solution containing D-glucose and incubate at 40-50°C for 20 min (see table below). Measure the absorbances at 510 nm against the reagent blank to obtain ΔA_{sample} and $\Delta A_{\text{D-glucose}}$ standard.

Calculation:

$$D - Glucose \ (\mu g/0.1 \ ml) = \frac{\Delta A Sample}{\Delta A D - Glucose \ standard(100 \mu g)} \times 100$$

	Reagent	**Standard Sample**	**Blank**
GOPOD reagent	3.0 ml	3.0 ml	3.0 ml
D-Glucose standard	-	0.1 ml	-
Sample	-	-	0.1 ml
Buffer or water	0.1 ml	-	-

APPENDIX B

B.1 Materials and methods

B.1.1 Materials

PS was purchased from Bangkok Inter Food Co., Ltd. (Bangkok, Thailand). Micellar casein concentrates powder with 82% (w/w) total protein was received from Vicchi Enterprise Co., Ltd. (Bangkok, Thailand). The SBO (Cook brand) used in this study was purchased from the Mall in Nakhon Ratchasima province, Thailand.

B.1.2 Sample preparation

The binary and ternary mixture was prepared according to the method of Farooq et. al (2018) and modified in consideration of a really real mashed potato system.

Potato starch (30 g, dry starch base) was weighted in a beaker and deionized water (nearly 200 g) was added into the beaker to prepare a suspension. The suspension was heated in a water bath at 95°C for 30 mins with a cover glass and then was stirred for 2 mins at the beginning to prevent the PS from caking, resulting in the GPS. The CA (3g, calculated as 10%, dry starch basis) was weighted in a beaker, and deionized water (nearly 40 g) was added to prepare a CA solution. The CA solution and SBO (1.5 g) were heated in a water bath at 95°C for 30 mins. To make the binary and ternary mixture system, the CA solution and SBO were added into the GPS with the 95°C water to make the total final weight of the mixture at 300 g. After the

mixture was completely mixed, it was cool down to 60°C and homogenized at 12500 rpm for 1 min and left until the temperature of the mixture was about 50°C. One-half of the mixture paste was hermetically kept in a 200mL-test tube for rheological determination. The one-half rest of the mixture was frozen immediately (-80°C). Then, the frozen sample was freeze-dried to prevent any further retrogradation. After freeze-drying, the binary and ternary mixtures were gently ground with a mortar and pestle and then passed through a 60-mesh screen sieve. The freeze-dried powder was stored in a sealed container at room temperature until further analysis. Potato starch paste (PSP) (only contained PS and water) was used as control. The composition of each sample is shown in Table B.1.

Table B.1 The samples with different compositions.

Number	Ingredients			
	Name	Potato starch	Casein	Soybean oil
1	PSP	√		
2	GPS-CA	√	√	
3	GPS-SBO	√		√
4	GPS-CA-SBO		√	√

B.1.3 Rheological measurements

The rheological property measurements were performed on an AR-G2 Rheometer (TA Instruments, New Castle, USA). Cup and bob geometry (cup radius 15 mm, bob radius of 14 mm and height of 42 mm) were used. Before the determination, the fresh samples of mixtures were left on the plate of rheometer at a given measurement temperature within 2 min in order to let the samples were in the

equilibrium state (Li, Ye, Zhou, Lei, and Zhao, 2019). The shear rate range in steady shear measurements was increased step-wise from 0.01 s^{-1} to 100 s^{-1}. The data of shear stress (τ) and shear rate ($\dot{\gamma}$) were fitted to the Herschel-Bulkley model (Equation (B.1)). Yield stress (τ_0, Pa), flow behaviour index (n, dimensionless) and consistency coefficient (K, Pa s^n) were used to characterize the rheological behavior of the samples (Wang et al., 2018). In Equation (B.1)), τ is the shear stress (Pa), while $\dot{\gamma}$ is the shear rate (s^{-1}).

$$\tau = \tau_0 + K\dot{\gamma}^n \tag{B.1}$$

In order to determine the linear viscoelastic region (LVR), strain sweep was performed at a constant frequency of 0.5Hz in the strain range of 0.01 ~ 100%. In the case of small amplitude oscillating shear, the frequency varied from 0.04 Hz to 4 Hz, and the strain amplitude is 0.5%.

B.1.4 FTIR spectroscopy

The FTIR spectroscopy was recorded using a Bruker Tensor 27 FT-IR Spectrometer (Bruker Optics Inc., Germany). The fine powder was pressed into transparent pellets after mixing and grinding, and detected by transmission method (Xiong, Li, Shi, and Ye, 2017). The infrared spectrum measurement range was 4000-400 cm^{-1}. The measured spectral resolution was 4 cm^{-1} and 64 scans were performed. The data were analyzed with OPUS software (Bruker, Germany).

B.1.5 XRD

The freeze-dried samples were equilibrated 7 days over a saturated sodium chloride solution at room temperature before analysis (Wang, Zheng, Yu, Wang, and Copeland, 2017). The X-ray diffractometer (D8 Advance, Bruker,

Germany) was operated at 40 kV and 40 mA with Cu tube (λ=1.5418 Å). The samples were placed in a grooved glass cell and scanned over the range of 4° to 30°(2θ) at 25 °C. The relative crystallinity (RC) of the samples was calculated using the following equation. In Equation (B.2), A_c is the area of the crystalline peak and A_a is the area of the amorphous peak.

$$RC = 100 \times \frac{A_c}{(A_c+A_a)} \tag{B.2}$$

B.1.6 Statistical analysis

Measurements of all experiments were carried out at least duplicate. The results were expressed as mean ± standard deviation. Statistical analyses were conducted using SPSS 23.0 (SPSS Inc., Chicago, USA). In all statistical analyses, $p<0.05$ was considered significant.

B.2 Results and discussion

B.2.1 Rheological properties

The steady shear flow curves of the PSP, binary, and ternary mixture are shown in Fig. B.1, and the rheological behaviors parameters (τ_0, n, and K) are summarized in Table B.2. All paste samples exhibited shear-thinning characteristic, despite slight shear thickening or transient Newtonian plateauing in the low shear rate range (0.1 to 0.2 s^{-1}). Similar trend was reported by Zhao et al (Li et al., 2019; Wang et al., 2018). In comparison with PSP, the effect of addition of SBO into the GPS on viscosity was not significant. Different from GPS-CA, the GPS mixed with CA/CA-SBO had a lower viscosity during all the shear rate. The decrease of viscosity after mixing with CA was related to the non-specific ionic strength effect of PS (Considine

et al., 2011). The decrease of viscosity after mixing with CA was related to the non-specific ionic strength effect of PS. The viscosity of PSP and GPS-SBO decreased greater than GPS-CA and GPS-CA-SBO when the shear rate was increased. This was also attributed by the rheological parameters of K (Table B.2). The higher the K value, the higher the viscosity of the mixture PSP and GPS-SBO presented the higher values in yield stress (τ_0) and consistency coefficient (K) but a lower value in flow behavior index (n) than GPS-CA and GPS-CA-SBO. This might be because the hydrophobic interaction between CA and GPS could inhibit the molecular rearrangement of GPS and reduce the viscosity of the GPS-CA mixture.
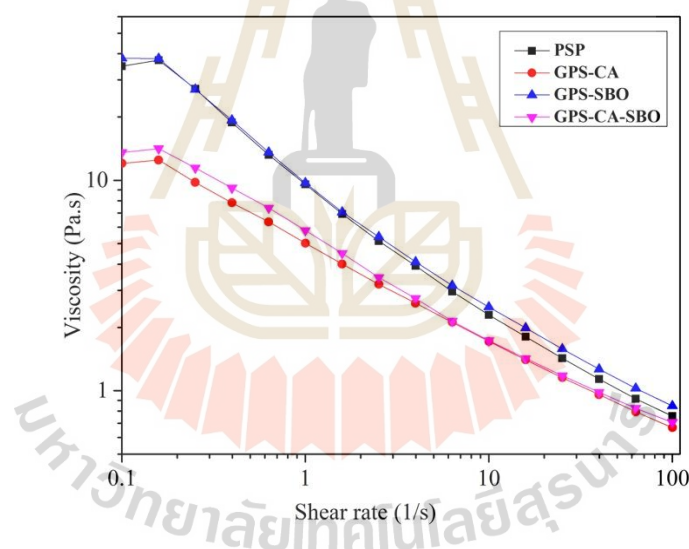
Figure B.1 Flow curves of the pastes (37°C) from PSP, GPS-CA, GPS-SBO and GPS-CA-SBO.

Table B.2 Rheological parameters of fresh sample pastes from steady shear.

Rheological parameters		PSP	GPS-CA	GPS-SBO	GPS-CA-SBO
steady	τ_0 (Pa)	4.11 ± 0.52^b	0.79 ± 0.30^a	4.03 ± 0.62^b	1.66 ± 1.12^a
	K(Pa s^n)	5.6 ± 1.61^a	4.05 ± 0.41^a	5.44 ± 1.23^a	3.59 ± 0.677^a
	n	0.58 ± 0.06^a	0.61 ± 0.01^a	0.59 ± 0.03^a	0.64 ± 0.01^a

[a-b]The rheological parameters of steady shear include yield stress (τ_0), consistency coefficient (K), flow behavior index (n). They were obtained by fitting the shear stress (τ) and shear rate ($\dot{\gamma}$) data from the steady shear rheological curves across the specific fitting range to Herschel-Bulkley model of $\tau = \tau_0 + K\dot{\gamma}^n$.

Fig. B.2 shows storage modulus (G'), loss modulus (G''), and loss tangent (*tan δ*) versus frequency plots of the fresh samples measured at 37°C. All the paste samples analyzed displayed a liquid-like behavior with higher G'' than G' over the entire frequency range. For all pastes (PSP, GPS-CA, GPS-SBO, and GPS-CA-SBO), both moduli exhibited strong frequency dependence. Also, all pastes revealed an almost linear in the double logarithm scale. In comparison with PSP, GPS-SBO possessed a higher G' and G''. The GPS-CA has the lowest G' and G'', the G' and G'' of the GPS-CA-SBO were between the G' and G″ of GPS-CA and GPS-SBO. The addition of SBO into GPS would promote a lower G' value more than the addition of CA into GPS, this was because the addition of SBO to GPS could enhance a solid-like characteristic of the GPS while the addition of CA might induce the GPS to lose its three-dimensional structure from the incompatibility between CA and GPS.

At any studied frequency, the *tan δ* values of all pastes were greater than 1.0, indicating that they behaved as a liquid-like matter with a G' value lower than the G'' value. This is due to the three-dimensional structure of the GPS was destroyed during the homogenization process. However, GPS-CA and GPS-CA-SBO exhibited much higher values of tan *tan δ* than PSP at any frequency. This implied that the structure of GPS accumulated more severe changes after the addition of CA. CA appeared to be an inactive filler which prevented the amylose rearrangement and weakened the gel formation of GPS (Thaiudom and Pracham, 2018). *Tan δ* value of GPS-SBO was close to that of PSP. This might be because the SBO could insert and exist in the GPS three-dimension networks as the oil droplets. Thus, the GPS structure was less damaged than that in GPS-CA system. However, all samples demonstrated a low frequency dependence for *tan δ* trace, indicating their high structural stabilities.
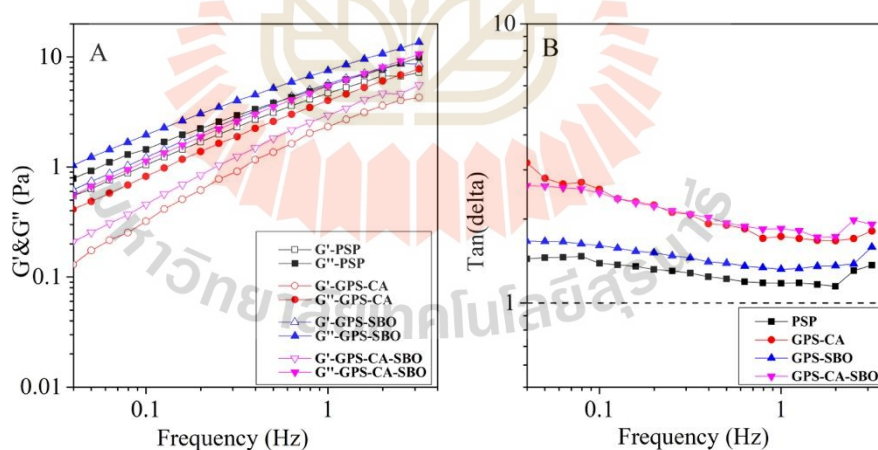
Figure B.2 G', G'' and tan δ (A and B) at a different frequency of PSP, GPS-CA, GPS-SBO and GPS-CA-SBO.

B.2.2 FTIR spectroscopy
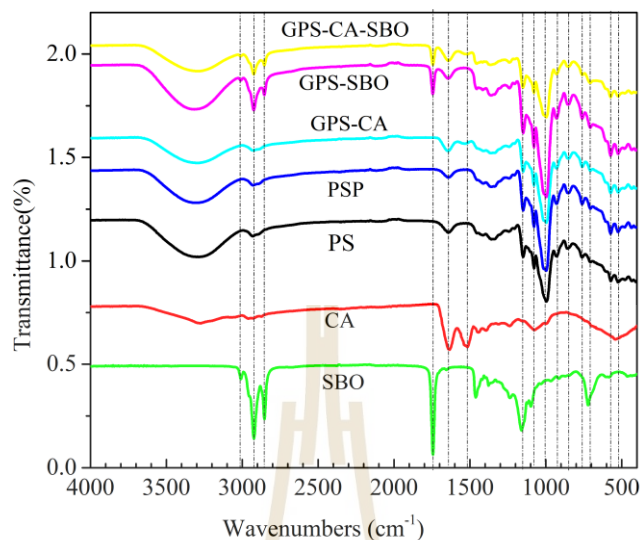
Figure B.3 FTIR spectra of PS, CA, SBO, PSP, GPS-CA, SBO, GPS-CA, and GPS-CA-SBO.

The FTIR spectroscopy of PS, CA, SBO, and the freeze-dried PSP, GPS-CA, GPS-SBO, and GPS-CA-SBO are presented in Fig.B.3. FT-IR spectroscopy of the PSP was almost the same as PS. The characteristic peak at about 3700-3000 cm^{-1} was due to the intermolecular bonding of hydroxyl group. The peak at 2937cm^{-1} attributed to the CH_2 deformation, and the characteristics peak at 1643 cm^{-1} assigned to the water adsorbed in the amorphous regions of starch (Kizil, Irudayaraj, and Seetharaman, 2002). After the addition of CA or CA and SBO into GPS, the GPS-CA and GPS-CA-SBO samples had a characteristic peak around 1541 cm^{-1}, which was assigned to the deformation vibration of amino acids and the amide II absorption in CA (Wang, M. Zheng, J. Yu, Wang, and L. Copeland, 2017; Zaleska, Ring, and Tomasik, 2001). While adding SBO into the systems, the GPS-SBO and GPS-CA-

SBO had characteristic peaks at about 2850 cm^{-1} and 1750 cm^{-1}, respectively, which is attributed to the vibration of carbonyl groups and the C−H asymmetric stretching vibration of the methylene groups of fatty acids (Yang, Irudayaraj, and Paradkar, 2005). The above observations However, the results showed that no new characteristic peaks appeared or shifted except those characteristic peaks of PS, CA, and SBO in the whole spectrum. The above observations suggested that only the characteristic peaks of PS, CA and SBO were detected in the entire spectra. This indicated that there was no covalent interaction among PS, CA, and SBO (Yang, Zhong, Goff, and Li, 2019).

B.2.3 XRD

The XRD patterns and RC of the samples are shown in Fig. B.4. PS displayed the B-type crystalline structure with strong reflections peaks at 5.7, 10.0,11.2,14, 15.0 17.0, 18.2, 19.5,24.0 and 26.2°(2θ) angles. In comparison with PS, the crystalline structure of the PSP was destroyed seriously. It only showed slight reflection peak at 17.0°(2θ) angles. It might be due to the incomplete gelatinization of the GPS. The addition of CA did not affect the crystalline structure of the GPS very much, but the reflection peaks at 5.7 disappeared. The addition of SBO showed a decrease in the RC compared with the PSP, it only showed slight reflections peaks at 17.0. From the RCs of the four samples, the addition of CA and/or SBO can enhance damage to the crystal structure of GPS, resulting in less structural existence. These results were relevant to the results of the rheological analysis which showed less solid-like characteristic.
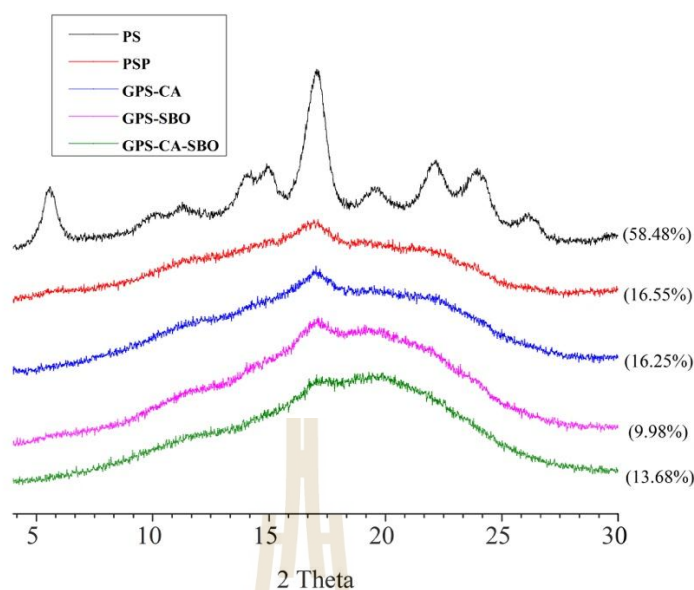
Figure B.4 X-ray diffraction of PS, GPS-CA, GPS-SBO and GPS-CA-SBO. Crystallinity (%) is given in parentheses.

B.3   Conclusions

The addition of CA and/or SBO to GSP could change the rheological properties of the mixture. Casein displayed more impact on the rheological properties than soybean oil. The addition of CA could reduce the viscosity of GPS significantly. All pastes (PSP, GPS-CA, GPS-SBO, and GPS-CA-SBO) possessed the liquid-like property. No covalent interactions between PS, CA, and SBO in this research. The degree of RC of PSP decreases after CA or both CA and SBO were added. This study provided a better understanding of binary and ternary interactions among PS, CA, and SBO.

B.4   References

Considine, T., Noisuwan, A., Hemar, Y., Wilkinson, B., Bronlund, J., and Kasapis, S. (2011). Rheological investigations of the interactions between starch and milk proteins in model dairy systems: A review. **Food Hydrocolloids.** 25(8): 2008-2017.

Farooq, A. M., Dhital, S., Li, C., Zhang, B., and Huang, Q. (2018). Effects of palm oil on structural and in vitro digestion properties of cooked rice starches. **International Journal of Biological Macromolecules.** 107: 1080-1085.

Kizil, R., Irudayaraj, J., and Seetharaman, K. (2002). Characterization of irradiated starches by using FT-Raman and FTIR spectroscopy. **Journal of Agricultural and Food Chemistry.** 50(14): 3912-3918.

Li, S., Ye, F., Zhou, Y., Lei, L., and Zhao, G. (2019). Rheological and textural insights into the blending of sweet potato and cassava starches: In hot and cooled pastes as well as in fresh and dried gels. **Food Hydrocolloids.** 89: 901-911.

Thaiudom, S., and Pracham, S. (2018). The influence of rice protein content and mixed stabilizers on textural and rheological properties of jasmine rice pudding. **Food Hydrocolloids.** 76: 204-215.

Wang, S., Zheng, M., Yu, J., Wang, S., and Copeland, L. (2017). Insights into the formation and structures of starch-protein-lipid complexes. **Journal of agricultural and food chemistry.** 65(9): 1960-1966.

Wang, S., Zheng, M., Yu, J., Wang, S., and Copeland, L. (2017). Insights into the Formation and Structures of Starch-Protein-Lipid Complexes. **Journal of Agricultural and Food Chemistry.** 65(9): 1960-1966.

Wang, Y., Ye, F., Liu, J., Zhou, Y., Lei, L., and Zhao, G. (2018). Rheological nature and dropping performance of sweet potato starch dough as influenced by the binder pastes. **Food hydrocolloids.** 85: 39-50.

Xiong, J., Li, Q., Shi, Z., and Ye, J. (2017). Interactions between wheat starch and cellulose derivatives in short-term retrogradation: Rheology and FTIR study. **Food Research International.** 100: 858-863.

Yang, C., Zhong, F., Goff, H. D., and Li, Y. (2019). Study on starch-protein interactions and their effects on physicochemical and digestible properties of the blends. **Food Chemistry.** 280: 51-58.

Yang, H., Irudayaraj, J., and Paradkar, M. M. (2005). Discriminant analysis of edible oils and fats by FTIR, FT-NIR and FT-Raman spectroscopy. **Food Chemistry.** 93(1): 25-32.

Zaleska, H., Ring, S., and Tomasik, P. (2001). Electrosynthesis of potato starch-casein complexes. **International Journal of Food Science & Technology.** 36(5): 509-515.
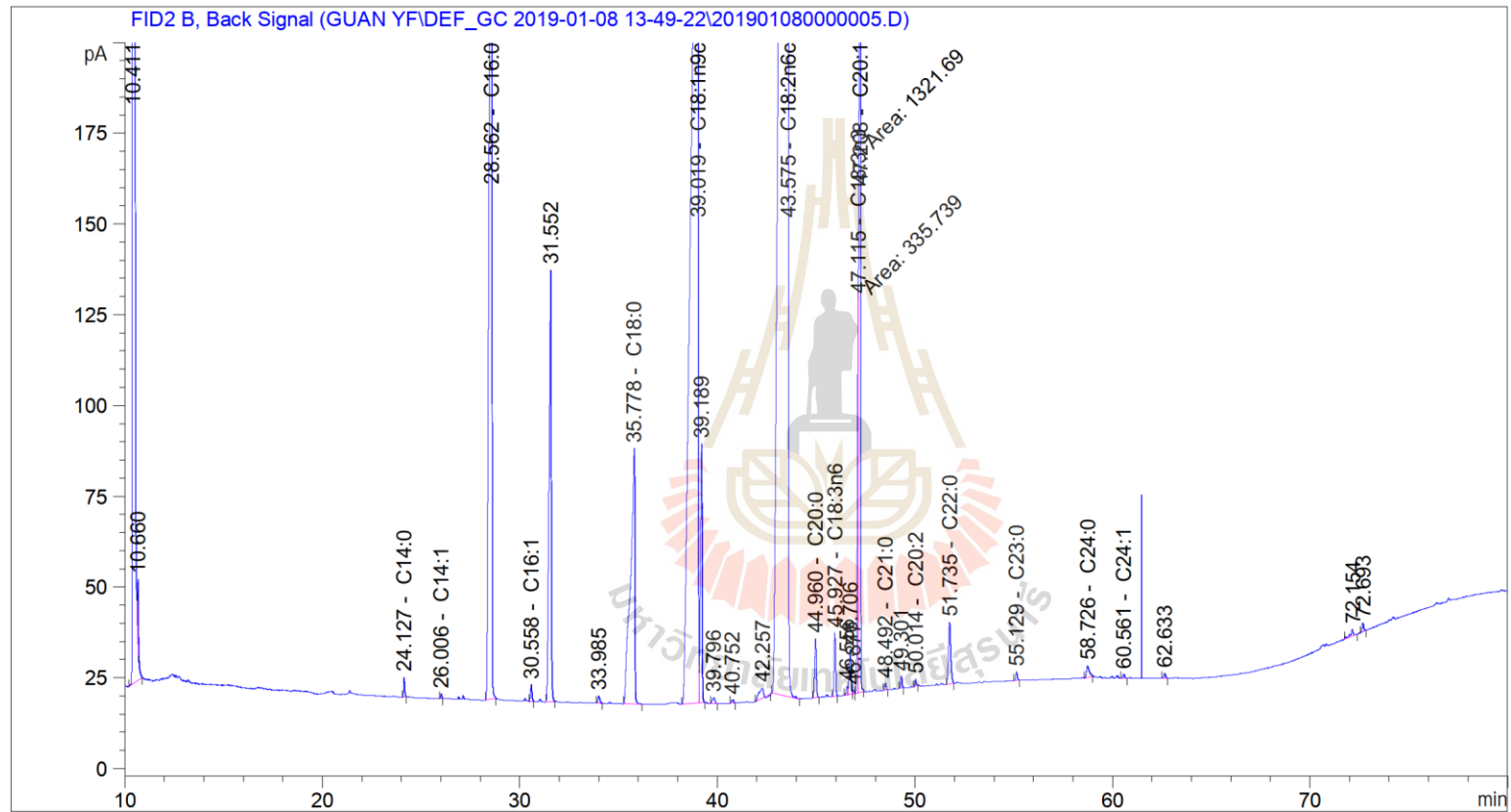
Figure C.1 The GC chromatogram of fatty acids in soybean oil.
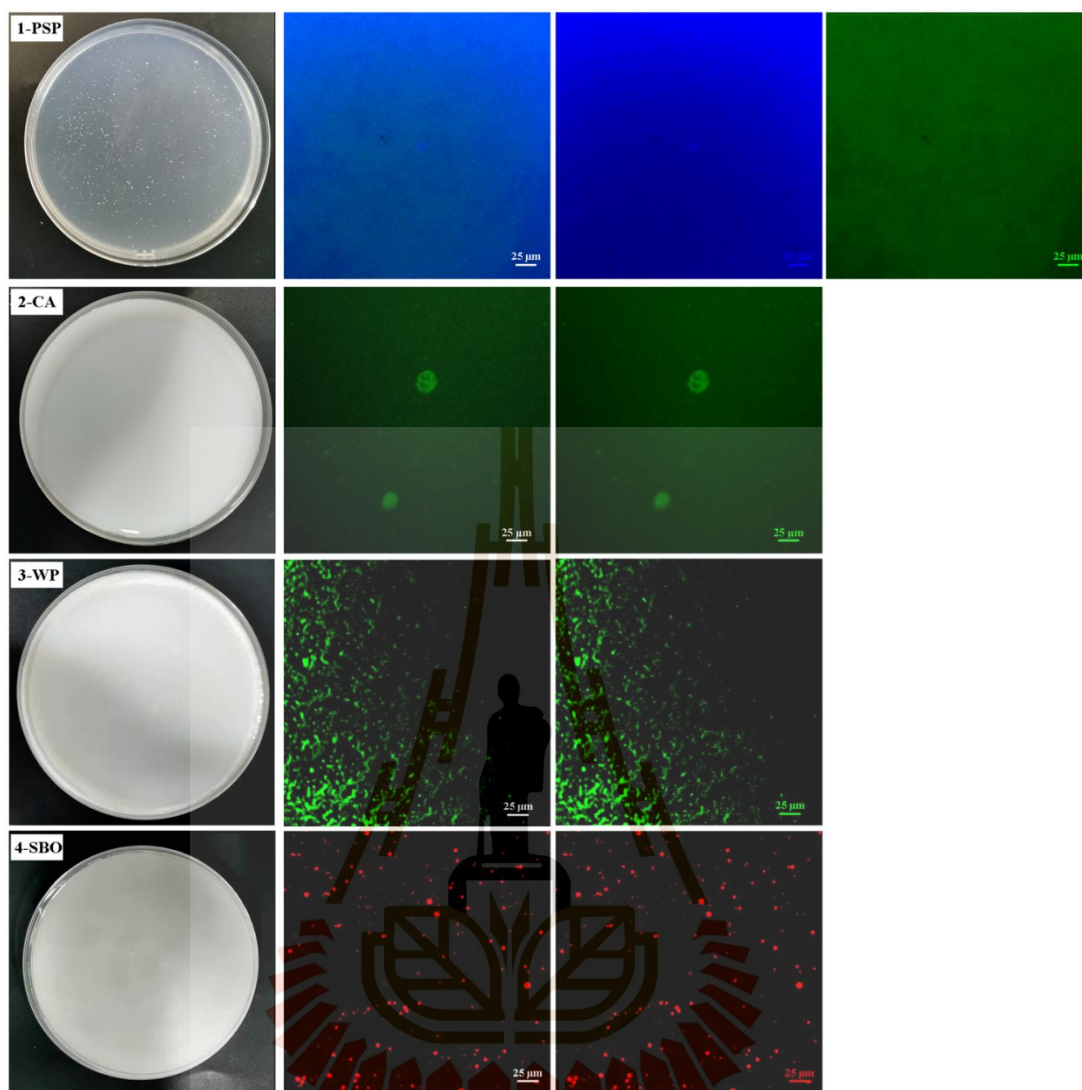
Figure C.2 Images of fresh samples (1, 2, 3, and 4) and their corresponding confocal microscope images. The first column is the picture of the fresh sample, and the second row is their corresponding confocal microscope images. The third and/or fourth columns are the images from different channels (405 nm, 488 nm, or 561 nm) of the second image.
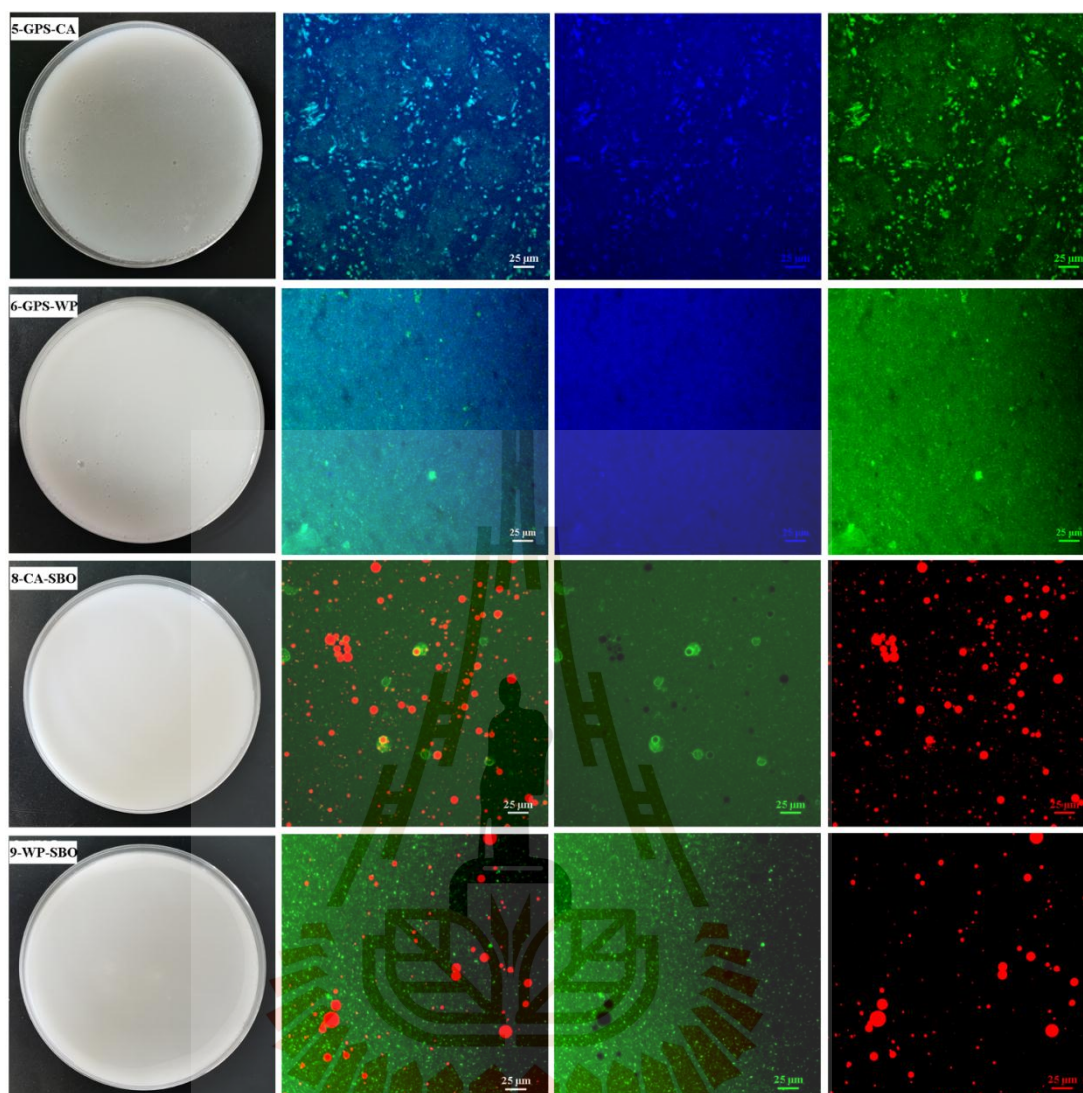
Figure C.3 Images of fresh samples (5, 6, 8, and 9) and their corresponding confocal microscope images. The first column is the picture of the fresh sample, and the second row is their corresponding confocal microscope images. The third and fourth columns are the images from different channels (405 nm, 488 nm, or 561 nm) of the second image.
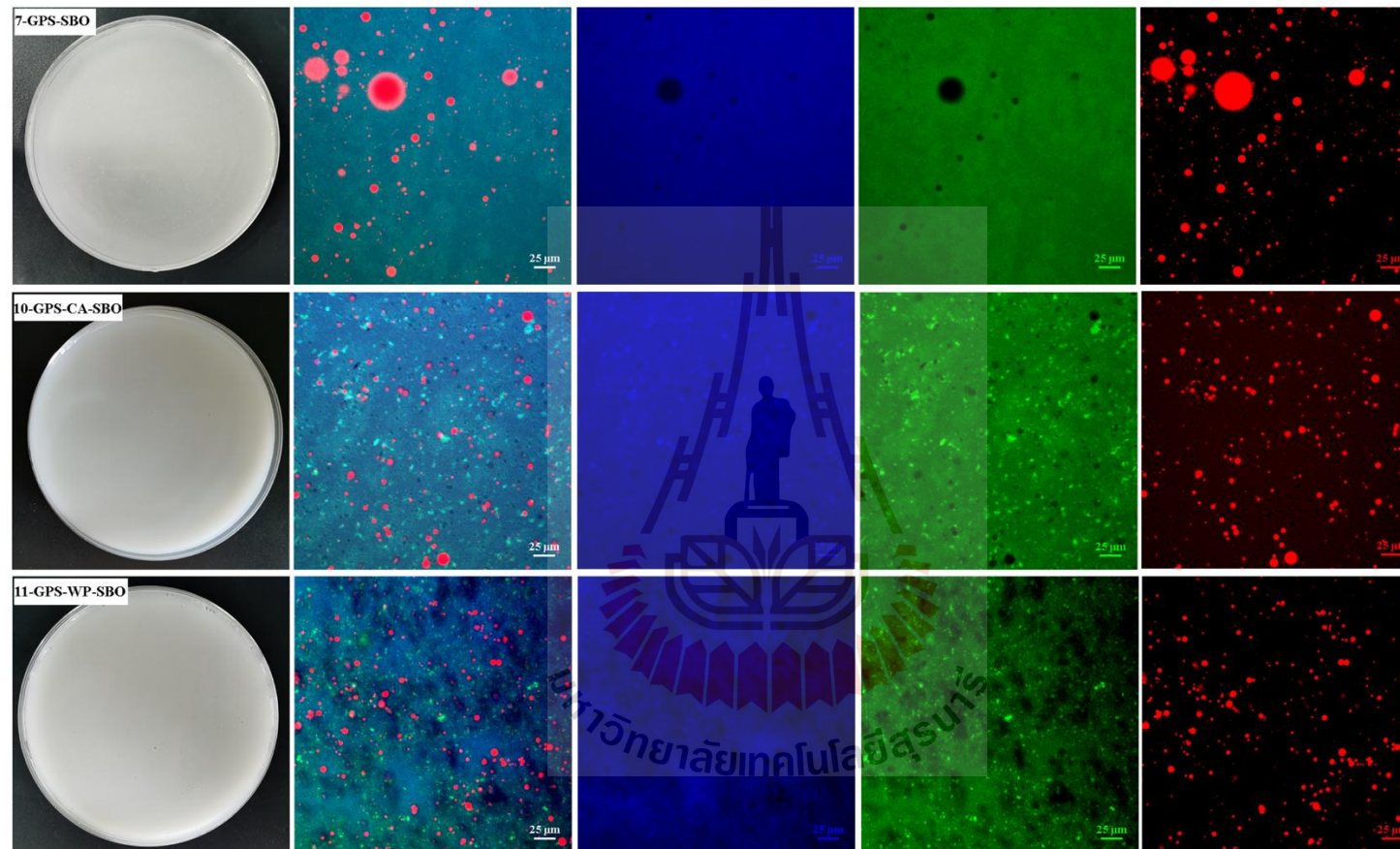
Figure C.4 Images of fresh samples (7, 10, and 11) and their corresponding confocal microscope images. The first column is the picture of the fresh sample, and the second column is their corresponding confocal microscope images. The third, fourth, and five columns are the images from different channels (405 nm, 488 nm, and 561 nm) of the second column image.
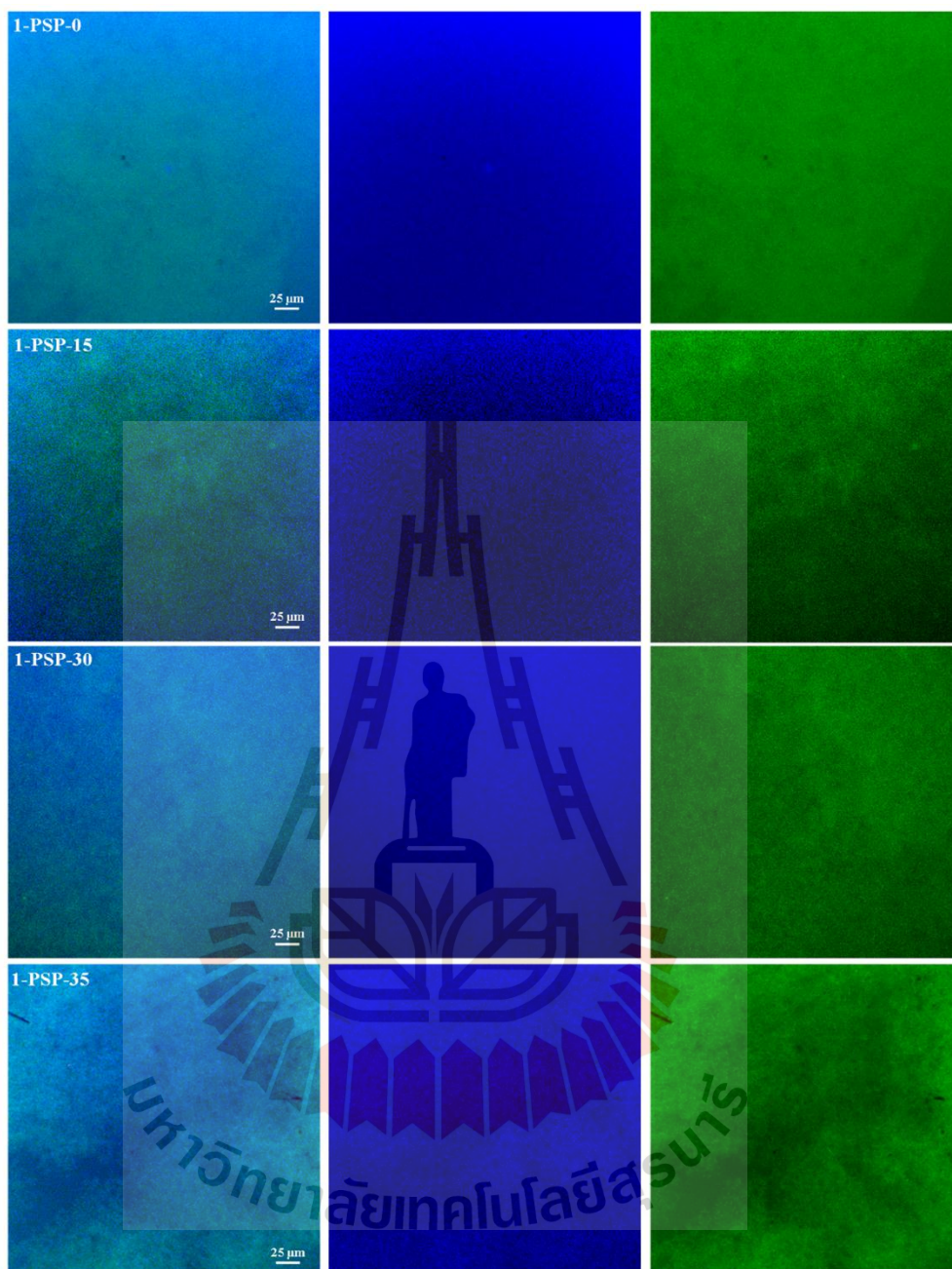
Figure C.5 Confocal microscopy images of PSP during *in vitro* digestion (Stomach phase 15 min and 30 min; Small intestine phase 5 min). The second and third columns are the images of different channels (405 nm and 488 nm) of the second column image.
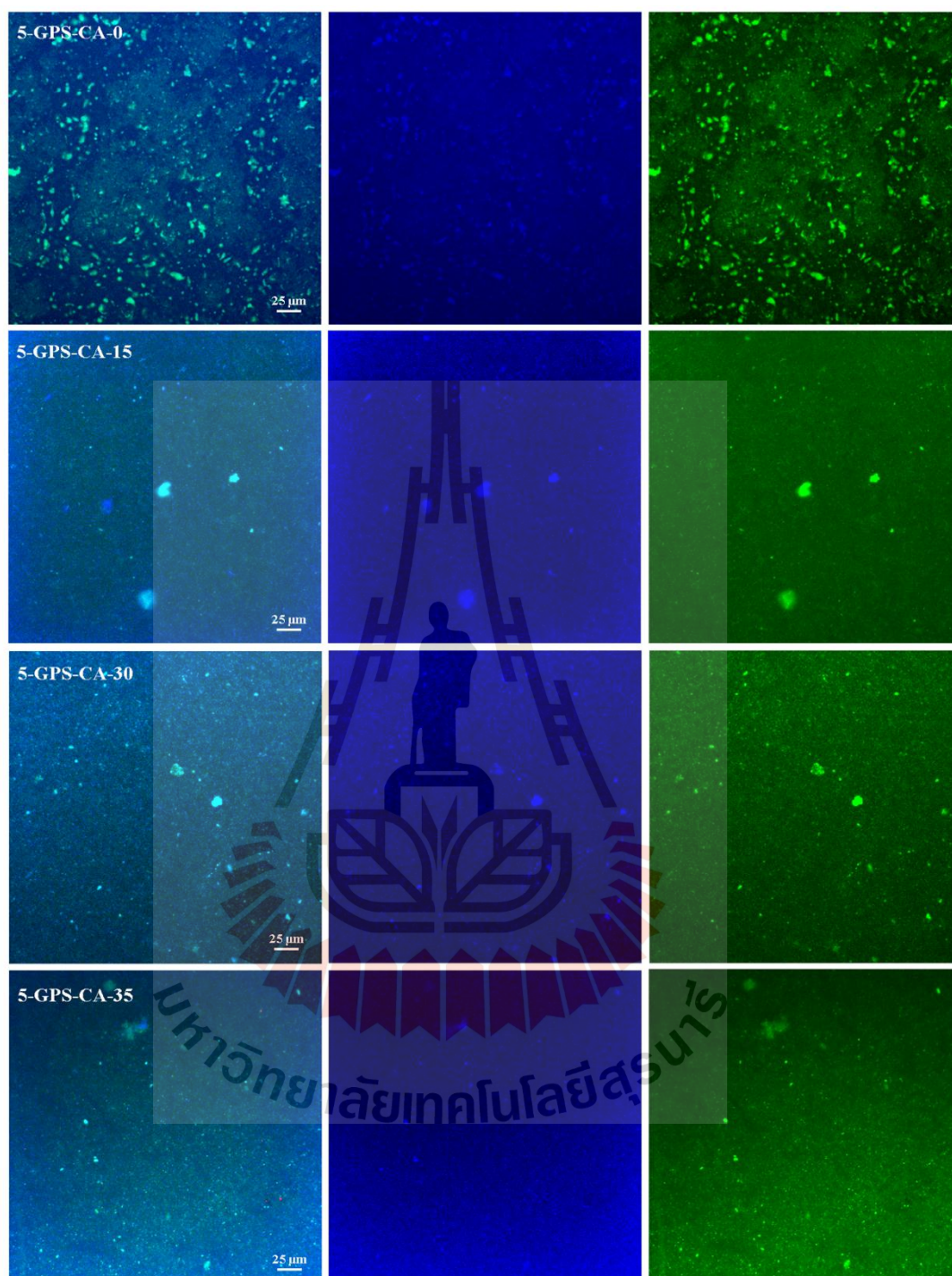
Figure C.6 Confocal microscopy images of GPS-CA during *in vitro* digestion (Stomach phase 15 min and 30 min; Small intestine phase 5 min). The second and third columns are the images from different channels (405 nm and 488 nm) of the second column image.
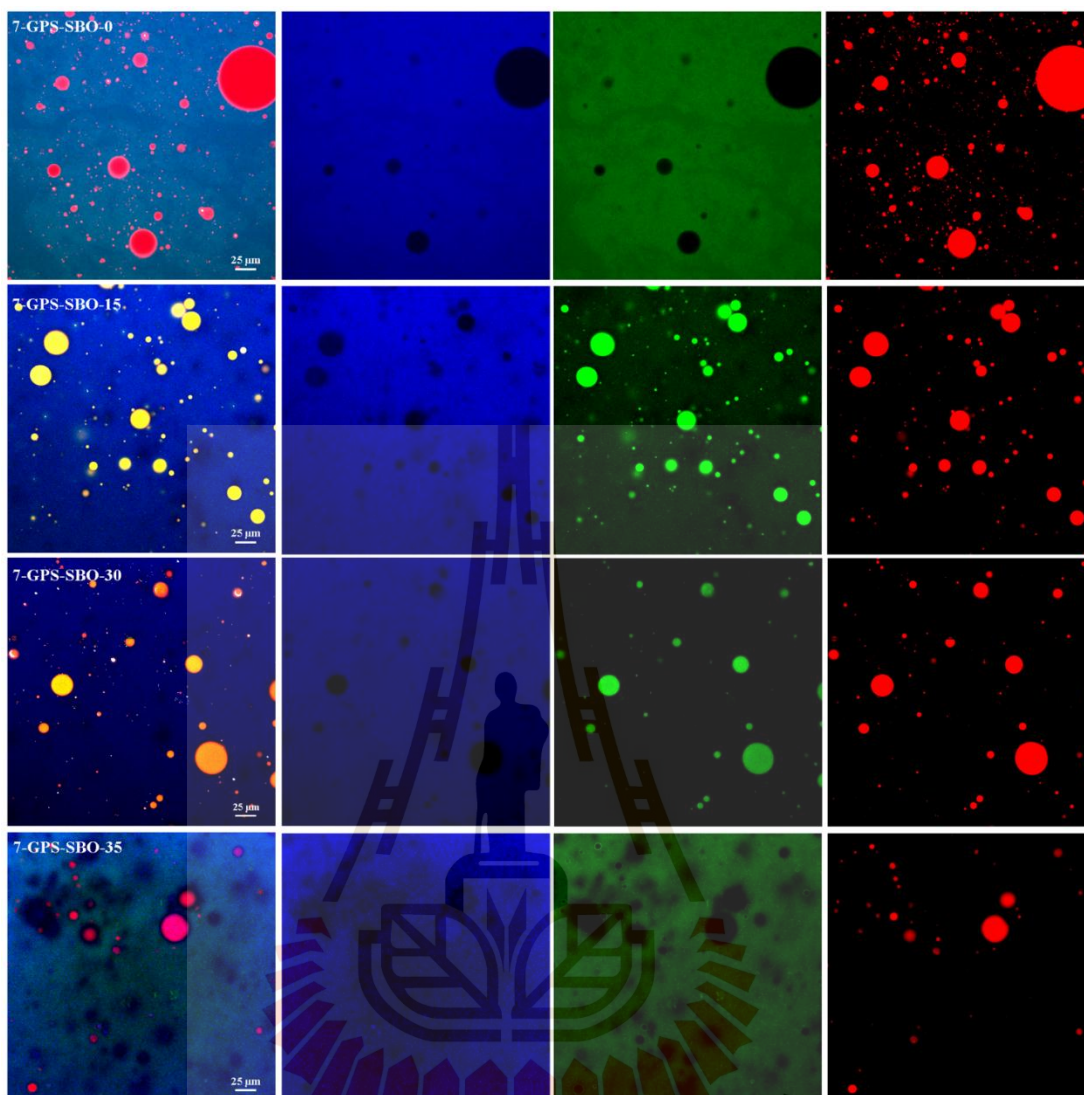
Figure C.7 Confocal microscopy images of GPS-SBO during *in vitro* digestion (Stomach phase 15 min and 30 min; Small intestine phase 5 min). The second, third, and fourth columns are the images from different channels (405 nm, 488 nm, and 561) of the second column image.
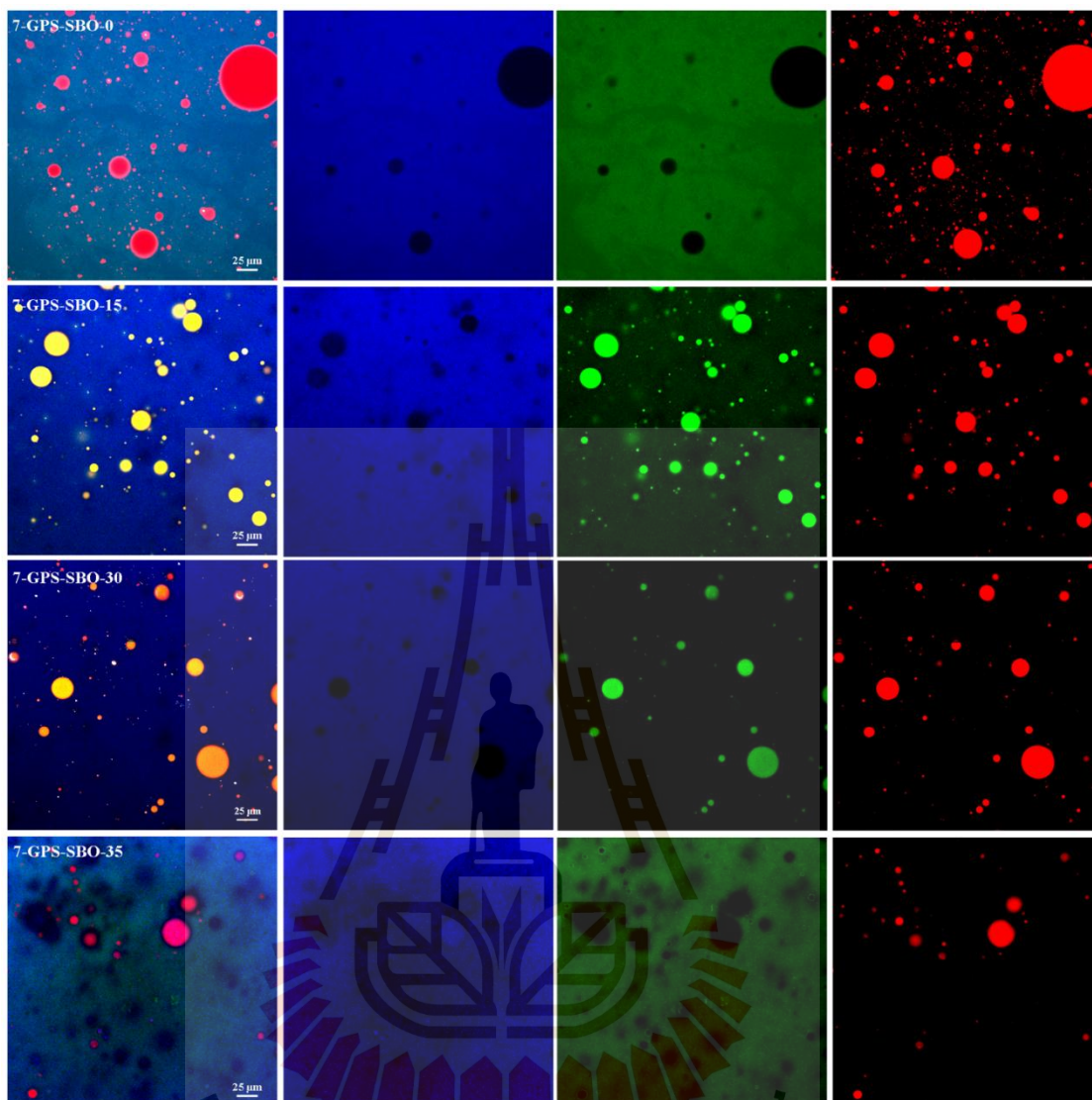
Figure C.8   Confocal microscopy images of GPS-SBO during *in vitro* digestion (Stomach phase 15 min and 30 min; Small intestine phase 5 min). The second, third, and fourth columns are the images from different channels (405 nm, 488 nm, and 561) of the second column image.
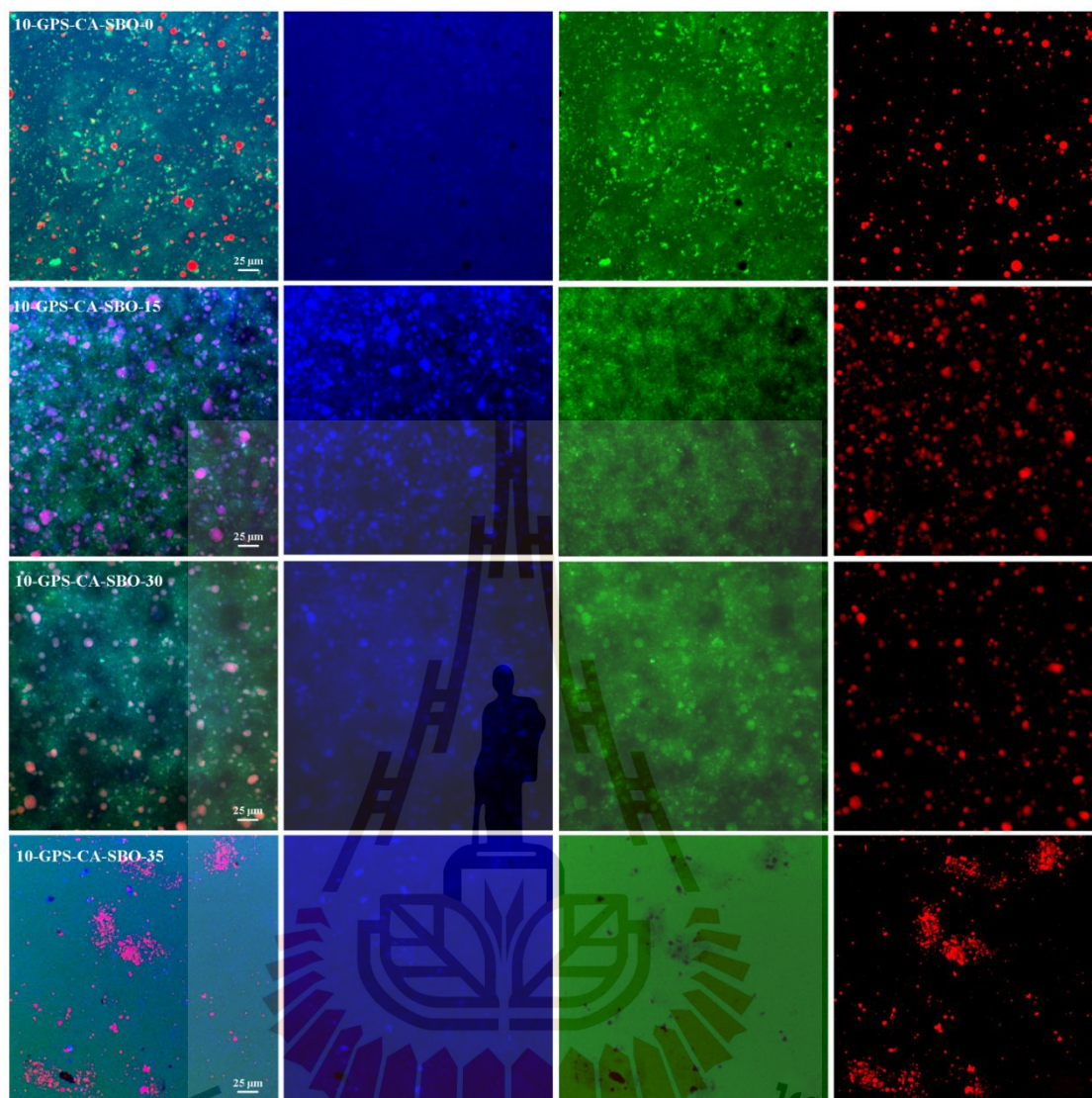
Figure C.9 Confocal microscopy images of GPS-CA-SBO during *in vitro* digestion (Stomach phase 15 min and 30 min; Small intestine phase 5 min). The second, third, and fourth columns are the images from different channels (405 nm, 488 nm, and 561) of the second column image.
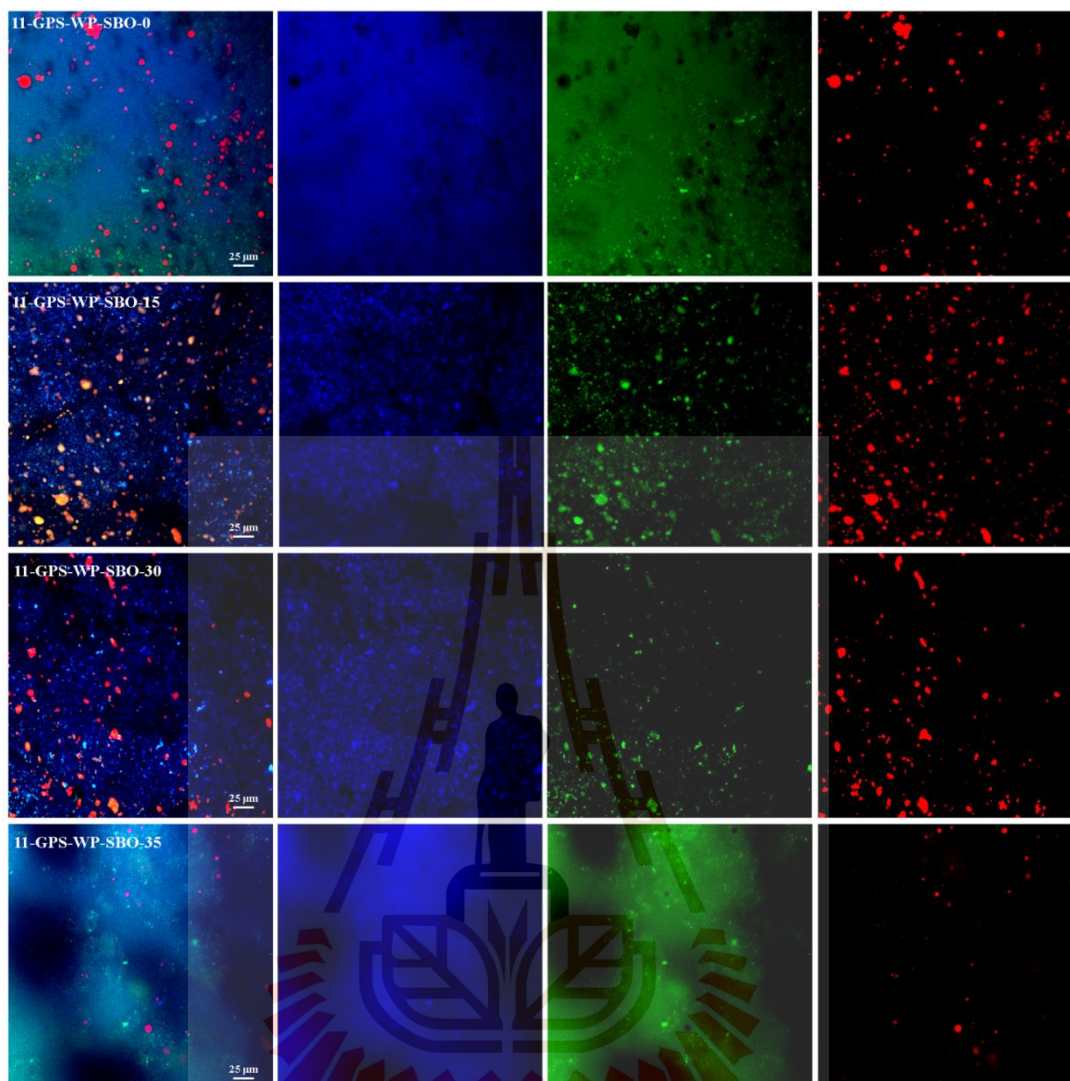
Figure C.10 Confocal microscopy images of GPS-WP-SBO during *in vitro* digestion (Stomach phase 15 min and 30 min; Small intestine phase 5 min). The second, third, and fourth columns are the images from different channels (405 nm, 488 nm, and 561) of the second column image.

BIOGRAPHY

Yufang Guan was born in July 22th, 1988 in Hunan, China. She received Bachelor Degree (Food Science and engineering) from Jishou University, Jishou, China in 2011. She received Master Degree (Food Science) from Southwestern University, Chongqing, China in 2014. During this period, she finished her graduation thesis: Interactions of Carboxymethyl modified polysaccharide with ε-Polylysine. She also published her research work under the title of "Interactions of ε-polylysine with carboxymethyl sweet potato starch with an emphasis on amino/carboxyl molar ratio" in Journal of agricultural and food chemistry (volume 61, page 11653-11659) in 2013. After graduated from Southwest University, she became a researcher at the Potato Research Institute of Guizhou Academy of Agricultural Sciences. She started her PhD study at SUT in November 2015.